Master thesis : Innovative joint configuration for structures subjected to highseismic actions and to exceptional events - Development of aspring model reflecting the joint behaviour in case of a columnloss scenario

Auteur : Milovanovic, Nemanja
Promoteur(s) : Jaspart, Jean-Pierre
Faculté : Faculté des Sciences appliquées
Diplôme : Master en ingénieur civil des constructions, à finalité spécialisée en "sustainable constructions unde natural hazards and catastrophic events (SUSCOS)"
Année académique : 2016-2017
URI/URL : http://hdl.handle.net/2268.2/2329

Innovative joint configuration for structures subjected to high seismic actions and to exceptional events – Development of a spring model reflecting the joint behaviour in case of a column loss scenario

Thesis Report

Author: Nemanja Milovanović

Supervisors:
Marina D'Antimo,Jean-François Demonceau & Jean-Pierre Jaspart

University: University of Liège

University: University of Liège

Date: 17.01.2017

Acknowledgements

First of all, I would like to thank my family for their support and for making this journey possible. Only people coming from Serbia know how challenging that could be.

I would like to express my gratitude to Prof. Jean-François Demonceau, Prof. Jean-Pierre Jaspart andMSc.Eng.Marina D'Antimo, promoters of my thesis, for sharing their knowledge, experience and providing guidance. Without their support, finalizing this work would not be possible.

My sincere gratitude once more to Prof. Jean-François Demonceau for providing me with acomputer after my stopped working. Without that, I would not have the means to finalize my thesis.

Special thanks to MSc.Eng. Angela Lemos and PhD.Eng. Hamra Lotfi, who provided me with useful data, constructive advices and their time without asking anything in return.

I would like to thank mycolleagues from the SUSCOS programme for their support and friendship.

Last but not least,I would like to thank my friends, both the ones I had before enrolling SUSCOS and the ones I made during this programme, for making this journey enjoyable.

Thank you all.

Summary

Structures made of steel have been widely used in areas where seismic activity is expected in the last decades. Their stable performance under cyclic loading conditions make them a desirable solution in earthquake prone areas. However when subjected to exceptional seismic events, like several times in the past, the fact that the input energy is dissipated by deformation of structural elements leads to severe damage and consequently high repair cost.

In order to overcome the above mentioned drawbacks innovative beam to column joint had been designed.This innovative beam-to-column joint is equipped with friction dampers which are located at the bottom flange level of the connected beam to dissipate the earthquake input energy. The friction resistance is calibrated by acting on the number and diameter of bolts and their tightening torque governing the preloading. The connections are conceived to exhibit wide and stable hysteresis loops without any damage to the connection steel plate elements.

The objective of the dissertation is to study the behaviour of a frame and the innovative joint forming the framewhen subjected to a column loss.In case of column loss scenario, this joint will be subjected to a specific loading (bending moment + axial loads) which will require the activation of ductile joint components to allow the activation of an alternative load path within the structure.

Within the thesis the behaviour and potential benefits of the joint under mention circumstances shall be assessed and pointed out.

Notations

θ - rotation at the extremities of the beam of the DAP

Φ - rotation of the joint

δ_{HOG} - elongation of the plastic hinge at the level of beam axis in case of hogging bending

ΔL - to the elongation of the beam under tension force

δ_{SAG} - elongation of the plastic hinge at the level of beam axis in case of sagging bending

$\delta_{slide.fd}$ – estimated length of the slip of the friction damper

δ_{slip} – dilatation of the spring at stroke end limit of the slip

δ_{slip1} – estimated length of the slip of the upper interface

β – transformation parameter for column panel in shear

δ_H – dilatation of the horizontal spring representing the IAP

$\delta_{i,HOG}$ – dilatation of the i spring of the joint subjected to hogging

$\delta_{i,SAG}$ – dilatation of the i spring of the joint subjected to sagging

$\delta_{N\_}$ elongation of the plastic hinge

F_H – horizontal force in the spring representing IAP

$F_{i,HOG}$ – force in the i spring of the joint subjected to hogging

$F_{i,SAG}$ – force in the i spring of the joint subjected to sagging

F_{RD} - design resistance

$F_{RD.H}$ – design resistance of the indirectly affected part

$F_{rd.slip.1}$ - force at slip of the upper joint interface

$F_{rd.slip.2}$ - force at slip of the friction damper

$F_{slip.rd}$ - design force for which the slip occurs

F_{slip_c} - slip resistance of the friction damper in compression

F_{slip_t} – slip resistance of the friction damper in tension

fsolve – matlab function used to solve the system of equations

h_i –distance from the spring row to the centre of compression

HOG 1 – equivalent spring in tension of a joint primarily subjected to hogging bending

HOG 2 – equivalent spring in compression of a joint primarily subjected to hogging bending

$K^*_{eq.T.1}$ – new value of the spring stiffness obtain after vertical translation of the spring

$K_{eff.i}$ – effective stiffness of the components at the level of the bolt row in tension

$k_{eq\_}$ equivalent stiffness of the spring

K_{fake} – "fake" stiffness

K_H – stiffness of the horizontal spring representing the IAP

$K_{i.c.no.slip}$ – stiffness of the equivalent compression spring before the slip

$K_{i.c.slip}$ – stiffness of the equivalent compression spring after the slip

$K_{i.t.no.slip}$ – stiffness of the equivalent tension spring before the slip

$K_{i.t.slip}$ – stiffness of the equivalent tension spring after the slip

K_N – axial stiffness of the plastic hinge

L - Initial length of the plastic hinge

L_0 - the initial length of the beam

M_{hog} – hogging bending moment

$M_{j.ini.limit}$ – moment in the joint limiting the behaviour governed by initial stiffness

$M_{j.slip1.limit}$ – moment in the joint limiting the behaviour governed by $S_{j.slip1}$

$M_{j.slip2.limit}$ – moment in the joint limiting the behaviour governed by $S_{j.slip2}$

M_{sag} – sagging bending moment

P – force applied at the upper node of the lost column simulating the column loss

SAG 1 – equivalent spring in tension of a joint primarily subjected to sagging bending

SAG 2 - equivalent spring in compression of a joint primarily subjected to sagging bending

$S_{j.i.ini}$ – initial rotational stiffness of the rotational spring i

$S_{j.i.slip1}$ –rotational stiffness of the rotational spring i valid after the slip of the upper interface

$S_{j.i.slip2}$ –rotational stiffness of the rotational spring i valid after the slip of the friction damper

$S_{j.ini}$ – initial joint stiffness

TolFun – fsolve function tolerance

TolX – fsolve function tolerance

U – vertical displacement at the upper done of the lost column

u_step – increment of vertical displacement

x0 – starting point of the iteration

$z_{eq\_}$ equivalent lever arm

z_i – lever arm of the rotational spring i

Table of contents

List of figures

List of tables

I INTRODUCTION

I.1. General

Inspite of the fact that the traditional weak beam – strong column- strong joint approach in seismic design had proven to be a reliable solution when designing Moment Resisting Frames, extreme events (e.g. earthquake Kobe 1995) have revealed its drawbacks. Therefore, the direction of the research shifted towards finding new solutions.

The possible solution was recognized in innovative type of connection, equipped with a friction damper, with the idea of using the friction damper as a primary dissipative element. The main idea is to develop connection capable ofdissipating all the seismic hazard energy without suffering any damage even is severe seismic conditions.

The innovative joint is being researched within the European project entitled "FREEDAM – Free From Damage Connections"which includes the participation of several international organisations: the University of Salerno (UNISA), the University of Naples (UNINA), the University of Coimbra (UC), the University of Liege (ULG),companies "FIP INDUSTRIALE" and "O FELIZ".

This Master thesis was proposed as a part ofproject "FREEDAM"

I.2. Objectives

The scope of the dissertation is to study the global behaviour of a 2D frame formed by connecting the beams and columns with the innovative joint equipped with friction damper when the frame is subjected to loss of a column. The part of the response when the membrane forces develop will be of main interest.

The work will concentrate on two main tasks in order to accomplish the above mentioned:

- Simulating the innovative joint behaviour by using the component method. New assembly model of the components forming the joint shall be developed and presented. The proposed assembly model should facilitate the introduction of the joint behaviour into the available analytical models.
- Implementing the developed joint model into the analytical procedure available for robustness assessment further to a column loss and studying the obtained results. Within this part a routine formed in programing language Matlab shall be modified so that it fits the analysed problem. The obtained result will be deeply analysed in order to confirm its validity and the validity of the program itself.

I.3. Structure of the dissertation

Five main chapters will be included within the master thesis. Chapter I contains general introduction explaining the origin of the studied problem, the objectives of the presented work and methods used in order to achieve them.

Chapter 2 presents the available state of the art related to the scope of the work. The development of Moment Resisting Frames from traditional one to the one equipped with the innovative joint studied within this work is included as well as the progress made concerning the analytical assessment of a frame subjected to a column loss. The existing analytical models are presented and the theoretical assumption they use are mentioned.

Chapter 3 is devoted to the description of the joints geometry and expected behaviour, relevant components are identified and then it is proceeded to development of a moment – rotational curve using the rotational spring model and development and validation of the moment – rotational curve using the 2-spring model approach. Significant calculations and consideration are presented.

In Chapter 4 implementation of the developed 2-spring model into the analytical procedure for assessing the global response of a structure further to a column loss is performed. The substructure modelling the behaviour of the global structure is described, the used equation are derived, the Matlab routine is briefly introduced, the modelled spring behaviour is explained and finally a parametric study is conducted and the results discussed.

Finally, conclusions and suggestions for future developmentare presented in Chapter 5.

II STATE OF THE ART

II.1. Beam-to-Column Connections in Moment Resisting Frames

Moment resisting frames(MRF) are widely used as structural systems in earthquake prone areas, due to their satisfying behaviour under seismic loading.

Traditional strategy for seismic design [Mazzolani, 2000] states that in case of a frequent earthquake, whose return period is comparable to the structures life cycle, structure must be design in such way that it remains in the elastic domain – the whole input energy must be dissipated by viscous damping. On the other hand, trying to keep the structure in the elastic range when subjected to rare and exceptionalseismic events which could happen once in 500 year or more would be very uneconomical. Therefore, in this case most of the earthquake input energy is dissipated by hysteresis, which leads to plastic deformationand damage of structural elements. Structural damage is accepted underthese circumstances, but only if compatible with the structure ductility and dissipation capacity, since the structural integrity must be maintained in order to avoid jeopardizing human lives and well-being.

Taking into the account the above mentioned, to remain in the elastic range structure needs to have sufficient lateral stiffness and strength. In particular, sufficient lateral stiffness is needed in order to assure that there will be no damage in non-structural elements, which is one of the demands of Serviceability Limit State (SLS). Conversely, for extra-ordinary seismic events the MRF has to be designed in such way that the energy is dissipated by the beam ends. To assure that the plastic hinges form at the beam ends,in which way we are able to utilize the greatest number of dissipative zones, sufficient over-strength needs to be provided for the beam-to-column connection and the column itself. The mentioned over-strength condition accounts for material variability and strain-hardeningassuring that the yielding will occur in the beam, not column or connection. Even though weak beam – strong column- strong joint approach is widely used and has plenty of advantages, like development of stable hysteresis loops and avoiding the soft-storey mechanism, the classical approach has also its disadvantages.

The main drawback of this approach is the fact that the plastic deformation and structural damage is the key for earthquake input energy dissipation, which, if a severe earthquake occurs, leads to high losses and refurbishment costs.

Another drawback is the necessity of over-strength elements which is not cost-effective, and demands additional elements and fabrication in order to guarantee the desired connection performance.

In order to evade the main drawbacks, a new strategy was introduces. The so-called strategy of supplementary energy dissipation or passive controlsuggested, among other things, friction dampers as elements reducing the lateral displacement for SLSand damage for Ultimate Limit State (ULS).

The door for this alternative approach was opened, and the subject became more interesting to the engineering society, when Eurocode 8 enabled the usage of partial strength connections, though only if previously checked by experimental test. Partial strength connections allowed the control of the bending moment being transfer to the column, and so, enabled the designer to prevent oversizing imposed by classical weak beam-strong column-strong joint approach.

Partial-strength connection became more interesting to researchers and Eurocode 8 [CEN 2004] introduces the concept ofdissipating the input earthquake energy within the elements of the connection. Double split tee connection emerged as a promising solution to be applied in the dissipative semi-rigid MRF because they can easily be replaced, which give a great benefit in terms of cost and sustainability [Iannone et al., 2011].

Latour et al. [2015] conducted a research of new type of beam-to-column connection with two friction dampers, one at each flange. After experimental tests, it was noted that despite the symmetry of the connection from geometrical point of view, the behaviourand displacements were not symmetric. This lead to the change of initial configuration, and friction damper was placed only at the bottom flange level. Connections are presented in Figure II-1. With the second configuration, under bending, the joint is forced to rotate around the upper T-stub and the energy dissipation is provided by the friction between lower beam flange and friction material layers.

In order to overcome the above presented drawbacks and for purpose of further improvement of dissipative beam-to-column connection, European project “FREEDAM” was proposed.

The aim of the project is to develop a new design strategy, whose goal is the design of connections able to withstand even the severe seismic event almost without any damage i.e. to develop a “Free from Damage Connection” which lead to the acronym “FREEDAM”.

The idea was based on the supplementary energy dissipation, but under new perspective. Unlike in passive control systems, the new proposed strategy is based on the use of the friction dampers not as additional dissipative element of primary structure, but as a way to substitute the traditional dissipative zones of MRFs i.e. the beam ends.

Beam-to-column connections are equipped with friction dampers which are located either at the bottom flange level or at the level of both flanges. Their role is to transfer the bending moment needed to fulfil the SLS requirement and to avoid slippage under gravity load. In addition, they need to provide earthquake input energy dissipation up to collapse prevention limit state, without any damage.

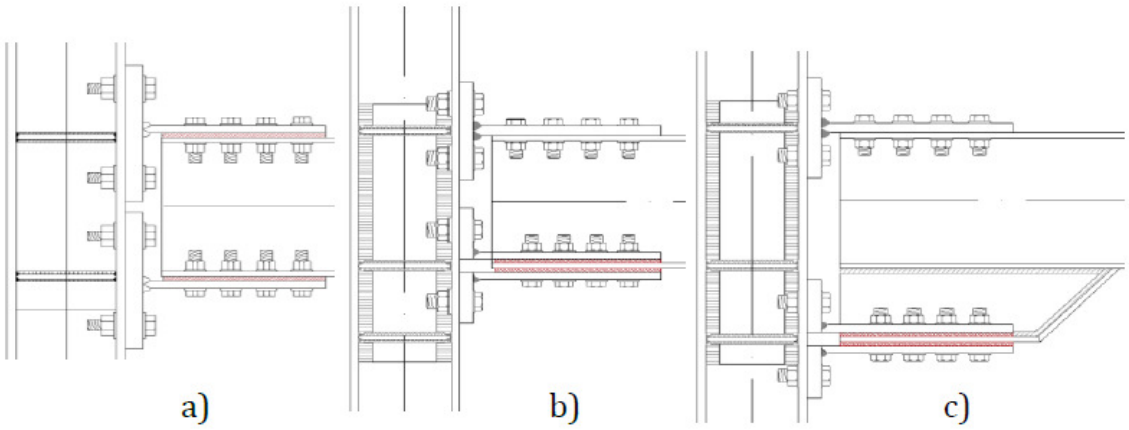

Figure II-1: Connection discussed: a) Connection with 2 friction dampers; b) Connection with one friction damper; c) Connection with a friction damper placed at the hammer-head flange [Lemos, 2015]

Friction damper is composed of L cleats, friction pads, and beam flange with slotted hole in order to allow displacement without any damage. This configuration enables high energy dissipation just due to the slippage of friction material. In addition, the costs are reduced for both connection and column, since we can control the bending moment transferred to the column.However, the main advantage of this kind of connection is that it works like a "Free from damage connection" up to the plastic rotation compatible with the stroke limit of the friction dampers.

It is important to emphasize one more important feature of the investigated connection, and that is its ultimate capacity. When the stroke end limit state is reached there is still some strength and rotation reserve. In case of a destructive event which demands exceeding the stroke end limit state, additional flexural strength and rotation are provided by activating new mechanisms – bolts and plates forming the friction damper subjected to shear and bearing, respectively.

Above mentioned property of the newly proposed joint should be very beneficial in term of robustness, in case of some exceptional loading condition like "loss of a column" scenario. Researching this feature will be the scope of the presented work.

II.2. Robustness

II.2.1. General

Maintaining the structural integrity under exceptional events started generating more and more interest among researchers and engineers in the last decades as catastrophic events, both natural (tsunami, hurricane…) and one caused by mankind directly (terrorist attack, car crashing into a building…), underlined the importance of the before mentioned which is the key to avoiding casualties, limiting and reducing loses in this exceptional situations.

Eurocodes and other national design codes demand ensuring structural integrity through appropriate measures, but in most cases there are no practical guidelines how those measuresshould

be provided. [Demonceau, 2007] Global design approaches like the activation of the alternative load path or the key element method were firstly introduced in British standards, and then more or less the same ideasspread to other national codes.One way of guaranteeing the structural integrity is to ensure appropriate robustness which is defined as the ability of the structure to remain globally stable in case of the event leading to local damage.[Huvelle C. et al.]

University of Liege gave a great contribution to the investigation of structural robustness being involved in projects like "Robust structures by joint ductility" [Kuhlmann U. et al. 2008] and conducting several numerical, experimental and analytical investigations, researches and PhD thesis.

The investigations done at University of Liege regarding robustness are mainly devoted to the exceptional event "Loss of a column in a building frame". In particular, two PhD theses[2], [Luu, 2008] were devoted to the development of the first analytical model for the prediction of the response of a frame subjected to a column loss situation, both before the mechanism is formed and after when the membrane forces, due to significant second order effects, start to develop.

Within the present work, the response of a frame equipped with the innovative joint containing friction damper shall be studied by implementing the joint characteristics into the developed analytical model.

The following subchapter will be dedicated to the explanation of the general concept used for the development of the analytical approach and the evolution of the analytical model from the simplest to the most advance one.

II.2.2. Development of analytical models

The analytical models discuses here are related to the prediction of the frame response in case of exceptional event occurring, in particular, loss of a column situation.

As stated in the article "Complete analytical procedure to assess the response of a frame submitted to a column loss" [3], when we have a frame subjected to a column loss situation we can divide the frame in two parts (Figure II-2a):

- The directly affected(DAP) part containing all the beams, columns and beam-to-column joints located above the lost column
- The indirectly affected(IAP) part which contains the remaining elements (storeys under the lost column and the lateral parts) forming the structure

The evolution of the compression force in the lost column is illustrated in Figure II-2b. As presented, in case of a column loss, we can distinguish three main phases:

- Phase 1: The event hasn't started yet and the column is supporting the loads coming from the floors above. It is assumed that there is no yielding and that the structure responds fully in the elastic range.

- Phase 2: The event occurred and the column is progressively losing its axial resistance. Two sub-phases can be distinguished[2]:
    - From point (2) to (3): The directly affected part gives a fully elastic behaviour until the first plastic hinge is formed at point (3).
    - From point (3) to (4): Change of the slope of the curve occurs each time a new plastic hinge is formed within the directly affected part until finally reaching the point (4) where a complete plastic mechanism is formed.

- Phase 3: The plastic mechanism is formed and large deformations are noted, inducing theprogressive development of membrane forces in the beams of the directly affected part. At point (5) the column is completely lost. Reaching point (5) would mean that the loads previously supported by the column are successfully transferredremainingpart of the structureand that we have avoided thecollapse.

Indirectly affected part has a role of providing lateral support to the developing membrane actions.The stiffness of the indirectly affected part governs the intensity of the catenary actions developing in the directly affected part. The higher the stiffness, the higher the membrane forces developing. In extreme case, no membrane forces will develop if there is not lateral stiffness provided by the indirectly affected part.

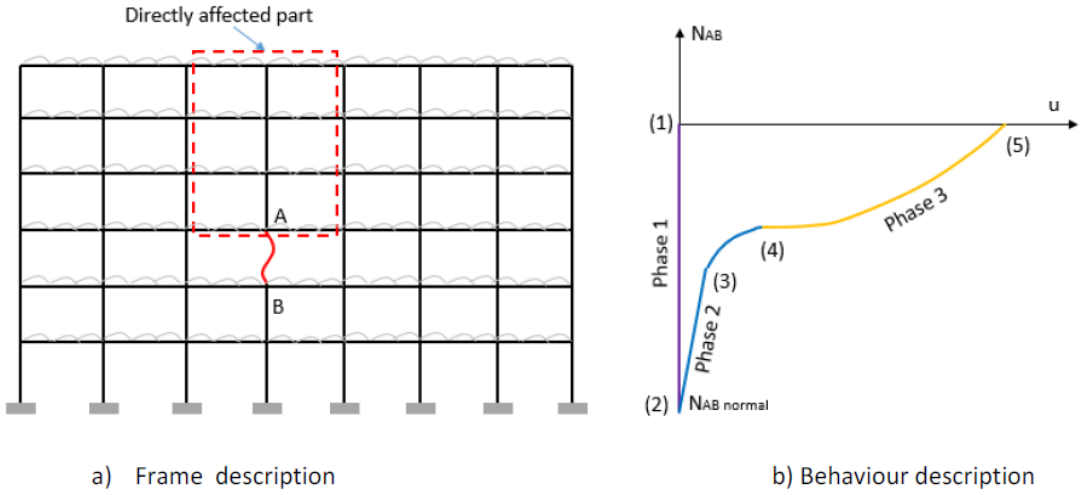

Figure II-2: Behaviour of a frame submitted to a column loss [3]

The behaviour of the structure when the event occurs, namely, Phase 2 and Phase 3, are of main interest when assessing robustness. Behaviour of the structure in these two phases can be simulated by assessing the behaviour of a structure presented in the Figure II-3; frame without the lost column subjected to a concentrated load **P** at the upper node of the lost column (node A). [3] The concentrated load **P**represents the force previously supported by the column which is transferred to the remaining structure due to the column progressive collapse.

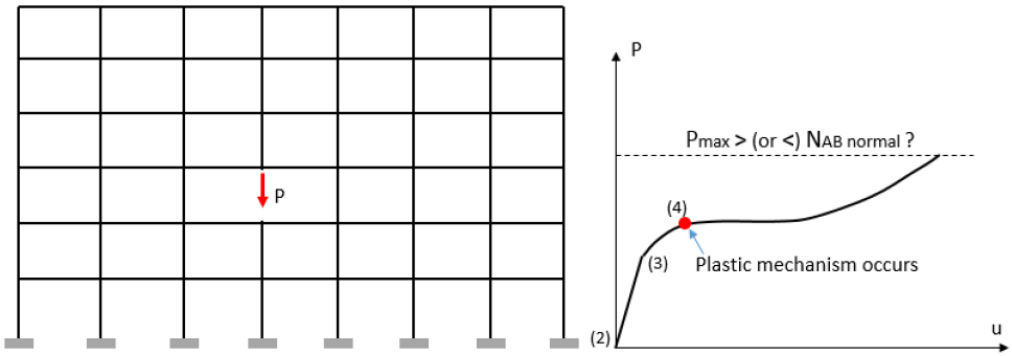

Figure II-3: Structure used for simulating the loss of a column [3]

Analytical models have been developed based on the problem formulation presented in the Figure II-3. The objective of the analytical models would be to estimate the redistribution of the load during Phases 2 and 3, and checking whether point (5) could be reached. In order to reach the mentioned point sufficient ductility of the deforming elements is needed as well asthe resistance from the remaining structure in order to sustain the membrane force developing. Robustness is required from the part of the structure not directly affected by the exceptional event.

II.2.3. Demonceau model

The first analytical model dedicated to the assessment of the response of a two-dimensional steel or composite structure was developed by Demonceau J. F., as part of his PhD thesis [2]. The main idea is to isolate a part of a frame and analyse the obtained simplified substructure.

It is important to note that the model is based on a static approach, and therefore, not accounting for dynamic effects. The model is focused on the Phase 3, when the catenary actions start to develop due to significant second-order effects.Therefore, rigid-plastic analysis had been used for this model.

After conducting parametrical studies, in was concluded in the [2] that the membrane forces developing in the beams just above the lost column are significantly more important the ones developing in the other beams of directly affected part. Consequently, it was decided to investigate only the behaviour of the lower beam of the directly affected part.

The isolated substructure is presented in (Figure II-4). To be able to isolate the substructure, several parameters had to be defined:

- $\mathbf{K_H}$ – the stiffness of the surrounding structure which is simulated by a horizontal spring. In this model it was assumed that the indirectly affected part remains elastic during whole phase 3. This represents a simplification since the IAP can yield during this phase.
- $\mathbf{F_{rd}}$ – the maximum load coming from the DAP that IAP can sustain;
- Distributed and concentrated load that the system needs to withstand.

It was later shown that the uniformly distributed load does not influence much the response during Phase 3. Therefore it was neglected, which made the equations used much simpler. For more information refer to [2].

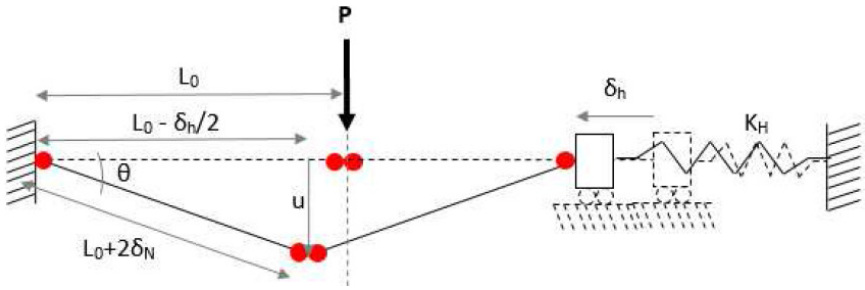

Figure II-4: Substructure of Demonceau [3]

During phase 2, the plastic hinges are subjected to bending moments only. After the plastic hinges areformed (beginning of Phase 3) normal forces, in particular, tension forces start to develop submitting the hinges to the interaction of **M** and **N**. In extreme cases, at the very end of Phase 3, they could be loaded only by **N** force.

That being said, to be able to use the presented model one needs to define the M-N interaction curve for both hogging and sagging bending in the plastic hinge, which can develop in the beam or in the joint.Axial stiffness of the plastic hinge submitted to both bending and axial force, named $\mathbf{K_N}$, is a necessary parameter used to define the relationship between the **N** force and plastic elongation of the hinge $\boldsymbol{\delta_N}$.

It is demonstrated in [2] that the substructure model gives results which accurately reflect the global frame behaviour during Phase 3 in case of a column loss if the parameters $\mathbf{K_H}$ and $\mathbf{K_N}$ are defined correctly.

Table II-1 presents the unknowns and equations in the substructure of Demonceau. For further information about the input data or the model itself, please refer to [2] and [3].

Table II-1: Unknowns and equations of the Demonceau model [3]

Unknowns	Equations
u	u = input data
θ	$\sin(\theta)= u/(L_0+2\ \delta_N)$
δ_h	$\cos(\theta)= (L_0- \delta_H/2)/(L_0+2\ \delta_N)$
δ_N	$\delta_H = F_H/K_H$
P	$\delta_N = N/K_N$
N	M = f(N) ([1] or [17])
M	$-0.25P(L_0-0.5\delta_H)+0.5F_Hu+2M=0$
F_h	$N = F_H\cos(\theta)+0.5P\ \sin(\theta)$

At the time being, no analytical procedure was available for definition $\mathbf{K_H}$ and $\mathbf{K_N}$so the values obtained experimentally or numerically had to be used. Further investigations lead to the analytical definition of both parameters leading to the complete analytical approach.

II.2.4. New approach

As previously stated for improving the existing model analytical definition of $\mathbf{K_N}$, parameter defining the behaviour of the yield zone in the DAP, was needed. Yield zones can occur in the beam or in the joint, if the partial strength joint is used. For both cases, the approach for the derivation of the new analytical method remains the same, with the exception of the hinge length, which in casethe hinge forms in the joint is equal to 0. Indeed, if the yield zone is located in the joint, which is assumed to be very short comparing to the length of the beam, the hinge length can be neglected as stated in [3].

A range of numerical tests have been conducted in order to understand whether $\mathbf{K_N}$ was a local parameter, depending only of cross section characteristic, or there is some coupling between the hinge behaviour and the global structure. The analysis was performed at University of Liege, using the homemade program FINELG. The results have shown that in addition of the dependence of$\mathbf{K_N}$ to the cross section characteristic, it also depends on the structure in which the hinge is developing. Therefore, a new definition of the $\mathbf{K_N}$was needed in order to consider the proven coupling.

The new approach for modelling $\mathbf{K_N}$ was firstly defined for the case of plastic hinge forming at the extremities of the beams and later extended for the case where the hinge forms within the joint. The hinge was modelled as a set of 6 parallel springs, assuming that the sections at the extremities of these springs remain straight, where each spring represents a part of a cross section. This is nicely presented in Figure II-5.

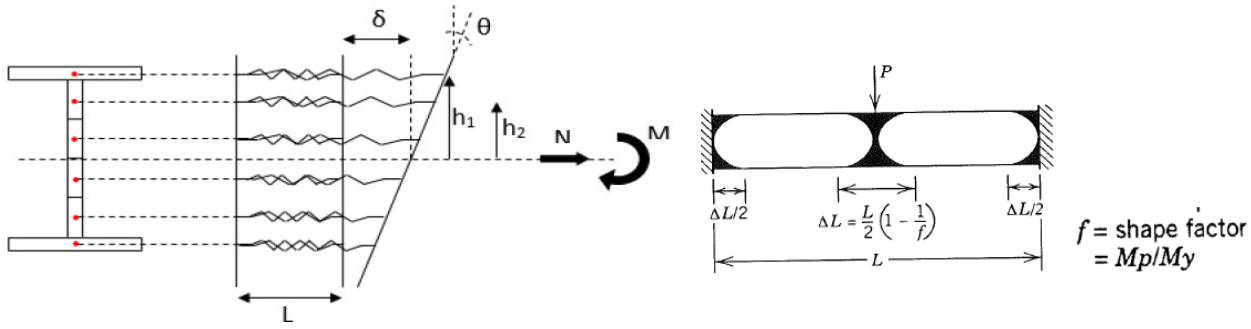

Figure II-5: The hinge model [3]

For fully defining the analytical model used for prediction of K_N, definition of plastic hinge length was required. The length was defined according to Figure II-6 [5]

Figure II-6: Plastic hinge length [5]

As it had been proven that there is coupling between the $\mathbf{K_N}$ and the global structure, the local hinge model was implemented into the substructure of Demonceau, forming a new substructure model presented in Figure II-7.

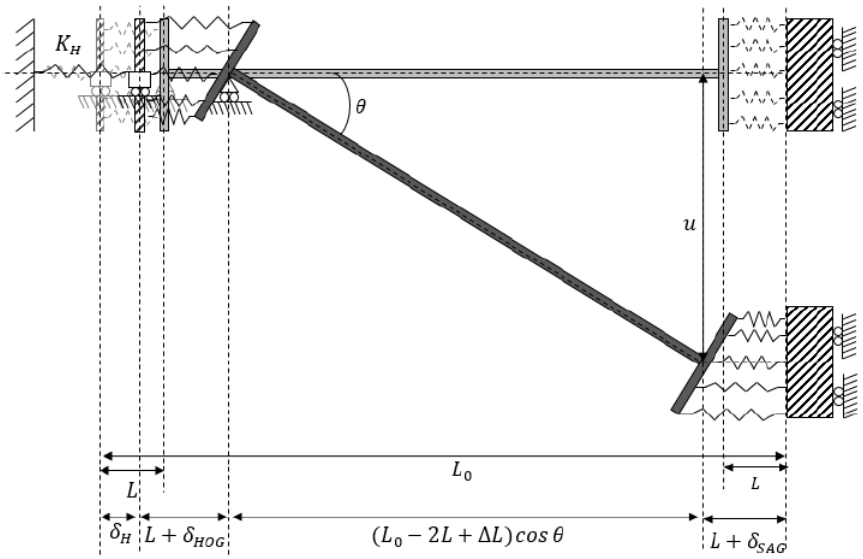

Figure II-7: New substructure model [3]

The main advantage of the above presented model is that by simulating the hinge by parallel set of springs we do not need any more to define an M-N resistance curve, nor is it necessary to explicitly define $\mathbf{K_N}$ because of all of this is included in the definition of the springs. By properly defining the properties of the springs, stiffness and resistance in particular, and accurately modelling their behaviour when subjected to the loss of a column situation, we can obtain satisfying results of the structure response.

If the hinge forms at the beam extremity, the spring model can be obtained by dividing the cross section area at the place of a hinge formation into several parts, and calculating the spring properties by using expressions $F_{rd.i} = A_i f_y$ and $K_i = EA_i/L$, where $\mathbf{A_i}$is the area of the part **i**and **L** is the length of the hinge considered, as presented in the [3].

If the hinge, on the other hand, forms in the partial strength joint, one spring could represents a component (or set of components) determined by component method recommended in EN 1993-1-8 for the characterization of joint properties. In that way, the same general approach could be used.It should be underlined that defining the behaviour of the springs in this case would be a bit more complex, due to the particularity of each component. This problem will be addressed later on in Chapter IIIand Chapter IV.

The presented approach is general and it can be applied for modelling the response of the substructure regardless of the place where the plastic hinges form (beam extremity or joint). The number of springs can also be modified to fit the user needs or the specificity of the problem analysed. It should be noted that in the present model $\mathbf{K_H}$ is still an input data.

The following table presents equations and unknowns needed for using the new substructure model. These equations will later be used and modifiedto fit a concrete problem – behaviour of a frame equipped with innovative partial strength joint further to a column loss.

Table II-2: Unknowns and equations for the new substructure model [3]

Unknowns	Equations
u	u = input data
θ	$\sin(\theta)=u/(L_0-2L+\Delta_L)$
δ	$\cos(\theta)=(L_0-2L-\delta_H-2\delta)/(L_0-2L+\Delta_L)$
δ_H	$\delta_H=F_H/K_H$
Δ_L	$\Delta_L=F_H(L_0-2L)/(EA)$
M	$M=\sum F_i h_i$
F_H	$F_H=\sum F_i$
F_i (i=[1:6])	$Fi=f(\delta_i)$
δ_i (i=[1:6])	$\delta_i=\delta+h_i\theta$
P	$-P(L_0-\delta_H)+F_Hu+2M=0$

The equations presented in Table II-2 can be solved using a mathematical solver, like the one Matlab programing language can provide. Matlabhad been used at University of Liege for performing most of the calculations of this type. It was decided, due to the fact that some programs based on this concept were made in Matlab and therefore they could be used asan example, that Matlab shall be used in this work as well.

II.2.5. The complete analytical model

The substructure presented earlier, composed by only the lower beam of the directly affected part and one horizontal spring simulating thebehaviour of the surrounding structure is only valid if the compression force in the column just above the lost one is constant during the whole Phase 3, which is not always the case. Important coupling effects develop between the storeys of the DAP and also between DAP and IAP and they should be taken into account [3]. That being so, a complete analytical model had been developed considering all the coupling, both of the storeys of the directly affected part and the coupling of the directly and indirectly affected part.

The substructure of Demonceau was generalized for all the storeys of the DAP as shown on the Figure II-8, while the plastic hinge was presented by springs in parallel. The influence of the IAP in taken into account by placing a horizontal spring at each extremity of the newly defined structure. Horizontal springs simulating the IAP are assumed to behave fully elastic.

The Figure II-9 shows how the flexibility matrix is defined and how the values forming the mentioned matrix are obtained.

*The horizontal displacement δ_{Hi} at the storey **i** is defined as follows: $\delta_{Hi}=\Sigma\, s_{ij} F_{Hj}$, in which the coefficients s_{ij} form the flexibility matrix of the indirectly affected part (i.e. s_{ij} is the horizontal displacement at the level i when a unitary horizontal force acts at the level j) and F_{Hj} is the horizontal load applied at storey **j**. In Figure 17, $s_{l,ij}$ $s_{r,ij}$ are respectively the displacements of the left ("l") and the right ("r") sides of the indirectly affected parts, then $s_{ij}=s_{l,ij}+s_{r,ij}$.[3]*

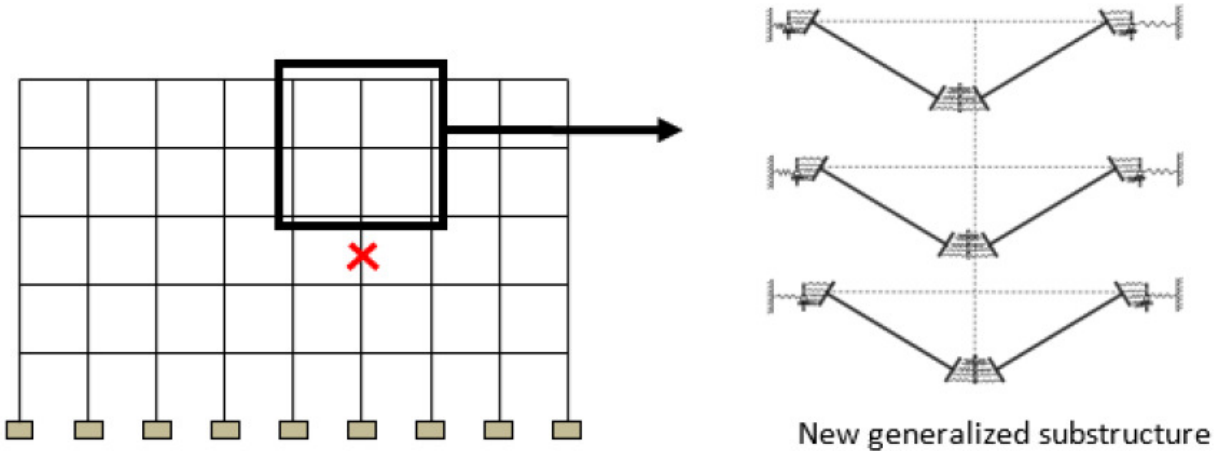

Figure II-8: New substructure [3]

The model presented in the Figure II-8had been validated by comparing with numerical results and it was concluded that the model gives sufficiently accurate results. For more information, input data, used equations please refer to the article of Huvelle C. et al. [3], where the problem is discussed in more detail.

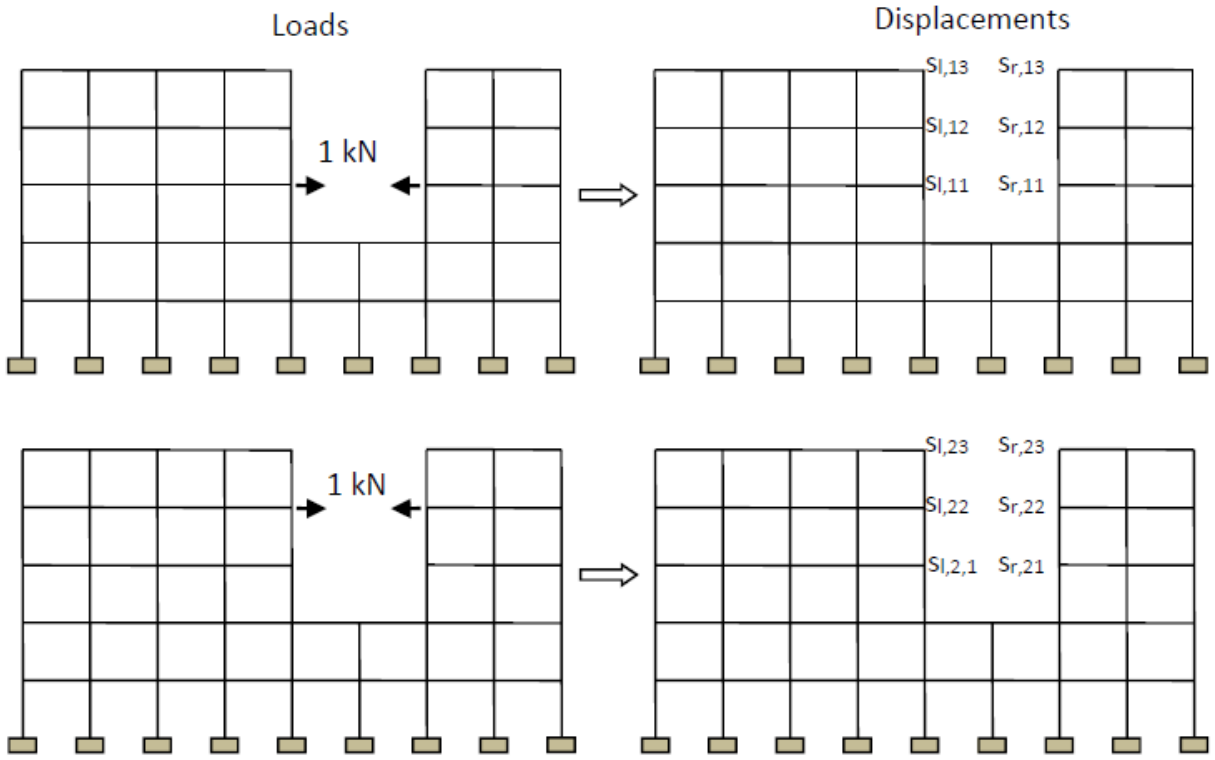

Figure II-9: Definition of the flexibility matrix [3]

II.3. Conclusions

The classical weak beam-strong column-strong joint approach in MRF provided a great way of dealing with seismic loads for many years, but the hazardous events during that time pointed out its weaknesses. In order to overcome the drawbacks of the traditional approach, new ideas and researches were needed. The "FREEDAM" project emerged bringing an idea of a new type of connection, equipped with friction dampers as dissipative elements, completely substituting the traditional dissipative zones.

Benefits coming from the new joint configuration:

- avoiding over-sizing by controlling the bending moment transferred to the column
- ability to dissipate large amount of earthquake input energy without taking damage
- expected enhanced behaviour of the structure interms of robustness(in case of exceptional events due to the strength and rotation reserve provided by activation of new failure mechanisms after reaching the stroke end limit state)

The last mentioned feature of the innovative joint could play an important role in placing this type of connection in front of others, as more and more attention is given to the subject of structural robustness in the recent years.

Developed analytical models for predicting the response of a frame submitted to loss of a column were presented, showing that the designer now has the possibility of calculating the frame response using only analytical expressions, avoiding preforming costly experiments.

By properly characterizing the joint where the plastic hinge forms, which shall be shown in the next chapter, analytical methods can be used to predict the behaviour of a frame equipped with the innovative joint further to a column loss.

III CHARACTERIZATION OF THE "FREEDAM" JOINT

III.1. Introduction

In the previous chapter it has been shown that analytical models for assessing the behaviour of a frame subjected to a column loss exist and that they give satisfying results if the springs are able to simulate the behaviour of the hinge accurately.

The present chapter aims at developing an effective spring model of the innovative joint which will then be implemented into the analytical model in order to simulate the behaviour of a frame further to a column loss.The following sequence of actions shall be used in order to achieve the before mentioned.

Firstly, the geometry and the expected behaviour of the joint shall be introduced and discussed.

Secondly, using thecomponent method recommended by the [6], the relevant components activated in both sagging and hogging bending will be defined and the characterisation of the joint components shall be performed.

By proper assembly of the components, a rotational spring model simulating the monotonic behaviour of the joint will be formed and compared with experimental data obtained from University of Salerno. The developed model shall beused later on as a reference for the validation of the following model.

Further on, the assembly of the joint components will be done is such way that we obtain a two-spring model, made of a pair of springs working in parallel, which will accurately simulate the monotonic behaviour of the joint in reality . Each of two horizontal springs will represent the behaviour of the whole set of components located in tension or compression. Therefore, the behaviour of the tension and compression zone of the joint shall both be modelled and represented by only one spring.

The newly developed 2-spring model will then be validated by comparing with results obtained from the reference model.

The above mentioned is performed with the idea to obtain a validated 2-spring model which can easily be implemented into the analytical routine.

III.2. Description of the joint

The connection presented here below was designed at University of Salerno, one of the partner Universities working on the "FREEDAM" project. Since the beginning of the research, several configurations have been considered. The joint configuration used in the present work was chosen

since, at the present time, it is believed that the following configuration (Figure III-1) will not suffer many changes in the future, at least not from the conceptual point of view.

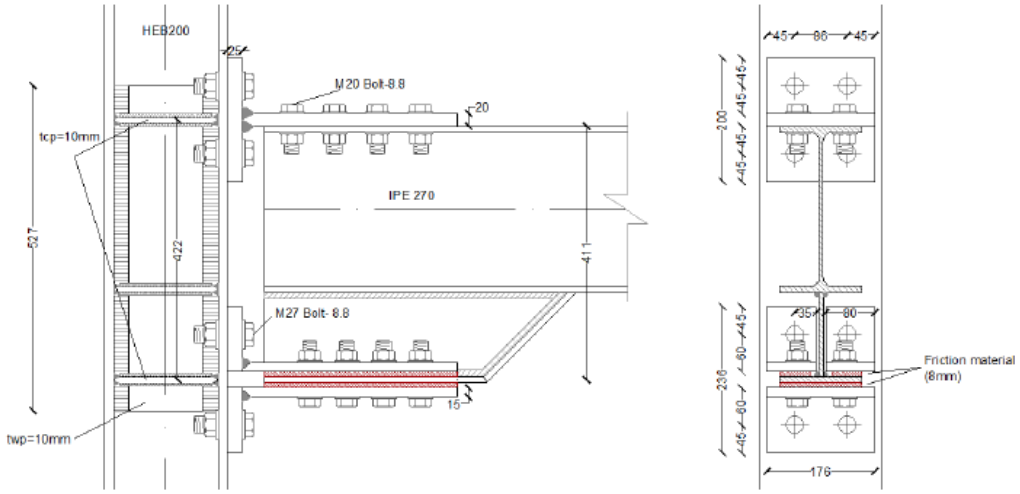

Figure III-1: Geometry of the specimen TSJ-H-SA300-260-CYC 13 (CYC 13) [1]

The configuration presented in the Figure III-1 came as a modification of previous specimen designed at University of Salerno, named TSJ-SA300-320-CYC 12 (CYC 12, for details refer to [1]). The main difference between CYC 13 compared to CYC 12 is the lever arm which was increased in case of CYC 13 by placing the friction damper on the "hammer head" added to the lower flange of the beam. This gave the upper hand to the CYC 13 configuration since in that case for the same value of friction force, due to the larger lever arm, we can obtain larger bending moment resistance.

The friction damper is formed, as presented in the Figure III-2, by inserting two 8mm steel plates, sprayed with a 300 μm think layer of aluminium in order to enhance the friction coefficient, in between the hammer head flange and L cleats. All the metallic elements are made out of steel S275. The two aluminium covered plates are connected to the L-stubs by bolts, passing through a regular bolt hole. This allows no slippage between them. The hammer head flange contains a slotted hole where the bolts pass, allowing the slip in the case when the slippage resistance is exceeded.

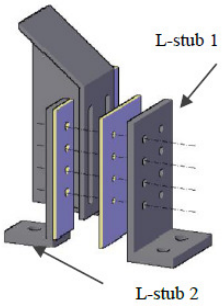

Figure III-2: Scheme of the friction damper [1]

The joint is connecting the beam IPE

270 and the column HEA 200, and the connection is formed on one side by bolting the web of a T-stub to the upper beam flange and the T-stub flange to the column flange, and on the other side by bolting the L-stubs forming the friction damper to the beam and the column. Both the beam and the column are made of steel S275.Bolts M27 were used in order to attach steel elements to the column, while bolts M20 were used to connect the elements to the beam flanges, both made out of steel class 8.8. The geometry of the T-stubs and L-stubs is presented in the Figure III-3 and Figure III-4, respectively.

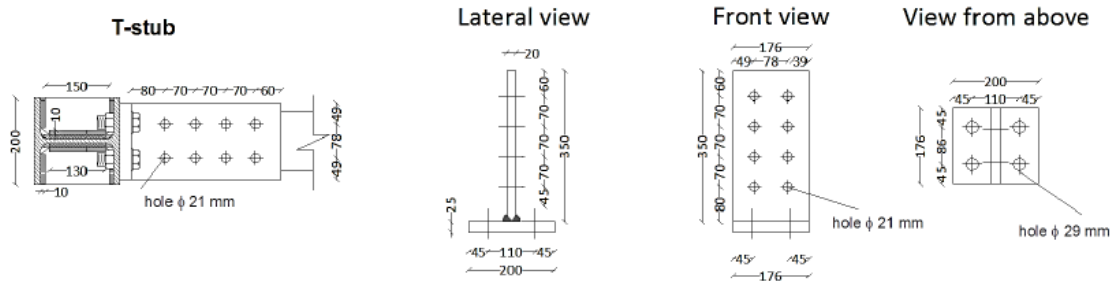

Figure III-3: Geometry of the T-stub [1]

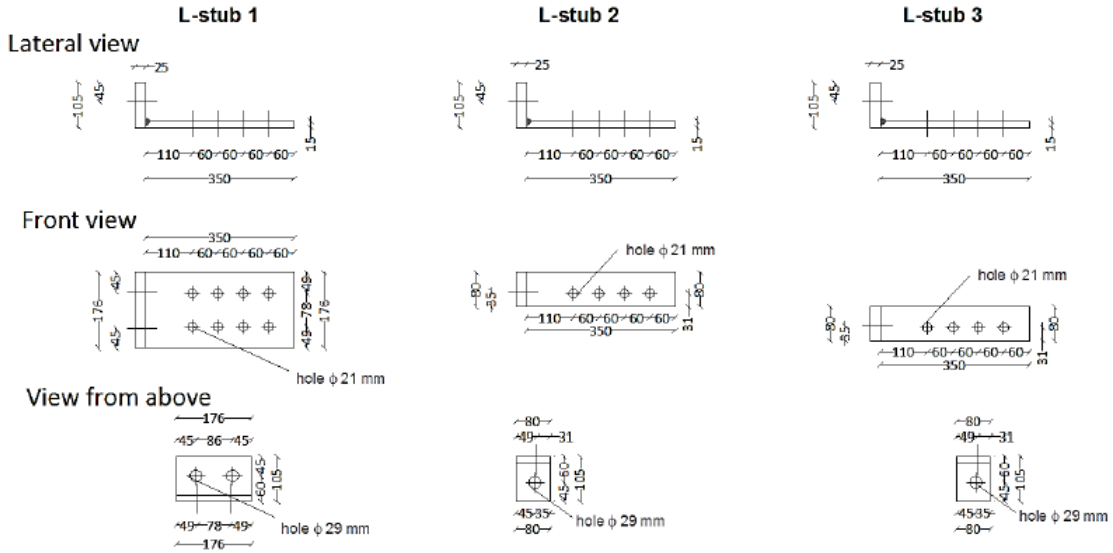

Figure III-4: Geometry of the L-stubs [1]

The joint is also equipped with web stiffeners and continuity plate designed in such way that the expected load could be safely withstand and transferred. More details can be found it the thesis of Lemos A. [1].

The main idea of this innovative joint is to dissipate energy using the friction provided by 2 slippage areas, namely, areas between the hammer head flange and aluminium coated steel plates. The expected behaviour of the joint shall be presented in the form of an M-Φ curve (Figure III-5) and discussed.

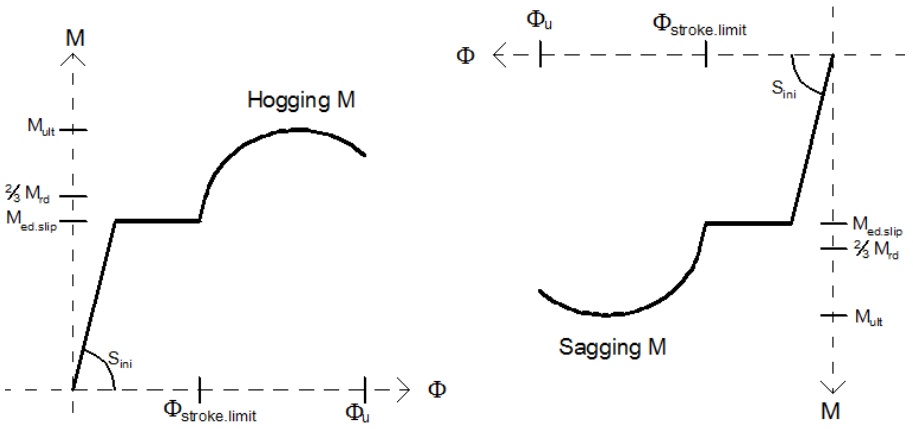

Figure III-5: Expected behaviour of the innovative joint under hogging moment

In the initial stage, namely before reaching the slip resistance, it is expected that the joint response is linear where the linearity factor would be the $\mathbf{S_{.ini}}$ – initial stiffness.

After reaching the slip resistance of the damper, the slip should occur.The slip is characterized by the rotation increasewithout any increment of the moment until reaching the stroke end limit, when the bolts hit the end of the slotted hole. When the stroke end limit is reached, new mechanisms are activated, namely the shearing of the bolts and the bearing of the plates, providing the additional strength and rotation to the joint.

It is reasonable to assume that after the activation of the new mechanism, the relation between bending moment and rotation will still be linear for some time. This is expected due to the fact that this connection was designed as a free from damage connection for SLS. The previous implies that, at the time when the slip resistance is reached, none of the elements initially activated in the load transfer should have reached 2/3 of their plastic resistance, which is the limit where yielding is expected. If the yielding of some element happens before we reach the slip resistance, that element will suffer some damage, and the connection could not be considered as free from damage.

After reaching the 2/3 of resistance of the joint, yielding of the elements transferring the load will commence, providing us with a relation between bending moment and rotation which is no longer linear. When the design resistance of the joint is reached, the increment of the rotation should be much higher for the same increment of bending moment, until reaching the ultimate bending resistance leading to progressive yielding and plastic rotation of the joint and, finally, failure.

The behaviour of the joint should be conceptually the same both for hogging and sagging bending, but due to the asymmetry of the joint the values of stiffness and resistance will be different. The joint shall be modelled using the component method having in mind the expected behaviour presented above. The behaviour of the joint shall be addressed in more detail in the following paragraphs.

III.3. Component method

Component method represents a widely used analytical solution for characterisation of joints in term of stiffness, resistance and ductility, since experimental and numerical approaches are not very practical for the designer.

This analytical procedure enables a prediction of the joint response based on the knowledge of the mechanical and geometrical properties of the "joint components", as stated in [Jaspart,Weynand 2016]. Component method represents a general analytical approach which can be used for both steel and composite joints, regardless of the geometrical configuration and type of loading. The approach used in the component method is to consider each joint as a set of individual basic components.

The application of the mentioned method requires the following steps:

- Identification of the active components relevant to the joint being considered
- Evaluation of the stiffness and/or resistance characteristics for each of the basic components
- Assembly of the components in order to evaluate the characteristics of the joint (strength, stiffness, full deformability curve)

Identification of the active components depends on the type of load that the joint is subjected to. Depending on the load transfer through the joint elements, the components active in the case of sagging and hogging bending can be different.

The assembly procedure is a step where the mechanical properties of the joint are derived from those of the individual basic components. That requires to know how the internal forces are distributed within the joint components. In fact, the external loads applied on the joint are distributed between the components according to the stiffness and resistance of the components at each loading step. Therefore, it is important to underline that only the monotonic behaviour of the joint shall be assessed within this work.

In the present work, firstly, component method shall be used in order to define the moment – rotation curve of the joint, for both hogging and sagging, using a rotational spring model. The obtained result shall then be used to verify the two-spring model solution.

III.3.1. Relevant components and rotational spring model

In order to assess the full joint behaviour under monotonic bending a rotational spring model shall be formed. The model will be obtained by cutting the connection at 3 relevant cross sections as shown on the figure, and simulating the components activated in the load transfer for each cross section by springs.

It is expected that the presented model will provide us with high result accuracy. The reason we can expecthigh accuracy comes from the fact than by making several cuts we have accounted for

the lever arm difference between different cross sections and therefore we are able to obtain more precise values of the points characterizing the joint behaviour.

The behaviour will be assessed separately for hogging and sagging bending moment since the connection is not symmetric. Depending on the external load, the components activated in in one case will differ from the components activated in the other case and that needs to be taken into account.

III.3.1.1. Rotational spring model – hogging bending moment

In order to form the mentioned rotational spring model, we firstly need to identify the components activated, this time, in case of hogging bending.

The model of main components activated in case of hogging bending,presented in the Figure III-7, is formed by analysing the load transfer sequence. Hogging bending can be presented as a pair of forces of opposite direction acting at a certain distance – lever arm. The force acting on the upper level of the connection in this case will be tensioning the components, while the opposite force will act as compression force. Therefore, upper end of our connection is in tension and the lower end in compression. In order to transfer the external load through the joint, tension force in the upper part, compression force in the lower part, joint components are activated.A brief explanation of the symbols used to present the components shall take place and them we will address the process of forming of the model.

Going through the literature [7] is was concluded that for the elements whose behaviour respect the rigid-plastic force-dilatation(F-δ) law, the symbol as the one used in this case for CWS (like the symbol used for a damper in dynamics) is used. For elements having linear-plastic behaviour, the classical spring symbol is used.

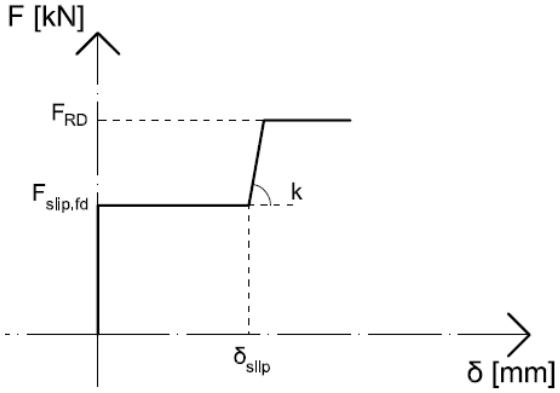

Figure III-6: Expected behaviour of the friction damper

Friction damper is an innovative component which was not referred in the component method up to now and therefore, there is no guidance how to consider it as a component in the Eurocodes.Its behaviour does not belong to any of the two mentioned cases, but it could be presented as a combination of a rigid-plastic (where the plateau would actually be caused by the slip) and a linear-plastic law (when the new elements are activated). Taking into consideration the before mentioned, no special symbol is available for representing the friction damper.

The behaviour of the friction damper is described in the Figure III-6. Initially, the stiffness of the friction damper is practically infinitive, since there should be no displacement i.e. no slip before reaching the $\mathbf{F_{slip.rd}}$. The value of $\mathbf{F_{slip.rd}}$corresponds to the slip resistance of the friction damper. When $\mathbf{F_{slip.rd}}$is reached the slip occurs leading to the increase of displacement without any change

of the value of the force, until reaching the stroke end limit which corresponds to δ_{slip}. When the bolts forming the friction damper reach the end of the slotted hole i.e. when we reach the δ_{slip}in the discus figure, new components activate providing additional stiffness. This provide us with additional rotation and resistance of the component. After reaching the design resistance of the component $\mathbf{F_{RD}}$ progressive deformations are expected with a small increment of force, leading to the collapse. In the presented model of the friction damper, for the sake of simplicity, the increment of the force after reaching the $F_{RD}$is neglected and therefore the ultimate resistance is not considered.

Next couple of paragraphs will be dedicated to the assembly of the componentsand modelling the joint behaviour by using the component method. The formed spring model will be analysed section by section. As visible in the Figure III-7, 3 cuts are made, 2 of them at the level of the connection and one level of the column panel in order to adequately "catch" the behaviour of the joint. The main idea is to recognize and characterize the components activated in the load transfer at the level of each section, then form a rotational spring for each of 3 sections, and finally combine the obtained rotational springs into one rotational spring which would represent the behaviour of the joint. The model will be analysed in the following section by section.

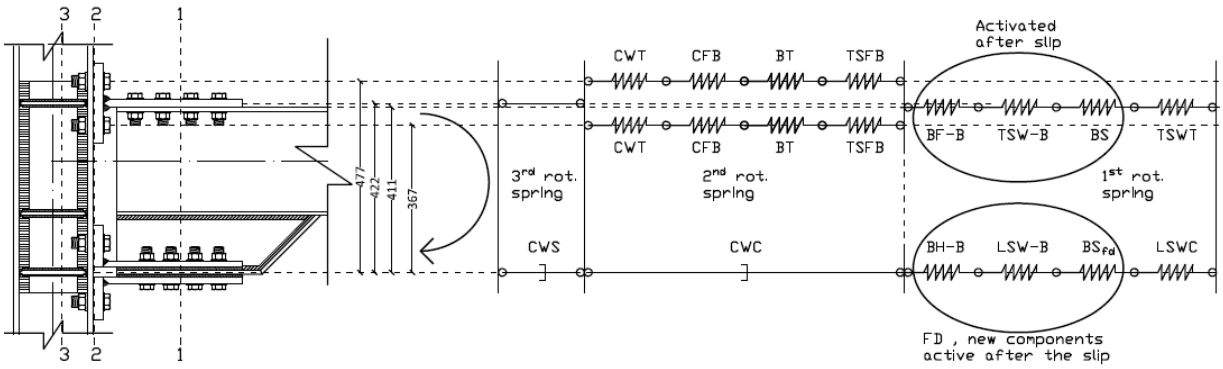

Figure III-7: Main components activated in case of hogging bending – horizontal spring model

- The first cut (1-1) is made at the connection of the beam to the T-stub and friction damper. Looking at the load transfer sequence in the tension part we can see that the tension force is transferred from the beam by activating the T-stub web in tension (TSWT). The connection between the T-stub and the beam is realized by preloaded bolts which means that after the tension forces reaches the slip resistance of the upper interface, new components shall be activated. The load will then be transferred by additional 3 components, namely,shearing of the bolts (BS), T stub web in bearing (TSW-B) and beam flange in bearing (BF-B). The same analogy can be used for explaining the behaviour as the one used for the friction damper, with the difference that the slip is very small and practically negligible.

  In the compression part we have a similar situation. A new element, namely, the friction damper (FD) and components forming it will be responsible for the load transferring. Eurocode or other literature [7] currently available does not present any data how to deal with this

innovative element nor how to represent it. Therefore the behaviour of the damper will be analysed by breaking it apart to more simple components. The same analogy will be used as in previous paragraph to describe the load transfer and component behaviour.

The friction damper is designed so that it remains rigid until reaching its slip resistance. Therefore, before reaching the slip resistance the load is transferred only by L-stub web in compression (LSWC). After the slip resistance of the friction damper is reached the slip occurs. The bolts forming the friction damper slide until reaching the end of the stroke. At that point, in order to transfer a higher force, new components forming the damper are activated. The load is transferred by bolts in shear ($BS_{.fd}$), L stub web in bearing (LSW-B) andbeamhammer head flange in bearing (BH-B).

The lever arm for this connection is taken as the distance between the slip interfaces, as shown on the Figure III-7.

- The second cut (2-2) in made at the level of the flange of the T and L stubs. The tension force is transferred from the T stub web to the T stub flange, activating itin bending (TSFB). The further transfer of stresses in done through bolts in tension (BT), activating the column flange in bending (CFB) and finally the column web in tension (CWT).
  As presented on the Figure III-7, there are 2 rows of each component forming the 2nd rotational spring. The lever arms to each spring row is taken as the distance from the compression centre to the axis of the corresponding bolts in tension.

  The compression force is transferred in this part only by activating the column web in compression(CWC) which is located at the centre of compression.

- The 3rd rotational spring refers to the behaviour of thecolumn panel activated in shear (CWS). The lever arm considered represents the distance from the centre of compression to mid thickness of the T- stub web.

It is now necessary to calculate the components characteristics, namely, resistance and stiffness. This was done as part of thethesis ofLemos A. [1], according to the recommendations presented in the Eurocode 3-1-8. The values obtained will be presented in the following table.

After having obtained the characteristics of the components, presented in the Table III-1, the behavior of the joint can be described.

In the beginning, there is no slip neither of the friction damper nor for the interface between the T-stub and the upper beam flange.As the force raises and reaches the value of $F_{rd.slip.1}$=186.6kN, the first slip occurs at the upper interface.

Table III-1: Stiffness and resistance of the components under hogging bending moment

Hogging bending moment					
Component	Acronym	F_{RD} per row [kN]	F_{RD} total [kN]	Coef from EC3-1-8	k_i [mm]
Components in tension					
Bolts in tension	BT	660.96	1321.92	k10	10.85
T-stub flange in bending	TSFB	414.51	829.02	k5	13.58
Column flange in bending	CFB	462.84	925.68	k4	32.86
Column web in tension	CWT	482.8	965.6	k3	9.97
T-stub web in tension	TSWT	x	968	k9	44
New components activated after the slip of the upper interface after $F_{rd.slip.1}$ =186.6kN is reached					
Bolts in shear	BS	x	1763	k11	6.1
T-stub web in bearing	TSW-B	x	3040.7	k12	9.21
Beam flange in bearing	BF-B	x	1446.34	k12	3.99
Components in shear					
Column web in shear	CWS	x	598.28	k1	inf
Components in compression					
Column web in compression	CWC	x	747.5	k2	inf
L-stub web in compression	LSWC	x	1386	k9	45.82
Friction damper	FD	x	450.8	x	inf
New components activated after the slip of the friction damper after $F_{rd.slip.2}$ =450.8kN is reached					
Bolts in shear	BS_{FD}	x	603.186	k11	3.05
Hammer head flange in bearing	BH-B	x	532.4	k12	2.995
L-stub web in bearing	LSW-B	x	893	k12	6.22

This might be a bit surprising since it is expected that the slippage would only occur in the case of friction damper, as the idea of this joint is to dissipate energy using the friction provided by the slippage of the damper without any damage. The slip of the upper interface will provoke a change in the initial stiffness and activation of new components. It was shown in the [1] that none of the components yield before the friction damper reaches its sliding limit. As mentioned before it is considered that the yielding of the component will occur when 2/3 of its resistance is reached. Therefore no damage will be made to the joint, making it free of damage despite the unexpected slip of the upper interface and making the joint configuration consistent with the research aim.

The second slip occurs when the force acting in the compression zone reaches a value of $F_{rd.slip.2}$=450.8kN. The slip ends when $\delta_{slip.fd}$(the value will be introduced later on) is reached and the new components are activated providing additional strength and rotation. It should be noted that the value of friction damper resistance in this work is not the calculated design resistance, but the "corrected" resistance calculated by modifying the friction coefficients to better fit the values obtain from the experiments. For more information refer to [1].

The component governing the failure mode is the hammer head flange in bearing. Bearing of a plate represents a ductile failure mode, which allows the force redistribution and is in accordance with the basic joint design recommendations.

Three new components activated when the slip resistance of the friction damper is exceeded, BH-B, LSW-B and $BS_{.fd}$, were not taken into account in [1]. They were calculated and considered in the present work. The results are presented in Table 3in the last 3 rows. The analytical procedure to calculate it was taken from the Eurocode 3. The detailed calculations can be found in Appendix A. It should be noted that no complete information about the geometry of the hammer head flange was found (it was not considered in [1] nor in other available documents) so some of the dimension have been assumed in accordance with the joint geometry and the scope of the work.

Now when we have all the necessary data, we can proceed with the forming of the rotational springs.

1st rotational spring

The components identified at the cut 1-1 (Figure III-7) will be transformed into equivalent springs, one for tension one for compression row, and then merged into a single rotational spring, as presented in Figure III-8.

Tension

The overall procedure would be to take all the elements of the analysed row and using the equation for the stiffness of springs in a row, presented here below as equation (3.1), form an equivalent spring with equivalent characteristics. But, since we have elements activated after slip, we can come to a conclusion that there are 2 situations we need to take into account.

$$k_{equivalent} = \frac{1}{\Sigma\left(\frac{1}{k_i}\right)} \qquad (3.1)$$

Case 1: Tension force $F_{t.ed} < F_{rd.slip.1}$

In this case only the TSWT is active, putting that into (3.1) we obtain:

$$k_{1.t.no.slip} := \frac{1}{\left(\frac{1}{k_{tswt}}\right)} = 44 \cdot mm$$

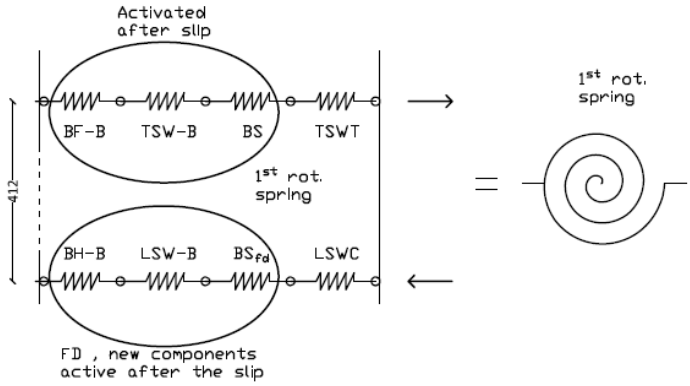

Figure III-8: 1st rotational spring

Case 2: Tension force $F_{t.ed} \geq F_{rd.slip.1}$

In the present case the additional 3 components are activated giving:

$$k_{1.t.slip} := \frac{1}{\left(\frac{1}{k_{tswt}} + \frac{1}{k_{tsw\text{-}b}} + \frac{1}{k_{bf\text{-}b}} + \frac{1}{k_{bs}}\right)} = 1.832 \cdot mm$$

It is obvious that the stiffness has dropped notably with the introduction of the new components. This is connected with the fact that the elements are all aligned in one row. Having one weak element can, in the present case, significantly influence the stiffness of the equivalent spring.

Compression

The procedure will be the same. We will consider the case before the damper slip, and after.

Case 1: Compression force $F_{c.ed} < F_{rd.slip.2}$

In this case only the LSWC is active, though we could consider the damper as an additional component being active before the slip occurs, but since its stiffness is in that case infinitive, we just consider the contribution of the LSWC:

$$k_{1.c.no.slip} := \frac{1}{\left(\frac{1}{k_{lswc}}\right)} = 45.82 \cdot mm$$

Case 2: Compression force $F_{c.ed} \geq F_{rd.slip.2}$

After the damper slips and reaches the stroke end, the additional 3 components are activated giving:

$$k_{1.c.slip} := \frac{1}{\frac{1}{k_{lsw\text{-}b}} + \frac{1}{k_{bh\text{-}b}} + \frac{1}{k_{bs.fd}} + \frac{1}{k_{lswc}}} = 1.184 \cdot mm$$

Stiffness of the rotational spring

The following expression recommended by the EC3-1-8, equation (6.27), is used to calculate rotational stiffness:

$$S_j = \frac{E \cdot z^2}{\mu \cdot \Sigma\left(\frac{1}{k_i}\right)}$$

Where: k_i is the stiffness of the basic com

μ is the ration between $S_{j.ini}/S_j$

z is the lever arm

Note: As the scope of this chapter is to formulate and validate the 2-spring-modelwhich will later beimplemented into the routine for calculating the response of the structure subjected to a column loss, a simplification was used regarding the behaviour of the joint, considering μ=1 when the rotational stiffness of the joint is formed, for both rotational and 2-spring model.

First rotational spring is defined by three different S_j:

$z_1 = 412\text{mm}$

- Rotational stiffness valid before the slip of the upper interface occurs

$$S_{j.1.ini} := \frac{E \cdot z_1^{\,2}}{\left(\frac{1}{k_{1.t.no.slip}} + \frac{1}{k_{1.c.no.slip}}\right)} = 8.001 \times 10^{5} \cdot \text{kN} \cdot \text{m}$$

- Rotational stiffness valid after the slip of the upper interface but before slippage of the damper

$$S_{j.1.slip1} := \frac{E \cdot z_1^{\,2}}{\left(\frac{1}{k_{1.t.slip}} + \frac{1}{k_{1.c.no.slip}}\right)} = 6.279 \times 10^{4} \cdot \text{kN} \cdot \text{m}$$

- Rotational stiffness valid after the slip of the friction damper

$$S_{j.1.slip2} := \frac{E \cdot z_1^{\,2}}{\left(\frac{1}{k_{1.t.slip}} + \frac{1}{k_{1.c.slip}}\right)} = 2.564 \times 10^{4} \cdot \text{kN} \cdot$$

Later the above presented stiffness values will be used to form the rotational stiffness of the whole joint.

2nd rotational spring

The components identifiedas the one forming the second rotational spring (Figure III-9) will be transformed into a rotational spring.

Tension

The present case shall be considered using EC3-1-8 section 6.3.3 - recommendations for an endplate joint with two bolt-rows in tension.

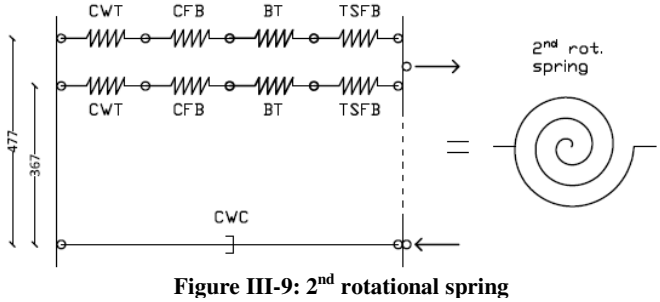

Figure III-9: 2nd rotational spring

It is questionable whether this consideration, using equations derived for a situation where the connection is formed using end-plate, is correct. In the case of an end-plate connection the deformation of the end-plateis considered plane, and the equations derived using that assumption. In the present case we do not have an end plate, but T-stub and L-stub instead. As presented in the

Figure III-9 by a dashed line, the flanges of the two stubs are not rigidly connected, and therefore may deform separately. Nevertheless, we shall consider the equations derived in EC 3-1-8 as suitable for the present case, and continue with the calculations as such. To validate the assumption made, the final result will be compared with the experimental obtained at University of Salerno result presented in the [1].

According to the EC3-1-8, firstly we transform the two rows of springs into equivalent springs:

$$k_{eff.1} := \frac{1}{\left(\frac{1}{k_{cwt}} + \frac{1}{k_{cfb}} + \frac{1}{k_{tsfb}} + \frac{1}{k_{bt}}\right)} = 3.372 \cdot \text{mm}$$

$h_{r.1} := 477\ \text{mm}$

$$k_{eff.2} := \frac{1}{\left(\frac{1}{k_{cwt}} + \frac{1}{k_{cfb}} + \frac{1}{k_{tsfb}} + \frac{1}{k_{bt}}\right)} = 3.372 \cdot \text{mm}$$

$h_{r.2} := 367\ \text{mm}$

The next step is to make an equivalent spring of those 2 parallel springs:

Equation provided by the EC3-1-8 for calculating the equivalent lever arm of the two bolt rows gives:

$$z_{eq} = \frac{\Sigma k_{eff.r} \cdot h_r^{\,2}}{\Sigma k_{eff.r} \cdot h_r} \qquad z_{eq.t2} := \frac{k_{eff.1} \cdot h_{r.1}^{\,2} + k_{eff.2} \cdot h_{r.2}^{\,2}}{k_{eff.1} \cdot h_{r.1} + k_{eff.2} \cdot h_{r.2}} = 429.17 \cdot \text{mm}$$

The final step is to obtain the equivalent stiffness of the spring presenting the two bolt rows:

$$k_{eq} = \frac{\Sigma\left(k_{eff.r} \cdot h_r\right)}{z_{eq}} \qquad k_{eq.t2} := \frac{\left(k_{eff.1} \cdot h_{r.1} + k_{eff.2} \cdot h_{r.2}\right)}{z_{eq.t2}} = 6.632 \cdot \text{mm}$$

$K_{eq.t2}$represents the value of the stiffness of a single equivalent horizontal spring located at $z_{ed.t2}$ distance from the centre of compression.

Compression

The only element active in compression is the column web in compression – CWC. As the column web is strengthen by use of stiffeners, its $k_{cwc} = \infty$ and therefore doesn't affect the stiffness of the rotational spring.

Stiffness of the rotational spring

$$S_{j.2.ini} := \frac{E \cdot z_{eq.t2}^{\,2}}{\left(\frac{1}{k_{eq.t2}}\right)} = 2.565 \times 10^{5} \cdot \text{kN} \cdot \text{m}$$

3rd rotational spring

The 3rd rotational spring represents the column panel in shear. It is a common practise to separate the behaviour of the column web in shear from the connection since its behaviour is not influenced by the same load.

In the present case the stiffness of the CWS will be taken as infinitive, $k_{cws} = \infty$, like in the work of [1]. This decision in questionable, since according to the literature [7], $k_{cws} = \infty$ can be taken in the case that appropriate diagonal stiffeners are provided, which is here not the case. Never the less, it is assumed that this consideration will not affect the final result much, and therefore we proceed like this.

Stiffness of the rotational spring

$S_{j.3.ini} = \infty$

Final rotational stiffness

Eurocode allows representing a joint as a single rotational spring located at the intersection of the axes of the connected members. Rotational springs formed at levels of the cuts made will be combined (Figure III-10), forming one rotational spring representing the behaviour of the whole joint when subjected to hogging bending.The value of the rotational stiffness of the joint varies depending on the value of the load i.e. depending on whether one of the slips occurred or not.

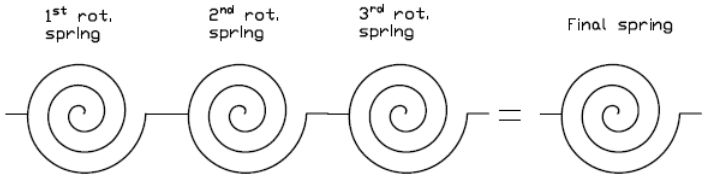

Figure III-10: Final rotational spring

Values of the forces in the springs and moments acting on the joint which define the limit for using a certain value of stiffness will also be presented. The moment at the point of stiffness change is calculated by multiplying the force at the stiffness change by the corresponding lever arm (lever arm of the rotational spring where the slip occurs)

- Rotational stiffness valid before the slip of the upper interface occurs

$$S_{j.ini} := \frac{1}{\frac{1}{S_{j.1.ini}} + \frac{1}{S_{j.2.ini}}} = 1.942406 \times 10^{5} \cdot kN \cdot m$$

$$F_{j.ini.limit} := 186.6\,kN \quad M_{j.ini.limit} := F_{j.ini.limit} \cdot z_1 = 76.879\ kN \cdot m$$

- Rotational stiffness valid after the slip of the upper interface but before slippage of the damper

$$S_{j.slip1} := \frac{1}{\frac{1}{S_{j.1.slip1}} + \frac{1}{S_{j.2.ini}}} = 5.044366 \times 10^{4} \cdot kN \cdot m$$

$$F_{j.slip1.limit} := 450.8kN \quad M_{j.slip1.limit} := F_{j.slip1.limit} \cdot z_1 = 185.73 \ kN \cdot m$$

- Rotational stiffness valid after the slip of the friction damper

$$S_{j.slip2} := \frac{1}{\frac{1}{S_{j.1.slip2}} + \frac{1}{S_{j.2.ini}}} = 2.331061 \times 10^{4} \cdot kN \cdot m$$

$$F_{j.slip2.limit} := 532.4kN \quad M_{j.slip2.limit} := F_{j.slip2.limit} \cdot z_1 = 219.349 \ kN \cdot m$$

With the data presented above, we can describe the behavior of the joint under hogging moment.

III.3.1.2. Rotational spring model – sagging bending moment

The same procedure shall be used to predict the behaviour of the joint under sagging moments. Firstly, the horizontal spring model is made using the load transfer sequence principle. Like in the previous case, three cutsare made in order to take into account the lever arm difference between the parts forming the joint. The horizontal spring model is presented in the Figure III-11.

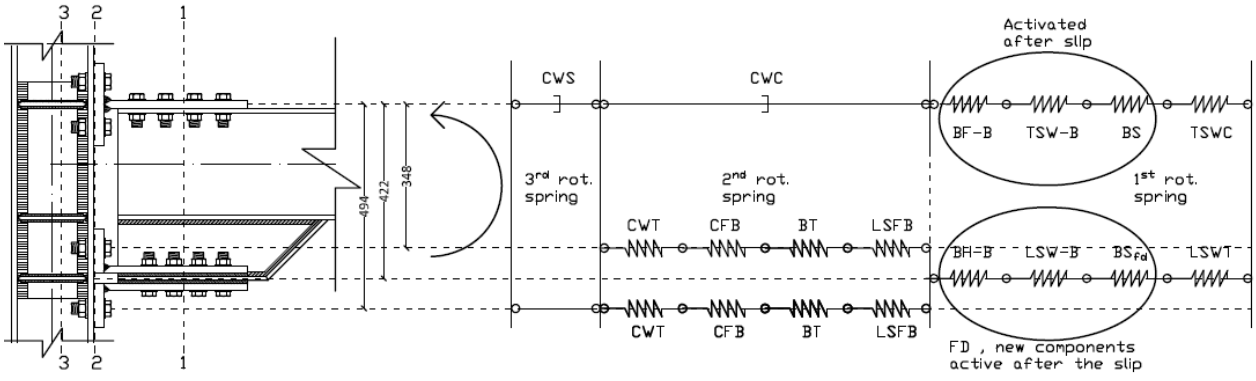

Figure III-11: Main components activated in case of sagging bending – horizontal spring model

The difference between the horizontal spring model for hogging and sagging moment is reflected in the fact that now the upper level of the joint is in compression, activating the T stub web in compression TSWC, and CWC.

The lower part of the joint is subjected to tension and therefore, the two bolt rows will be activated in tension, as well as the L-stub web which will also be activated in tension. Other than that, all the other components and the joint global behaviour remains the same. The slip limit and behaviour does not depend on the force direction.

The values of the stiffness and resistance of the components are presented in the Table III-2.

The joint under sagging bending experiences the same overall behavior. Only difference is reflected in stiffness, which slightly varies from the one obtained for hogging, and in the failure governing component.

Value of $F_{rd.slip.1}$=186.6kN represents the value when the first slip will occur and the new components will activate, only this time under compression. The slip of the friction damper is expected when the force acting at the tension side reaches a value of $F_{rd.slip.2}$=450.8kN. Reaching the slip limit the same 3 components are additionally activated providing more strength and rotation. Failure is governed by a ductile failure mode L-stub flange in bending this time with a value of $F_{RD.lsfb}$ = 490.1kN. The design moment resistance is therefore, in case of sagging bending, lower when compared to hogging.

We now move to the analytical procedure of forming the rotational spring model for the case of sagging bending.

Table III-2: Stiffness and resistance of the components under sagging bending moment

Sagging bending moment					
Component	Acronym	F_{RD} per row [kN]	F_{RD} total [kN]	Coef from EC3-1-8	k_i [mm]
Components in tension					
Bolts in tension	BT	660.96	1321.92	k10	10.85
L-stub flange in bending	LSFB	x	490.1	k5	16.32
Column flange in bending	CFB	462.84	925.68	k4	32.86
Column web in tension	CWT	482.8	965.6	k3	9.97
L-stub web in tension	LSWT	x	1386	k9	45.82
New components activated after the slip of the friction damper after $F_{rd.slip.2}$=450.8kN is reached					
Bolts in shear	BS_{FD}	x	603.186	k11	3.05
Hammer head flange in bearing	BH-B	x	532.4	k12	2.995
L-stub web in bearing	LSW-B	x	893	k12	6.22
Components in shear					
Column web in shear	CWS	x	598.28	k1	inf
Components in compression					
Column web in compression	CWC	x	679.5	k2	inf
T-stub web in compression	TSWC	x	968	k9	44
Friction damper	FD	x	450.8	x	inf
New components activated after the slip of the upper interface after $F_{rd.slip.1}$=186.6kN is reached					
Bolts in shear	BS	x	1763	k11	6.1
T-stub web in bearing	TSW-B	x	3040.7	k12	9.21
Beam flange in bearing	BF-B	x	1446.34	k12	3.99

1st rotational spring

The same procedure as for the hogging bending shall be used. The components activated are presented in the Figure III-12.

Tension

We need to account for two situations:

Case 1: Tension force $F_{t.ed} < F_{rd.slip.2}$

In this case only the LSWT is active, so we obtain:

$$k_{1.t.no.slip} := \frac{1}{\left(\frac{1}{k_{lswt}}\right)} = 45.82 \cdot mm$$

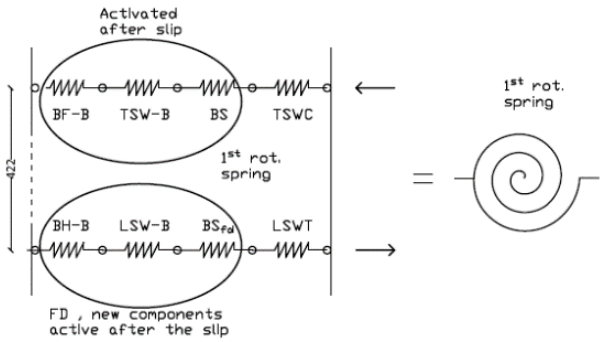

Figure III-12: 1st rotational spring

Case 2: Tension force $F_{t.ed} \geq F_{rd.slip.2}$

After the slip of the dumper 3 new components are activated giving:

$$k_{1.t.slip} := \frac{1}{\left(\frac{1}{k_{lswt}} + \frac{1}{k_{lsw\text{-}b}} + \frac{1}{k_{bh\text{-}b}} + \frac{1}{k_{bs.fd}}\right)} = 1.184 \cdot mm$$

Compression

The procedure will be the same. The stiffness will change after the slip of the upper interface.

Case 1: Compression force $F_{c.ed} < F_{rd.slip.1}$

Before the slip only TSWC is active:

$$k_{1.c.no.slip} := \frac{1}{\left(\frac{1}{k_{tswc}}\right)} = 44 \cdot mm$$

Case 2: Compression force $F_{c.ed} \geq F_{rd.slip.1}$

$$k_{1.c.slip} := \frac{1}{\frac{1}{k_{tsw\text{-}b}} + \frac{1}{k_{bf\text{-}b}} + \frac{1}{k_{bs}} + \frac{1}{k_{tswc}}} = 1.832 \cdot mm$$

Stiffness of the rotational spring

First rotational spring is defined by three different S_j:

$z_1 = 412\text{mm}$

- Rotational stiffness valid before the slip of the upper interface occurs

$$S_{j.1.ini} := \frac{E \cdot z_1^{\,2}}{\left(\frac{1}{k_{1.t.no.slip}} + \frac{1}{k_{1.c.no.slip}}\right)} = 8.394 \times 10^5 \cdot \text{kN} \cdot \text{m}$$

- Rotational stiffness valid after the slip of the upper interface but before slippage of the damper

$$S_{j.1.slip1} := \frac{E \cdot z_1^{\,2}}{\left(\frac{1}{k_{1.t.no.slip}} + \frac{1}{k_{1.c.slip}}\right)} = 6.588 \times 10^4 \cdot \text{kN} \cdot \text{m}$$

- Rotational stiffness valid after the slip of the friction damper

$$S_{j.1.slip2} := \frac{E \cdot z_1^{\,2}}{\left(\frac{1}{k_{1.t.slip}} + \frac{1}{k_{1.c.slip}}\right)} = 2.69 \times 10^4 \cdot \text{kN} \cdot \text{m}$$

Later the above presented stiffness values will be used to form the rotational stiffness of the whole joint.

2nd rotational spring

The components identified as the one forming the second rotational spring (Figure III-14) will be transformed into a rotational spring.

Tension

The present case shall be considered using EC3-1-8 section 6.3.3 - recommendations for an endplate joint with two bolt-rows in tension. The present situation has already been analysed when the 2nd rotational spring in the case of hogging bending was formed, therefore we proceed without

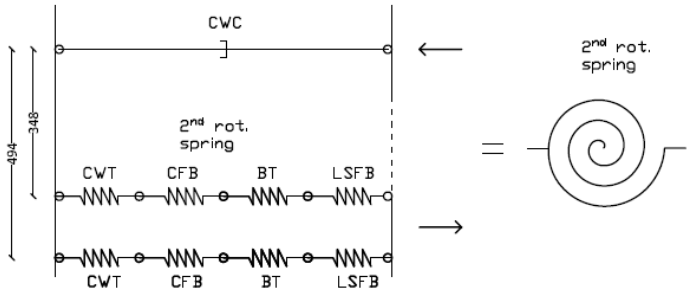

Figure III-13: 2nd rotational spring

detailed explanation.

According to the EC3-1-8, firstly we transform the two rows of springs into equivalent springs:

$$k_{eff.1} := \frac{1}{\left(\frac{1}{k_{cwt}} + \frac{1}{k_{cfb}} + \frac{1}{k_{lsfb}} + \frac{1}{k_{bt}}\right)} = 3.519 \cdot mm \qquad h_{r.1} := 494\ mm$$

$$k_{eff.2} := \frac{1}{\left(\frac{1}{k_{cwt}} + \frac{1}{k_{cfb}} + \frac{1}{k_{lsfb}} + \frac{1}{k_{bt}}\right)} = 3.519 \cdot mm \qquad h_{r.2} := 348\ mm$$

The next step is to make an equivalent spring of those 2 parallel springs:

Equation provided by the EC3-1-8 for calculating the equivalent lever arm of the two bolt rows:

$$z_{eq} = \frac{\Sigma k_{eff.r} \cdot h_r^{\,2}}{\Sigma k_{eff.r} \cdot h_r} \qquad z_{eq.t2} := \frac{k_{eff.1} \cdot h_{r.1}^{\,2} + k_{eff.2} \cdot h_{r.2}^{\,2}}{k_{eff.1} \cdot h_{r.1} + k_{eff.2} \cdot h_{r.2}} = 433.66 \cdot mm$$

The final step is to obtain the equivalent stiffness of the spring presenting the two bolt rows:

$$k_{eq} = \frac{\Sigma k_{eff.r} \cdot h_r}{Z_{eq}} \qquad k_{eq.t2} := \frac{\left(k_{eff.1} \cdot h_{r.1} + k_{eff.2} \cdot h_{r.2}\right)}{z_{eq.t2}} = 6.833 \cdot mm$$

$K_{eq.t2}$represent the value of the stiffness of a single equivalent horizontal spring located at $z_{ed.t2}$ distance to the centre of compression.

Compression

The only element active in compression is the column web in compression. As it was addressed previously, when hogging bending was analysed, the column web is strengthen by use of stiffeners, its $k_{cwc} = \infty$ and therefore doesn't affect the stiffness of the rotational spring.

Stiffness of the rotational spring

$$S_{j.2.ini} := \frac{E \cdot z_{eq.t2}^{\,2}}{\left(\frac{1}{k_{eq.t2}}\right)} = 2.698 \times 10^{5} \cdot kN \cdot m$$

3rd rotational spring

The stiffness of the component column web in shear is $k_{cws} = \infty$ and therefore doesn't affect the stiffness of the rotational spring.

Stiffness of the rotational spring

$S_{j.3.ini} = \infty$

Final rotational stiffness

The calculated rotational stiffness is presented in the following along with the forces and moments limiting its use:

- Rotational stiffness valid before the slip of the upper interface occurs

$$S_{j.ini} := \frac{1}{\left(\frac{1}{S_{j.1.ini}} + \frac{1}{S_{j.2.ini}}\right)} = 2.041944 \times 10^{5} \cdot kN \cdot m$$

$$F_{j.ili.limit} := 186.6\,kN \quad M_{j.ini.limit} := F_{j.ili.limit} \cdot z_1 = 78.745\ kN \cdot m$$

- Rotational stiffness valid after the slip of the upper interface but before slippage of the damper

$$S_{j.slip1} := \frac{1}{\left(\frac{1}{S_{j.1.slip1}} + \frac{1}{S_{j.2.ini}}\right)} = 5.294972 \times 10^{4} \cdot kN \cdot m$$

$$F_{j.slip1.limit} := 450.8\,kN \quad M_{j.slip1.limit} := F_{j.slip1.limit} \cdot z_1 = 190.238\ kN \cdot m$$

-
- Rotational stiffness valid after the slip of the friction damper

$$S_{j.slip2} := \frac{1}{\left(\frac{1}{S_{j.1.slip2}} + \frac{1}{S_{j.2.ini}}\right)} = 2.446183 \times 10^{4} \cdot kN \cdot m$$

$$F_{j.slip2.limit} := 490.1\,kN \quad M_{j.slip2.limit} := F_{j.slip2.limit} \cdot z_1 = 206.822\ kN \cdot m$$

With the data presented above, we can describe the behavior of the joint under sagging moment.

III.3.2. **M-Φ of the joint - rotational spring model**

The general response of a joint can be presented by M-Φ curve, where **M** represents the bending moment to which the joint is subjected and **Φ** represents the relative rotation between connected elements. The behaviour of the innovative joint shall be expressed using the M-Φ curve.

The necessary characterization of the components for forming the M-Φ curve of the joint is done. Stiffness governing the behaviour of the joint has also been defined. The information missing for assessing the behaviour of the joint regards the length of the stroke. Indeed, in order to obtain the M-Φ curve of the joint we need to assess the stroke length.

The length of the slotted hole is $L_{slotted.hole}$=270 mm. Four bolts M20 with the pitch p=60mm are forming one side of the friction damper. If we assume that the bolts are initially placed in the middle of the slotted hole, using the following equation we obtain:

$$\delta_{slide.fd} = (L_{slotted.hole} – (n_{bolt} - 1)p – 2d_b/2)/2$$

$$\delta_{slide.fd} = (270 – (4 - 1)\ 60 – 2\ (20/2) / 2 = 35mm$$

It should be emphasized that in the present case we are developing the monotonic behaviour of the joint. Since the aim of the rotational spring model is to represent a reference model, which will be compared with the innovative 2 spring model in order to validate it, it will be sufficient to assess the monotonic behaviour of the joint. Therefore, we can assume that the obtained value of $\delta_{slide.fd}$is adequate for the present situation.

The length of the slip of the upper interface shall also be calculated. Since the slip is quite small, and hard to predict due to the fact that it is not realistic to expect the bolt to be places exactly in the middle of the hole, δ_{slip1} shall be neglected.

$$\delta_{slip1} = (d_0 – d) / 2 = 0.5mm$$

In the following comments shall be made with respect to the Figure III-14.

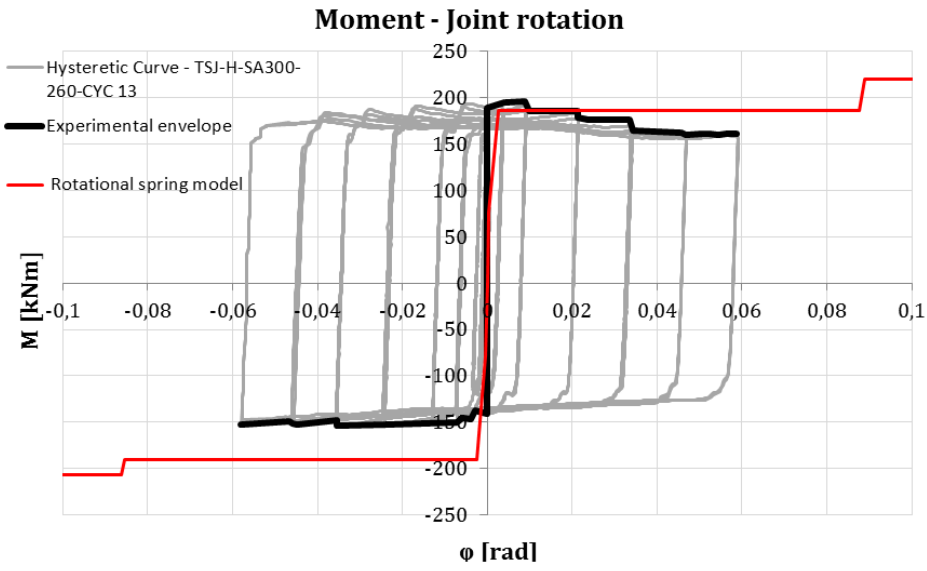

Figure III-14: M-Φ curve of the joint. Rotational spring model. Experimental data.

Figure III-14 represents the comparison of the modelled joint behaviour for monotonic loading and the obtained joint behaviour from the test performed at University of Salerno. [1] The aim of the test performed at Salerno on a full scale connection was to assess the behaviour of the new joint typology in terms of hysteresis stability, behaviour of the friction damper and the friction coefficient stability when subjected to cyclic loading. Therefore, the test was conducted only up to the slip limit. More about the test layout and the test in general can be found in [1].

Due to the lack of any other useful information, the envelope was formed out of the results obtained from the experiment and it was decided to compare the so-obtained experimental M-Φ curve with the one modelled by the rotational spring model. The comparison can be provided for the part of the curve describing the behaviour up to point where the slip is reached.

As noticeable, the result are in good agreement up to the slip though the change of the stiffness after the slip of the upper interface is not that obvious in the experimental curve. We can also say that the part of the curve representing hogging bending is in good agreement with the experimental results, with the exception of the decrease of the force at slip for each cycle. It will be assumed within this work that the friction force will remain constant. The rotational spring model over-estimates the joint resistance in is sagging according to the experimental data. Even though the friction force should be the same as for hogging bending, the experiment proves otherwise. The reason for such behaviour was not explained. Some assumptions have been made including the one stating that the force might not be the same due to the direction of the loading, as the different direction of the loading could affect the preloading of the bolts.

As the reason for a lower friction force in sagging is not certain, taking into account the fact that the presented experimental results are not representing the monotonic behaviour of the joint and considering that the modelled behaviour in hogging is in good agreement with the experimental result, the decision was made to assume that the modelled behaviour is acceptable and that it can be used further on.

The modelled joint behaviour is generally the same in case of hogging and sagging, with the difference in values at the points defining a change of the behaviour.

The $S_{j.ini}$ is valid until the bending moment reaches a value of around 77 kNm for both cases, when the slip of the upper interface occurs. The change of stiffness is notable as the new components

activate. Newly obtained modified stiffness $S_{j.slip.1}$ is governing the M-Φ dependence law until reaching the values 185.7 kNm and 190.2 kNm, for hogging and sagging bending, respectively.

When latter is reached, the friction damper slips, causing a rotation of more than 0.08 rad before reaching the stroke end. Here we can note one of the obvious advantages of the innovative connection. From the Figure III-14 we can conclude that, according to the modelled behaviour, we can reach a rotation larger than 0.08 rad without any damage of the elements forming the connection which is significantly higher than the minimum required by the EN 1998-1 for frames in ductility class high (DCH), which is 0.035 rad for using partial strength connections.

Further on, after reaching the stroke end limit of the friction damper, additional stiffness will be provided by newly activated elements, until finally reaching the $\mathbf{M_{rd}}$.

As notable, the post-limit behaviour of the joint was not considered and it is assumed that the plateau occurs when the design resistance is reached. The ultimate resistance of the joint and the influence of strain hardening was neglected. It should also be emphasized that the presented rotational limit is chosen arbitrary, as no data about this subject is available.

The developed rotational spring model will serve as a reference model for validation of the proposed 2-spring model.

III.3.3. Spring model in case of a column loss scenario - 2-spring model

Following pages are dedicated to the development of a new spring model.The main idea behind the following development is to obtain a model which should trustworthy represent the behaviour of the joint and be easy to implement into the robustness assessment routine.

It was concluded that a model containing 2 horizontal parallel spring, where each of them would represent the full behaviour of the zone to which they correspond, would be quite convenient for the implementation in the robustness assessment procedure.

The basic idea is to start from the horizontal spring model we already developed, and by forming equivalent springs, come to a model with 2 parallel springs, one in tension and the other in compression zone, which would be able to characterize the behaviour of the whole zone.

Considering the above mentioned, the model was named 2-spring model. Figure III-15picturesquely explains the mentioned steps for a joint subjected to hogging moment.

III.3.3.1. Hogging bending

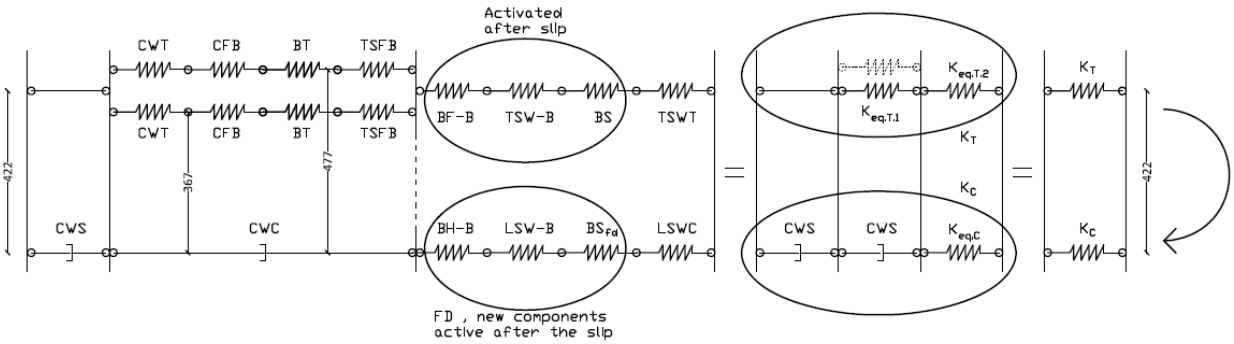

Figure III-15: Steps to come from the horizontal spring model to 2-spring model

Tension zone

The first step would be forming the $K_{eq.T.1}$which contains the components activated at the level of the bolt rows, namely, CWT – CFB – BT-TSFB. Again, we shall use the recommendation provided by the EC3-1-8 for the bolted connection with an end plate. As already commented when rotational spring model was made, this is a questionable assumption but we shall consider it accurate enough. Therefore:

$$k_{eff.1} := \frac{1}{\left(\frac{1}{k_{cwt}} + \frac{1}{k_{cfb}} + \frac{1}{k_{tsfb}} + \frac{1}{k_{bt}}\right)} = 3.372 \cdot mm \qquad h_{r.1} := 477\,mm$$

$$k_{eff.2} := \frac{1}{\left(\frac{1}{k_{cwt}} + \frac{1}{k_{cfb}} + \frac{1}{k_{tsfb}} + \frac{1}{k_{bt}}\right)} = 3.372 \cdot mm \qquad h_{r.2} := 367\,mm$$

The equivalent spring and lever arm have values of:

$$z_{eq.T.1} := \frac{k_{eff.1} \cdot h_{r.1}^{2} + k_{eff.2} \cdot h_{r.2}^{2}}{k_{eff.1} \cdot h_{r.1} + k_{eff.2} \cdot h_{r.2}} = 429.17 \cdot mm$$

$$k_{eq.T.1} := \frac{\left(k_{eff.1} \cdot h_{r.1} + k_{eff.2} \cdot h_{r.2}\right)}{z_{eq.T.1}} = 6.632 \cdot m$$

Next, we form the $K_{eq.T.2}$ from TSWT - BS- TSW-B - BF-B. We need to account for the two situations:

Case 1: Tension force $F_{t.ed} < F_{rd.slip.1}$

In this case only the TSWT is active, therefore we obtain:

$$k_{eq.T.2.no.slip} := \frac{1}{\left(\frac{1}{k_{tswt}}\right)} = 44 \cdot \text{mm} \qquad z_{eq.T.2} := 422\,\text{mm}$$

Case 2: Tension force $F_{t.ed} \geq F_{rd.slip.1}$

After the slip of the dumper 3 components are activated giving:

$$k_{eq.T.2.slip} := \frac{1}{\left(\frac{1}{k_{tswt}} + \frac{1}{k_{tsw\text{-}b}} + \frac{1}{k_{bf\text{-}b}} + \frac{1}{k_{bs}}\right)} = 1.832 \cdot \text{mm} \qquad z_{eq.T.2} := 422\,\text{mm}$$

It should be noted that the lever arm considered here is different than the one considered in the rotational spring model. The reason for that is the necessity of having all of the springs in one row in order to be able to combine them into an equivalent spring. Therefore, a simplification was used and present spring was assigned with the same lever arm as for the column panel in shear.

The final step is merging $K_{eq.T.1}$ and $K_{eq.T.2}$ into the equivalent spring K_T. As addressed in the previous paragraph in order to make $K_T$we need spring which are in row. It is obvious from the presented calculations that the two springs, $K_{eq.T.1}$ and $K_{eq.T.2}$, have different lever arms with respect to the compression centre. Therefore we shall move the $K_{eq.T.1}$, as presented in the Figure III-16, and place it in the same row with the others spring in tension. Of course, the change of the lever arm has to be accompanied with the corresponding change of the stiffness. Indeed, in order to keep the M constant at the level of analysed cross section, the above mentioned must be done. The problem presented in the current paragraph shall be addressed in more detail in III.3.3.3.

In order to change the stiffness of $K_{eq.T.1}$in respect to the lever arm, we shall use and expression derived in III.3.3.3:

$$z_{eq.T.1} = 429.168\ \text{mm} \qquad z_{eq.T.2} := 422\,\text{mm}$$

$$k_{eq.T.1} = 6.632\ \text{mm} \qquad k^*_{eq.T.1} := \left(\frac{z_{eq.T.1}}{z_{eq.T.2}}\right)^2 \cdot k_{eq.T.1} = 6.859\ \text{mm}$$

It is noticeable that the defence between the old $K_{eq.T.1}$ and the new value $K^{*}_{eq.T.1}$is quite small, around3%, which implies that neglecting this change would not make much difference on the final result. Nevertheless, the new value of $K_{eq.T.1}$shall be used in the final formulation.

Finally, the values of stiffness of the equivalent tension spring representing the behaviour of the whole tension part, for $z_{.eq.T}$ = 422mm, are:

$$K_{T.no.slip} := \frac{1}{\left(\frac{1}{k_{eq.T.2.no.slip}} + \frac{1}{k_{eq.T.1}}\right)} = 5.934 \cdot mm \qquad K_{T.slip} := \frac{1}{\left(\frac{1}{k_{eff.t2c2}} + \frac{1}{k_{eq.T.1}}\right)} = 1.446 \cdot mm$$

The behaviour of the spring shall be shown in a form of an F - δ diagram.

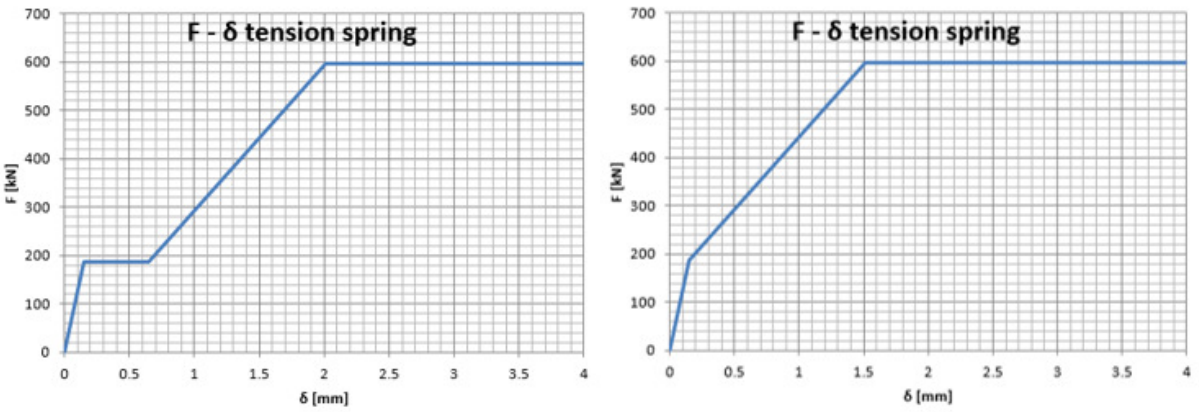

Figure III-16: F - δ diagram of the equivalent tension spring when considering δ_{slip1} (left) and without considering δ_{slip1} (right)– hogging bending

In Figure III-16 (right) we can clearly see the influence of the slip to the change of the behaviour of the spring. The initial stiffness changes after $F_{slip.1}$ is reached, providing a more flexible response.The designed resistance of the spring corresponds to the minimum value of the resistance of all of the components forming the spring. In this case the design resistance is governed by component CWS and therefore F_{RD} = 598.28 kN. In the presently discussed picture $\delta_{slip.1}$was not considered.

Figure III-16 (left) represent the behaviour of the same spring but when $\delta_{slip.1}$is included. In this case the behaviour of the tension part is quite similar to the behaviour of the friction damper, except the slip is much smaller. Due to uncertainty of the slip length, the fact that it will not influence the response much and for the sake of the simplicity, the slip of the upper interface shall be neglected.

The ductility of the presented spring should also be addressed. In the present case, ductility is taken as infinite. Therefore, the limit presented on the graph (4mm) is completely arbitrary and chosen so that the behaviour of the spring is fully presented.

Compression zone

The same procedure shall be conducted in order to obtain the equivalent spring K_C.

Fistly, we form the $K_{eq.C}$ from LSWC – BS_{fd} – LSW-B – BH-B.

Case 1: Compression force $F_{t.ed} \leq F_{rd.slip.2}$

In this case only the LSWT is active, therefore we obtain:

$$k_{eq.C.no.slip} := \frac{1}{\left(\frac{1}{k_{lswc}}\right)} = 45.82 \cdot mm$$

Case 2: Compression force $F_{t.ed} \geq F_{rd.slip.2}$

After the slip of the dumper 3 components are activated giving:

$$k_{eq.C.slip} := \frac{1}{\frac{1}{k_{lsw\text{-}b}} + \frac{1}{k_{bh\text{-}b}} + \frac{1}{k_{bs.fd}} + \frac{1}{k_{lswc}}} = 1.184 \cdot mm$$

As the CWS and CWC have infinite stiffness, the stiffness of the equivalent compression spring K_C is:

$$k_{C.no.slip} := \frac{1}{\left(\frac{1}{k_{lswc}}\right)} = 45.82 \cdot mm \qquad k_{C.slip} := \frac{1}{\frac{1}{k_{lsw\text{-}b}} + \frac{1}{k_{bh\text{-}b}} + \frac{1}{k_{bs.fd}} + \frac{1}{k_{lswc}}} = 1.184 \cdot mm$$

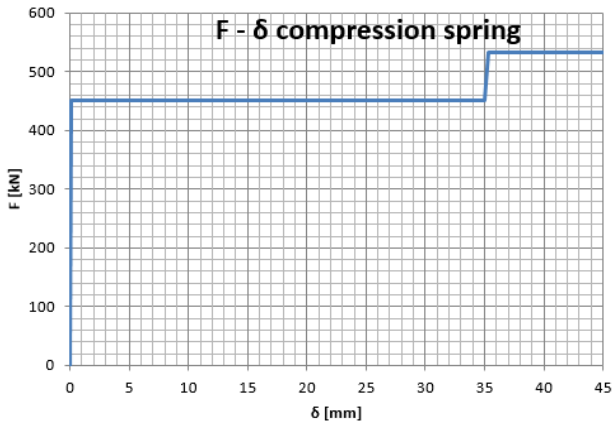

Figure III-17: F - δ diagram of the equivalent compression spring – hogging bending

Figure III-17 represents the behaviour of the equivalent compression spring. We can conclude that due to the high initial stiffness, the spring behaves up to the slip limit as practically rigid. When the slip occurs there is not force increment up to the stroke end, when the new stiffness is provided. The designed resistance of the spring corresponds to the minimum value of the resistance of all of the components forming the spring and in this case is governed by component BH-B. Therefore, $F_{RD} = 532.4$ kN.

The ductility of the spring is taken as infinite and the graph ends at arbitrary value of δ as previously explained.

With the data we now have, we can form the $S_j$for the hogging bending:

- Rotational stiffness valid before the slip of the upper interface occurs

$z_{eq} := 422\,\text{mm}$ $E := 210\,\text{GPa}$

$$S_{j.ini} := \frac{E \cdot z_{eq}^{2}}{\left(\frac{1}{k_{C.no.slip}} + \frac{1}{K_{T.no.slip}}\right)} = 1.964723 \times 10^{5}\ \text{kN} \cdot \text{m}$$

$F_{j.ini.limit} := 186.6\,\text{kN}$ $M_{j.ini.limit} := F_{j.ini.limit} \cdot z_{eq} = 78.745\,\text{kN} \cdot \text{m}$

- Rotational stiffness valid after the slip of the upper interface but before slippage of the damper

$$S_{j.slip1} := \frac{E \cdot z_{eq}^{2}}{\left(\frac{1}{k_{C.no.slip}} + \frac{1}{K_{T.slip}}\right)} = 5.241551 \times 10^{4}\ \text{kN} \cdot \text{m}$$

$F_{j.slip1.limit} := 450.8\,\text{kN}$ $M_{j.slip1.limit} := F_{j.slip1.limit} \cdot z_{eq} = 190.238\,\text{kN} \cdot \text{m}$

- Rotational stiffness valid after the slip of the friction damper

$F_{j.slip2.limit} := 532.4\,\text{kN}$ $M_{j.slip2.limit} := F_{j.slip2.limit} \cdot z_{eq} = 224.673\,\text{kN} \cdot \text{m}$

$$S_{j.slip.2} := \frac{E \cdot z_{eq}^{2}}{\left(\frac{1}{k_{C.slip}} + \frac{1}{K_{T.slip}}\right)} = 2.434719 \times 10^{4} \cdot kN \cdot m$$

With the data presented above, we can describe the behavior of the joint under hogging moment using the 2-spring model. We now move to the sagging bending.

III.3.3.2. Sagging bending

Figure III-18 explains the steps used to form the 2-spring model of the joint when subjected to

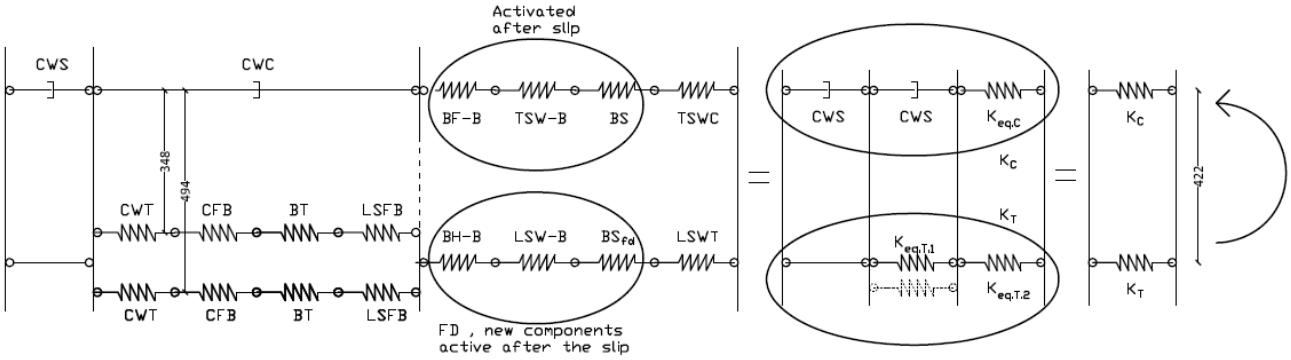

Figure III-18: Steps to come from the horizontal spring model to 2-spring model

sagging moment. The procedure is generally the same as for the hogging bending.

Tension zone

Firstly we shall make $K_{eq.T.1}$ which contains the components activated at the level of the bolt rows, namely, CWT – CFB – BT - LSFB. Therefore:

$$k_{eff.1} := \frac{1}{\left(\frac{1}{k_{cwt}} + \frac{1}{k_{cfb}} + \frac{1}{k_{lsfb}} + \frac{1}{k_{bt}}\right)} = 3.519 \cdot mm \qquad h_{r.1} := 494\,mm$$

$$k_{eff.2} := \frac{1}{\left(\frac{1}{k_{cwt}} + \frac{1}{k_{cfb}} + \frac{1}{k_{lsfb}} + \frac{1}{k_{bt}}\right)} = 3.519 \cdot mm \qquad h_{r.2} := 348\,mm$$

The equivalent spring and lever arm have values of:

$$z_{eq.t1} := \frac{k_{eff.1} \cdot h_{r.1}^{2} + k_{eff.2} \cdot h_{r.2}^{2}}{k_{eff.1} \cdot h_{r.1} + k_{eff.2} \cdot h_{r.2}} = 434 \cdot mm$$

$$k_{eq.t1} := \frac{k_{eff.1} \cdot h_{r.1} + k_{eff.2} \cdot h_{r.2}}{z_{eq.t1}} = 6.833 \cdot mm$$

The next step would beforming of the $K_{eq.T.2}$ from LSWT – BS_{fd} – LSW-B – BH-B. We need to account for the two situations:

Case 1: Tension force $F_{t.ed} < F_{rd.slip.2}$

In this case only the LSWT is active, therefore we obtain:

$$k_{eq.T.2.no.slip} := \frac{1}{\left(\frac{1}{k_{lswt}}\right)} = 45.82 \cdot mm \qquad z_{eq.T.2} := 422\ mm$$

Case 2: Tension force $F_{t.ed} \geq F_{rd.slip.2}$

After the slip of the dumper 3 components are activated giving:

$$k_{eq.T.2.slip} := \frac{1}{\left(\frac{1}{k_{lswt}} + \frac{1}{k_{lsw\text{-}b}} + \frac{1}{k_{bh\text{-}b}} + \frac{1}{k_{bs.fd}}\right)} = 1.184 \cdot mm \qquad z_{eq.T.2} := 422\ mm$$

The final step is merging $K_{eq.T.1}$ and $K_{eq.T.2}$ into the equivalent spring K_T. As addressed when hogging bending was discussed, in order to make K_T we need spring which are in row. In order to move $K_{eq.T.1}$ we will need to account for the change of the stiffness of $K_{eq.T.1}$ with respect to the lever arm as explained in III.3.3.3:

$$z_{eq.T.1} := 434\,mm \qquad z_{eq.T.2} := 422\,mm$$

$$k_{eq.T.1} = 7.021\ mm \qquad k^{*}_{eq.T.1} := \left(\frac{z_{eq.T.1}}{z_{eq.T.2}}\right)^{2} \cdot k_{eq.T.1} = 7.426\ mm$$

The new value of $K_{eq.T.1}$ shall be used in the final formulation.

Finally, the values of stiffness of the equivalent tension spring representing the behaviour of the whole tension part, for $z_{eq.T}$ = 422mm, are:

$$K_{T.no.slip} := \frac{1}{\left(\frac{1}{k_{eq.T.2.no.slip}} + \frac{1}{k_{eq.T.1}}\right)} = 6.39 \cdot mm \qquad K_{T.slip} := \frac{1}{\left(\frac{1}{k_{eq.T.2.slip}} + \frac{1}{k_{eq.T.1}}\right)} = 1.021 \cdot mm$$

The behaviour of the spring shall be shown in a form of an F - δ diagram.

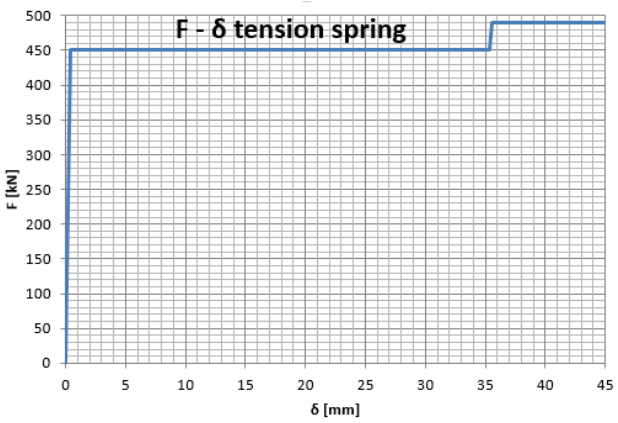

Figure III-19: F - δ diagram of the equivalent tension spring– sagging bending

Similarly to hogging bending situation, the spring containing the friction damper has firstly a behaviour very close to a rigid one(Figure III-19).Then the slip occurs inducing large dilatation, until the new components are activated.The designed resistance of the spring corresponds to the minimum value of the resistance of all of the components forming the spring. In this case the design resistance is governed by component LSWB and therefore F_{RD} = 490.1 kN.

The ductility limit of the spring is taken as infinite and the graph ends at arbitrary value of δ as previously explained.

Compression zone

The same procedure shall be conducted in order to obtain the equivalent spring K_C.

Fistly, we form the $K_{eq.C}$ from TSWC – BS – TSW-B – BF-B.

Case 1: Compression force $F_{t.ed} \leq F_{rd.slip.1}$

In this case only the TSWC is active, therefore we obtain:

$$k_{eq.C.no.slip} := \frac{1}{\left(\frac{1}{k_{tswc}}\right)} = 44 \cdot mm$$

Case 2: Compression force $F_{t.ed} \geq F_{rd.slip.1}$

After the slip, 3 components are activated giving:

$$k_{eq.C.slip} := \frac{1}{\frac{1}{k_{tsw\text{-}b}} + \frac{1}{k_{bf\text{-}b}} + \frac{1}{k_{bs}} + \frac{1}{k_{tswc}}} = 1.832 \cdot mm$$

As the CWS and CWC have infinite stiffness putting them into the expressions presented below would not change anything, therefore the stiffness of the equivalent compression spring K_C is:

$$k_{C.no.slip} := \frac{1}{\left(\frac{1}{k_{tswc}}\right)} = 44 \cdot mm \qquad k_{C.slip} := \frac{1}{\frac{1}{k_{tsw\text{-}b}} + \frac{1}{k_{bf\text{-}b}} + \frac{1}{k_{bs}} + \frac{1}{k_{tswc}}} = 1.832 \cdot mm$$

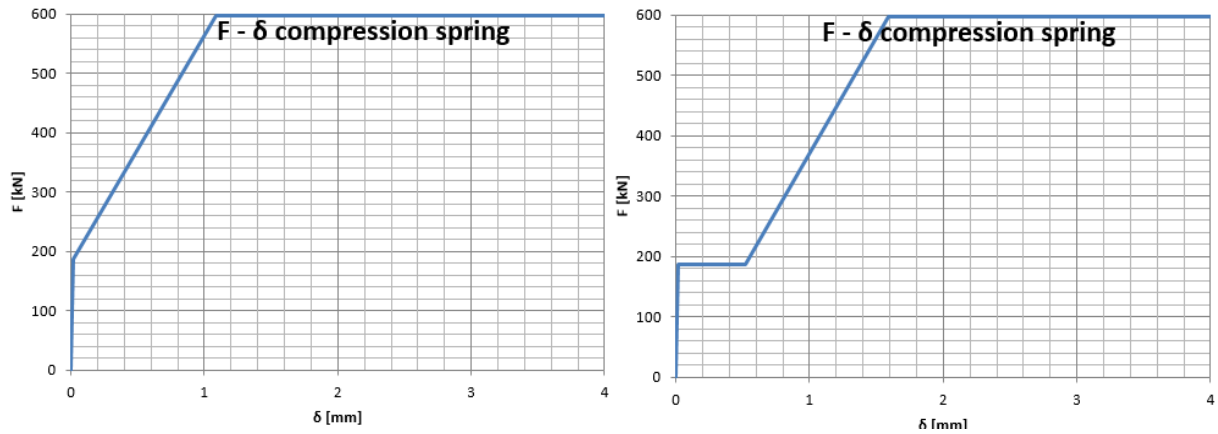

Figure III-20: F - δ diagram of the equivalent compression spring when considering δ_{slip1} (right) and without considering δ_{slip1} (left)– sagging bending

In Figure III-20 (right) represents the behaviour of the equivalent compression spring. We can note that until reaching the first slip, the behaviour is close to rigid. The initial stiffness changes after $F_{slip.1}$ is reached, providing a more flexible response until we finally reach the design resistance governed by CWS. Therefore F_{RD} = 598.3 kN.In the presently discussed picture $\delta_{slip.1}$was not considered.

Figure III-21 (left) represent the behaviour of the same spring but when $\delta_{slip.1}$is included. As mentioned, due to uncertainty of the slip length, the fact that it will not influence the response much and for the sake of the simplicity, the slip of the upper interface shall be neglected.

In the present case, ductility is taken as infinite and therefore, the limit presented on the graph is completely arbitrary and chosen so that the behaviour of the spring is fully presented.

With the data we now have, we can form the $S_j$for the sagging bending:

- Rotational stiffness valid before the slip of the upper interface occurs

$E := 210\,GPa$ $z_{eq} := 422\,mm$

$$S_{j.ini} := \frac{E \cdot z_{eq}^{2}}{\left(\frac{1}{k_{C.no.slip}} + \frac{1}{K_{T.no.slip}}\right)} = 2.086761 \times 10^{5} \cdot kN \cdot m$$

$F_{j.ini.limit} := 186.6\,kN$ $M_{j.ini.limit} := F_{j.ini.limit} \cdot z_{eq} = 78.745\,kN \cdot m$

- Rotational stiffness valid after the slip of the upper interface but before slippage of the damper

$$S_{j.slip1} := \frac{E \cdot z_{eq}^{2}}{\left(\frac{1}{k_{C.slip}} + \frac{1}{K_{T.no.slip}}\right)} = 5.324626 \times 10^{4} \cdot kN \cdot m$$

$F_{j.slip1.limit} := 450.8\,kN$ $M_{j.slip1.limit} := F_{j.slip1.limit} \cdot z_{eq} = 190.238\,kN \cdot m$

- Rotational stiffness valid after the slip of the friction damper

$$S_{j.slip.fd} := \frac{E \cdot z_{eq}^{2}}{\left(\frac{1}{k_{C.slip}} + \frac{1}{K_{T.slip}}\right)} = 2.452493 \times 10^{4} \cdot kN \cdot m$$

$F_{j.slip2.limit} := 490.1\,kN$ $M_{j.slip2.limit} := F_{j.slip2.limit} \cdot z_{eq} = 206.78\,kN \cdot m$

With the above presented we have fully defined the monotonic behavior of the joint for both hogging and sagging bending using two parallel spring, one representing tension and the other compression zone. We proceed to the validation of the so-called 2-spring model to evaluate whether this model can fairly represent the behavior of the joint.

III.3.3.3. Theoretical background of the spring translation

Earlier, when we were forming the 2-spring model of the innovative joint, it was needed to translate one of the horizontal springs to a different position, in order to be able to form an equivalent spring. The mentioned problem shall be addressed in the following paragraphs.

Let us imagine that we have a joint where the connection is realized by an end plate, subjected to bending. We make two cuts in order to form the horizontal spring model and we calculate the characteristics of the springs by using the component method. Let us assume our formed model has 2 springs, spring 1 with its stiffness K_1, resistance and lever arm from the compression centre h_1 and spring 2 with its stiffness K_2, resistance and lever arm from the compression centre z_{eq}. (Figure III-21)

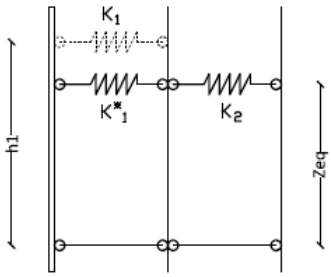

Figure III-21

In order to form an equivalent spring from springs 1 and 2, we need to move one of them and place them in a row. We will move the spring 1to be in line with the spring 2. The characteristics of the new spring will contain a sign *. To assess what kind of influence the change of the lever arm has on the stiffness we start from the following statement:

Bending moment is constant at the level of the cross section where the cut was made. Therefore:

$$M_1 = M_1^*(1)$$

Where moments for the different position of the spring can be expressed as:

$$M_1 = h_1F_1 = h_1k_1\delta_1 \;/\; (:\, h_1)$$

$$M_1^* = z_{eq}\, F_1^* = z_{eq}\, k_1^*\delta_1^* \;/\; (:\, z_{eq})$$

where $\delta_1$is the dilatation of the spring 1 and $\delta_1^*$is the dilatation of the spring 1^*.

If we divide both of the expressions with the corresponding lever arm and then place them into (1) we obtain the following:

$$h_1^2\Phi\, k_1 = z_{eq}^2\Phi^*\, k_1^*$$

whereΦ is the rotation of the section at position of spring 1 and $\Phi^*$is the rotation of section at position of spring 1^*.

From the Bernoulli theorem saying that the plane section remains plane after the deformation we can say that the rotation of a cross section is constant:

$$\Phi=\Phi^*$$

Bringing us finally to the wanted expression for the new stiffness when the spring is vertically moved to a different lever arm:

$$k_1^* = (h_1 / z_{eq})^2 k_1$$

From the derivation presented above we can conclude that the change of the stiffness of a spring when vertically moved depends on the squared value of the ratio between the previous and final position. When forming the M - Φ curve of a joint, we needed to account for the change of stiffness of a spring since we moved it. This expression was used to obtain the "new" value of the stiffness of the spring moved in case of hogging and sagging bending.

III.3.4. Validation of the 2-spring model

The present chapter will be dedicated to comparison between the results obtained by using the rotational spring model and the ones obtained from the 2-spring model in order to estimate the expected joint behaviour under the monotonic bending. The rotational spring model shall be used as a reference in order to validate the 2-spring model. Results are given ina form of M - Φ curves, presented in the Figure III-22.

If we look at the part of the curve presenting the behaviour under sagging bending, we can notice that we have obtained a full match. The behaviour obtained by using 2-spring model, referred as the Model 2, is identicalto the behaviour obtained by the rotational spring model, referred as Model 1. This is due to the match of the lever arms. Namely, when a rotational spring model is formed, the failure of the joint is governed by the failure of one of the rotational springs with the corresponding lever arm of that spring. Likewise, the change of the overall behaviour of the joint is governed by the slip occurrence that takes place in the 1st rotational spring, with a lever arm of 422mm in the case of sagging bending. The value of the M for each point is calculated by multiplying the force acting on the springs with the lever arm. Therefore, in the present case where the lever arm has a value of 422mm for both models in all significant points, the bending moment will be the same in each point. Similar thing happens with the rotation Φ. Since the rotation of the cross section can be obtained by dividing the dilatation of the horizontal springs by the lever arm, it is expected to have equal rotations for both models.

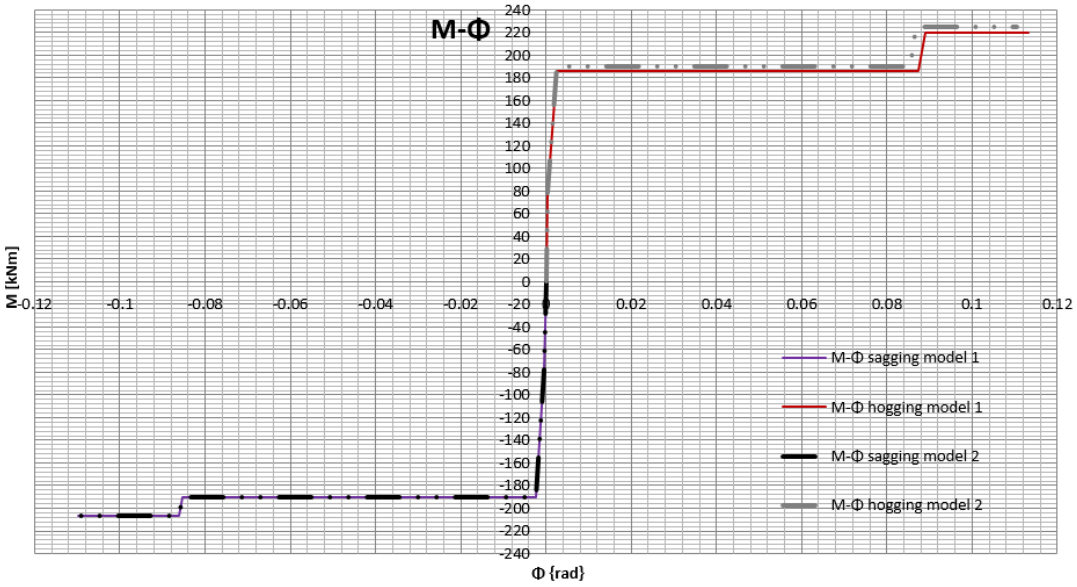

Figure III-22: Monotonic M - Φ curve comparison between Model 1 – Rotational spring model and Model 2 – 2-spring model

The difference between the results of the two models is visible in the part representing the behaviour under hogging bending. In the Model 1, both slip and the design resistance governing components are located in the 1st rotational spring with the lever arm of 412mm, while the Model 2 has a constant lever arm of 422mm. Due to the difference in lever arms we can notice that the 2-spring model is slightly overestimating the moment design resistance as well as the bendingmoment at slip, but the difference is below 3% and therefore negligible. Opposite happens for the joint rotation. As we already mentioned, rotation can be obtained by dividing the dilatation by the lever arm. If we look at the estimated slip of the friction damper, inducing a dilatation of 35mm, we will obtain different rotations depending on the lever arm we used, explaining the negligible underestimating of the joints rotation.

The comparison of the rotational stiffness of models 1 and 2 are presented below, in the Table 5. The difference between the rotational stiffness provided by the two models does not exceed 4.4% in any case, and mostly it stays below 2.2%, proving that the 2-spring model can fairly represent the stiffness of the joint.

Table III-2: Comparison of the rotational stiffness

/	Hogging			Sagging		
	S.j.ini [kNm]	S.j.slip1 [kNm]	S.j.slip.2 [kNm]	S.j.ini [kNm]	S.j.slip1 [kNm]	S.j.slip.2 [kNm]
Model 1	194240.6	50443.66	23310.61	204194.4	52949.72	24461.83
Model 2	196472.3	52415.51	24347.19	208676.1	53246.26	24524.93
F_{RD} [kN]	186.6	450.8	532.4	186.6	450.8	490.1
Δ 1-2 [%]	1.1	3.9	4.4	2.2	0.6	0.3

The literature [7] provide us with a criteria that can be used to check whether a difference between approximate joint stiffness and the actual joint stiffness has a significant influence on the frame behaviour. If the actual joint stiffness, which will in our case be the stiffness obtained from the rotational spring model, fits between the boundaries for variance of the actual and approximate stiffness, where the approximate stiffness is the stiffness obtained from the 2-spring model, then we can say that the difference has less than 2% influence on the frames bearing capacity, and therefore is negligible. In this way we can prove that the 2-spring model provides us with a satisfying value of initial stiffness. It should be noted that this approach is applicable only for the initial stiffness. The approach explain it this paragraph will be presented below.

The presented calculation are done for the case of anunbraced frame, with the dimensions equal to ones used later for the robustness assessment. Only the stiffness with the larges difference shall be checked, which will in this case be the initial stiffness under sagging bending.

According to the table 9.3 in the [7]the boundaries for the unbraced frame are given as:

$$S_{j.ini.lo} \geq \frac{24 S_{j.app} \cdot E \cdot I_b}{30 \cdot \left(E \cdot I_b\right) - L_b \cdot S_{j.app}} \qquad S_{j.ini.up} \leq \begin{cases} \dfrac{30 S_{j.app} \cdot E \cdot I_b}{24 \cdot \left(E \cdot I_b\right) - L_b \cdot S_{j.app}} & \text{if } S_{j.ini} \leq S_{j.ini.limit} \\ \text{infinitive} & \text{otherwise} \end{cases}$$

The needed input data are:

$S_{j.app} := 208676.1\,kN \cdot m$ approximate joint stiffness (Model 2)

$S_{j.ini} := 204194.4\,kN \cdot m$ actual joint stiffness (Model 1)

$E := 210GPa$ modulus of elasticity

$L_b := 5m$ beam length

$I_b := 5790\,cm^4$ second moment of area of the beam cross section

The result is presented in the Figure III-24. The red lines on the presented figure represent the upper and lower boundary limit. If the actual initial joint stiffness, in our case the one obtained from the rotational spring model presented with the grey line, is within the boundaries which as shown depend on the value of the approximate initial stiffness, presented with a blue line and

obtained from the 2-spring model, than the influence that the change has on the frames bearing capacity is negligible and the approximate value can be used for the frame analysis.

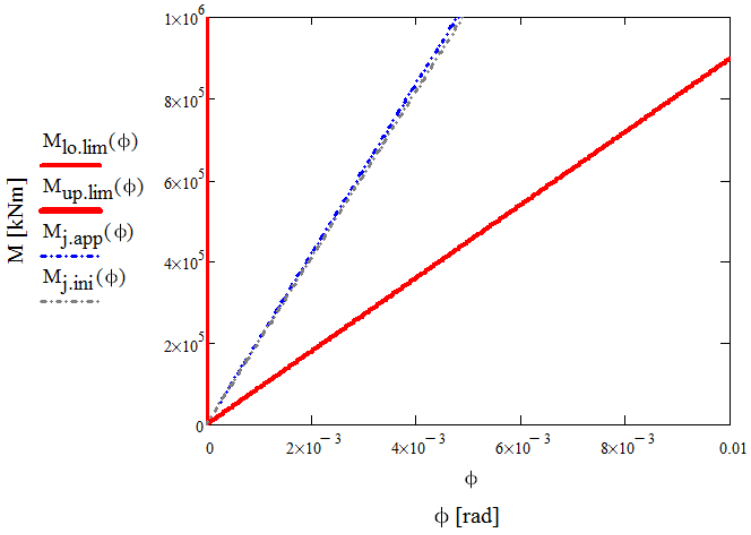

Figure III-23: Boundaries for variance between the actual and approximate initial stiffness

As seen on the graph presented in the Figure III-23, the $S_{j.ini}$is well within the boundaries, even almost completely matching the $S_{j.app}$. Therefore we can conclude that the 2-spring model provides us with a very accurate representation of the joints behaviour and that it can be used further on.

III.4. Conclusion

In the present chapter, in it was shown that the component method is a very useful approach which allowed us to estimate the behaviour of the innovative joint even thoughthis type of joint was not directly considered when the method was developed.

The friction damper as a component is not mentioned up to now and it could be that a way to improve and update the component method is by including the friction damper as a new type of component. Nevertheless, it was possible to analyse the joint by presenting the friction damper as a set of elements already included in the component method and therefore we were able to estimate the behaviour of the joint.

The 2-spring model had been developed and validated, leading to a conclusion that it is possible to represent a joint in such way, which will latter prove to be of great use in terms of analytical robustness assessment.

IV IMPLEMENTATION OF THE "FREEDAM" JOINT BEHAVIOUR INTO THE ANALYTICAL MODEL FOR ROBUSTNESS ASSESSMENT

IV.1. Introduction

In the previous chapters the available state of the art regarding analytical assessment of a frame response when subjected to the column loss situation had been presented. Several possibilities were given starting from the simplestmodel all the way up to the most complex and most complete one. The behaviour of the innovative joint was adequately modelled using the 2-spring modeland later validated, allowing its usage further on.

The present chapter aims at implementing the behaviour of the innovative joint defined by the 2-spring model into the routine, which will be formed in programing language Matlab, based on the model presented in II.2.4.

Analytical model addressed in II.2.4 represents the simplest model which considers the coupling between the hinge and global structure behaviour and it had been proven that it gives satisfying results of the frame behaviour during Phase 3 (Figure IV-1). Therefore, it was decided to use this simplifiedapproachtoanalyse the frame equipped with the innovative joint, as the present work representsthe first step towards fully modelling the behaviour of the a frame equipped with the innovative joint submitted to a column lost.

Primarily, the necessary properties of the frame shall be defined. A simplified substructure shall be extracted from the DAP followed by explanation of the expected behaviour of the substructure and the problem itself.

Further on, equations describing the behaviour of the substructure shall be derived usingstatic approach and introducing several assumptions. The obtained equations will be introduced into a solver using the programming language Matlab along with the definition of the behaviour of the spring. Parameters influencing the used solver shall be mentioned and the optimized for each case in order to obtain satisfying results. The path from the simplest programed behaviour to the full spring model behaviour shall be briefly explained

Finally, parametric study shall be conducted, and the obtained results analysed and discussed. The main idea is to show the different possible response of the substructure depending on the stiffness of the indirectly affected part and to discuss the behaviour and possible contribution of the innovative joint to structural robustness.

IV.2. Substructure model

The following subchapter shall be dedicated to the explanation of the sequence of getting from the frame submitted to a column loss to the simplified substructure that will be analysed.

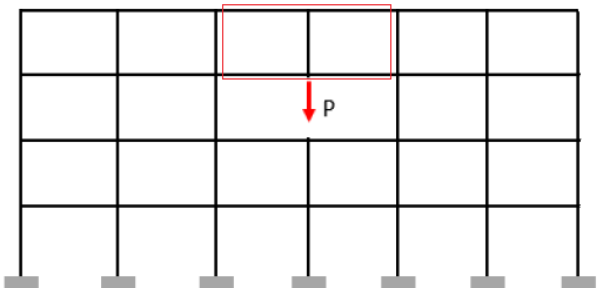

Figure IV-1: Frame subjected to a column loss simulation model [3]

As mentioned earlier, the behaviour of a frame submitted to a column loss can be simulated by a frame without the lost column subjected to a concentrated force **P**applied at the upper node of the mentioned column, as shown in Figure IV-1.

Following the procedure described in the state of the art, the considered frame presented in the Figure IV-1 will be divided into the directly affected part and indirectly affected part. The joints connecting the frames members have the same configuration as the innovative joint CYC 13 analysed in the previous chapter.Beams and columnsof the DAP are the same one forming the joint.

The directly affected part contains all the beams, columns and joints located just above the lost column, and is marked with a red rectangle in the Figure IV-1.In the present work, only the response of the lower beams of DAP will be investigated, as it had been proven that they adequately model the behaviour of the frame in the Phase 3. Indeed, as discussed in [2], the highest membrane forces develop at the lower beams of the DAP and therefore those will be the beams analysed. The beams and the joints of the substructure are the ones meet in the storey just above the column loss.

We extract the lower beams from the DAP, as shown in the Figure IV-2, and form the substructure which is defined as in the Demonceau model.

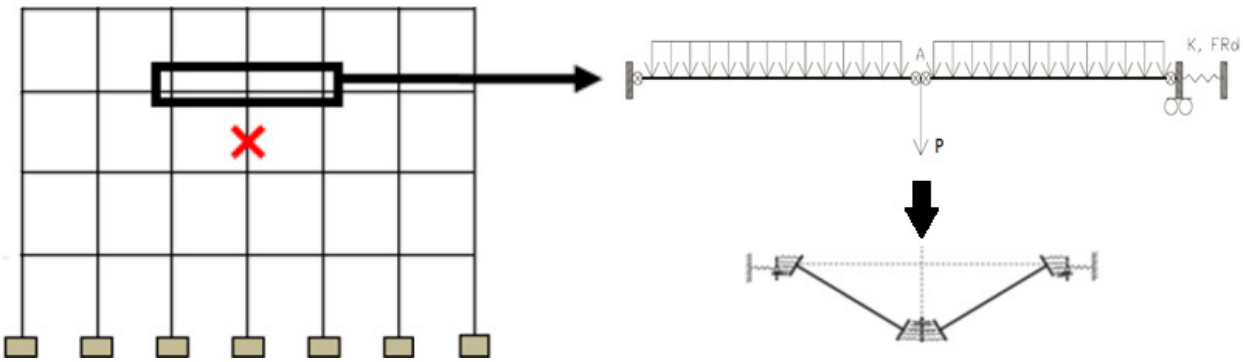

Figure IV-2: Definition of the substructure

Plastic hinges which develop at the beginning of the Phase 3 in the joints as the joints are partial strength, are modelled by horizontal springs. By modelling the plastic hinges as horizontal springs,

we are accounting for the coupling effect of the hinge and global frame behaviour. Moreover, as already mentioned, we are avoiding the direct definition of the M-N interaction curve of the joint, as this data is implicitly included in the definition of the springs. Finally, by simulating the hinges behaviour with horizontal springs we pass from the Demonceau model tothe new substructure, one as presented in II.2.4.

In the new substructure, apart from representing the hinge behaviour by the 2-spring model, we shall neglect the contribution of the uniformly distributed load as it was proven in [2] that it doesn't significantly affect the response of the structure during Phase 3.

Indirectly affected part is defined as the remaining part of the structure when we exclude the directly affected part. The geometry of the IAP will not be introduced, as we will include the behaviour of the IAP by placing a horizontal spring at the level of the analysed substructure. The only data needed to define the IAP is the stiffness $\mathbf{K_H}$ and design resistance $\mathbf{F_{RD.H}}$.The stiffness$\mathbf{K_H}$ of the spring represents the stiffness provided by the whole IAP of the frame. The ideaistovary the $\mathbf{K_H}$and perform a parametric study by varying the value of $\mathbf{K_H}$ in order to assess the response of frames with different properties.

A simplification shall be made within this work assuming that the IAP remains in elastic range during whole Phase 3 even though there is a possibility of forminga mechanism within IAP followed by failure. Therefore, the failure will not be governed by the IAP and there is no need to estimate the $F_{RD.H}$.Information on how to assess the characteristics of the IAP can be found in [4].

It should also be noted that the present analysis will consider the case of a 2-dimensional structure statically losing a column. No dynamic influences shall be considered. The work will be focused on the so-called Phase 3, when the mechanism forms and second order effects are developing. The behaviour during Phase 2, before the mechanism occurs, will be included in the result but as an approximation. The used model is not validated for simulating the behaviour during Phase 2.Coupling effects between the storeys of the DAP are not included by this model.

The substructurediscussed herein is taken to be symmetric for the sake of simplicity. That being so, the substructure shall be simplified even further by considering only half of it. The final substructure representing the half of the extracted one is formed respecting the theory of static symmetry. Thefinal substructure that will be analysed is presented in the following paragraphs.

IV.2.1. The final substructure disposition

The final substructure model, both in deform and initial stage, is presented in the Figure IV-3.The model consists of a beam supported on the left side by a restrain that can horizontally slide, and on the right side by a restrain which can freely slide in vertical direction. The slidingrestrain on the left is supported by a spring in horizontal direction, representing the influence of the indirectly affected part.

The plastic hinges formed in the partial strength joint are represented by 2 springs, one simulating the behaviour of the tension zone and another simulating the behaviour of compression zone. The springs activated in tension are labelled with number 1 while the ones acting in compression are marked as number 2. The detailed behaviour of the springs further to a loss of a column shall be addressed in IV.3.

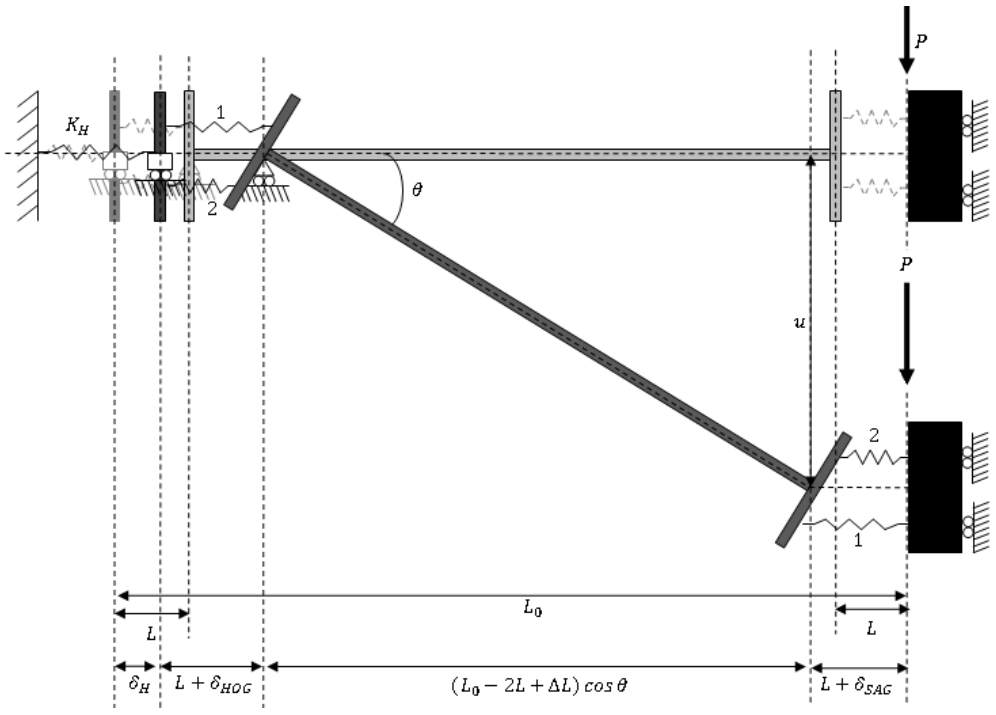

Figure IV-3: Final substructure model – compatibility of deformations

The value $\mathbf{L_0}$ represents the initial length of the beam. In this work length of the beam considered will be taken as $\mathbf{L_0 = 5m}$.

Initial length of the plastic hinge label as **L** in the Figure IV-3 for the case where the hinge develops in the joint is taken as equal to **0**. According to [3], when the yield zone is localized in the joint, which is assumed to be very short compared to the length of the beam.

ΔL corresponds to the elongation of the beam under tension force when the membrane forces develop and it is defined by the equation $\mathbf{\Delta L = F_H\,(L_0\text{-}2L)\,/\,(EA)}$.

Values $\mathbf{\delta_{HOG}}$ and $\mathbf{\delta_{SAG}}$ represent, respectively, the elongation of the plastic hinge at the level of beam axis in case of hogging and sagging bending.

Vertical displacement at the upper node of the lost column is labelled as **u**, while the rotation of the beam axis is referredas **θ**(rotation of the hinge).

P corresponds to the concentrated force associated to the column loss and is applied at the upper node of the lost column.

The horizontal spring characterised by stiffness$K_H$represents the influence of the indirectly affected part of the structure. The behaviour of the IAP, as previously explained, will be taken as fully elasticduring the whole Phase 3.

The following (Figure IV-4) figure will address the equilibrium of forces in the beam of the substructure.

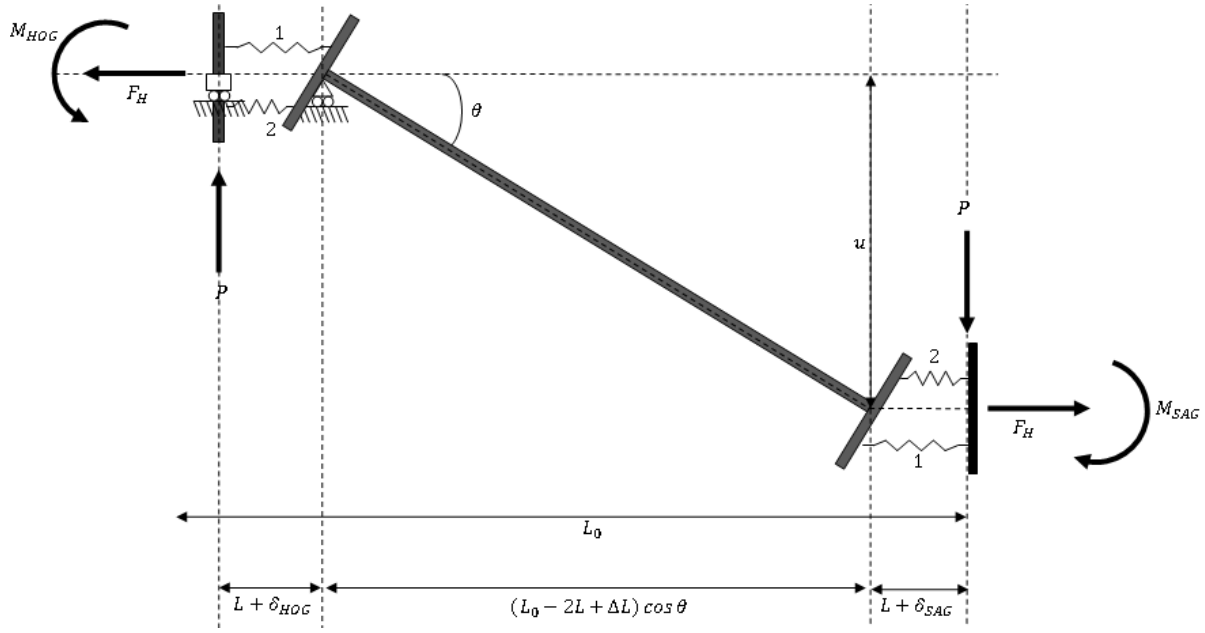

Figure IV-4: Equilibrium of forces

When thevertical displacement **u** reaches a significant value within the described substructure the membrane forces $\mathbf{F_H}$startdeveloping in the beams compensating the loss of the column carrying capacity and maintaining the structural integrity.Of course, the membrane forces cannotcarry the total load of the column unconditionally. The development of the catenary actions depends on the anchorage provided by the indirectly affected part and the ductility of the members forming the structure. In order to have a robust structure, ductility isnecessary condition.

The development of the P is limited by maximal deformation which can be reached, in the present case,within the joint. Unfortunately, for the given joint configuration no tests were performed assessing the joint ultimate rotation capacity or ductility of the components forming it. Therefore, we cannot claim with certainty what the ultimate plastic rotation of the joint will be. The problem will be addressed later, when the particular result of the analysis will be discussed.

The developed tension forces are transferred to the hinges, as presented in the Figure IV-5.The equilibrium in the hinge is obtained by the activation of the springs forming the joint. The sum of the forces in the springs equal the F_H, while the bending moment is equal to the forces in the springs multiplied with the corresponding lever arm.

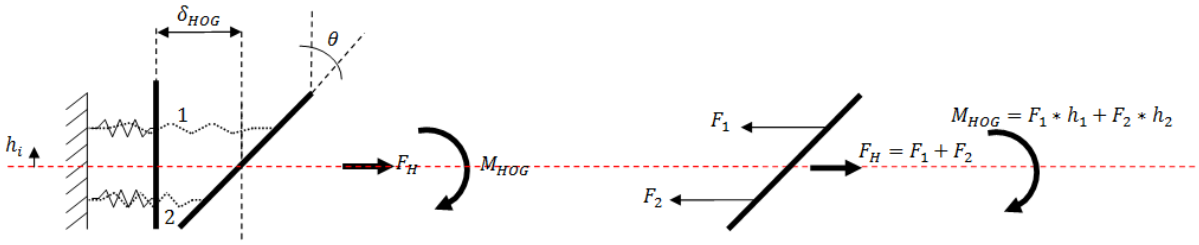

Figure IV-5: Forces in the hinge model [8]

The beams axis is taken as a reference line and therefore the distance h_i, which corresponds to the spring **i**,is taken as the distance from the spring to the axis of the beam. The beam forming the frame is IPE 270. Therefore, the distance from the level of springs to the beam axis are:

$h_{1.hog}$ = 142.5mm $h_{2.hog}$ = -269.5mm

$h_{1.sag}$ = -269.5mm $h_{2.sag}$ = 142.5mm

Considering all mentioned before, we can now derive the equations which analytically characterise our problem.

Table IV-1: Equations and unknowns used in the analytical procedure

Unknowns	Equations		
u	u = input data	(1)	
θ	$\sin(\theta) = u/(L_0-2L+(F_H*(L_0-2L)/(E_s*A_s)))$	(2)	Figure IV-3
δ_{HOG}	$L0-2L = \delta_H+\delta_{HOG}+\delta_{SAG}+\cos(\theta)*(L_0-2L+(F_H*(L_0-2L)/(E_s*A_s)))$	(3)	
δ_{SAG}	$\delta_H=f(F_H)$	(4)	
$\delta_{1,HOG}$	$\delta_{1,HOG} = \delta_{HOG} + h_{1.hog}*\theta$	(5)	Figure IV-5
$\delta_{2,HOG}$	$\delta_{2,HOG} = \delta_{HOG} + h_{2.hog}*\theta$	(6)	
$\delta_{1,SAG}$	$\delta_{1,SAG} = \delta_{SAG} - h_{1.sag}*\theta$	(7)	
$\delta_{2,SAG}$	$\delta_{2,SAG} = \delta_{SAG} - h_{2.sag}*\theta$	(8)	
$F_{1,HOG}$	$F_{1,HOG}=f(\delta_{1,HOG})$	(9)	IV.3
$F_{2,HOG}$	$F_{2,HOG}=f(\delta_{2,HOG})$	(10)	
$F_{1,SAG}$	$F_{1,SAG}=f(\delta_{1,SAG})$	(11)	
$F_{2,SAG}$	$F_{2,SAG}=f(\delta_{2,SAG})$	(12)	
F_H	$F_{1,HOG} + F_{2,HOG} = F_H$	(13)	Figure IV-5
δ_H	$F_{1,SAG} + F_{2,SAG} = F_H$	(14)	
M_{HOG}	$M_{HOG} = h_{1.hog}*F_{1HOG} + h_{2.hog}*F_{2HOG}$	(15)	
M_{SAG}	$M_{SAG} = h_{1.sag}*F_{1SAG} + h_{2.sag}*F_{2SAG}$	(16)	
P	$F_H*u+M_{HOG}-M_{SAG} - P\,(L_0-\delta_H) = 0$	(17)	Figure IV-4

The equations and the unknowns used to analytically address the problem of the frame behaviour further to a column loss will be presented in the Table IV-1. Most of the equations are derived from the above presented figures i.e. compatibility of deformations, force equilibrium and geometry. It should be underlined once more that the presented equations are derived based on a static approach, analysing the behaviour of a 2D frame subjected to a column loss, considering the response of the DAP.

For solving the presented system of equations the definition of the spring behaviour under the discussed situation is needed. This will be the subject of the following subchapter.

IV.3. The behaviour of the springs simulating the hinge

Earlier we have defined the behaviour of the joint when subjected to monotonic bending. The 2-spring model was formed, and the force-displacement law of springs forming the model was presented. The modelled behaviour of the springs is adequate for assessing the behaviour under monotonic loading,but to apply it in the robustness assessment model it will need to undergo some changes.

In order to define the F-δ laws of the springs forming the hinge we first need to address the behaviour of the substructurebefore and after the mechanism is formed.

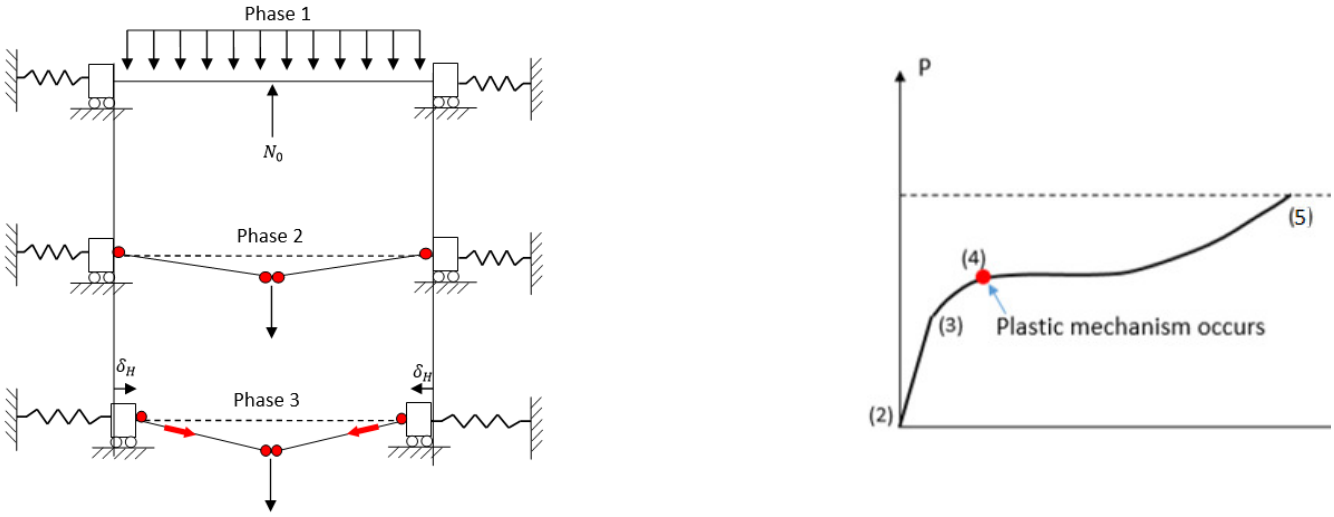

Figure IV-6: General behaviour

Figure IV-6 is introduced as a reminder of the expected general behaviour of the analysed frame. When the column starts to progressively collapse(Phase 2 from point (2) to (4) in theFigure IV-6),the load which the column cannot support anymore will be redistributed to the remaining structure. The joints in that case will be subjected to bending moments, loading one side of the joint in tension and another in compression.

As the collapse is progressing, the first plastic hinge will form at point (3). This would mean that one of the springs representing the joint reached the plateau. At this point we still consider our joint is subjected to pure bending.

With the further increase of vertical displacement, more of the springs will enter the plastic domain until finally all of them reached the plateau and the mechanism is formed at point (4). Until reaching this point the spring are still loaded in the same direction as in the beginning, tension springs in tension, springs firstly activated in compression further in compression.

Further vertical deformation, since now the mechanism is formed, will induce the formation of tension forces in the beams, related to the catenary actions. The tension forces are transferred to the hinges formed in the joints loading them with the combination of **M** and **N**. At this point, with the newly developed axial load included, the springs in tension are subjected further to tension, but for the springs in compression the unloading phase begins.

The growth of the vertical displacement generate larger tension forces in the hinges and the springs which were in compression start to unload and potentially, if the structure is able to develop significant membrane forces, pass from being active in compression to being active in tension.

Taking into consideration the above mentioned, we come to conclusion that in order to properly define the behaviour of the springs we need to take into account the possibility of the load changing direction in the case of springs subjected to compression. This will generate some changes in the 2-spring model we have derived.

Namely, the behaviour of the springs derived in the Chapter III concerned the behaviour valid under monotonic bending which means that the load acting on the spring does not change direction. That would mean that the derived behaviour laws are valid up to the development of the membrane forces. As the forces developing with the increase of the deformation are tension forces,the only the springs suffering some changes will be the ones primarily activated in compression.

The behaviour of the springs in tension is presented in Figure IV-7 and Figure IV-8.

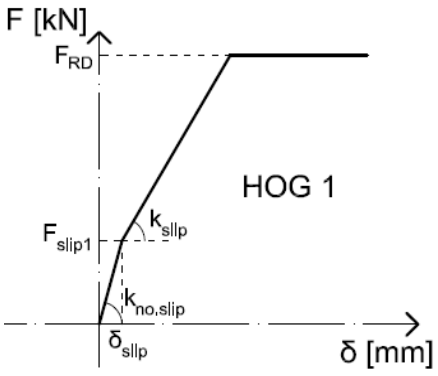

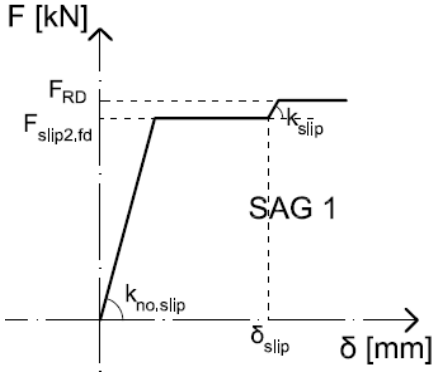

Figure IV-8: F - δ law of the tensions spring under hogging bending labelled as HOG 1

Figure IV-7: F - δ law of the tensions spring under sagging bending labelled as SAG 1

The presented springs, named**HOG1** and **SAG1** are just like the ones defined in the 2-spring model. The label**HOG** corresponds to the spring primarily subjected to hogging bending, while the label**SAG** represents the springfirstly subjected to sagging bending. Their behaviour was been discus in the Chapter III. The only thing that should be addressed is the ductility. The ductility of the components forming the springs will be considered unlimited within this work. When the result are obtained, they will be discus in terms of requested ductility needed to reach certain value of **P**. The values defining the presented spring behaviours can be found in Table IV-2.

Spring subjected to compression in Phase 2 are presented in Figure IV-9and Figure IV-10.

If we want the springs primarily activated in compression to adequately model the expected behaviour when membrane forces start to develop, defining their behaviour becomes a bit more complex.

In order to explain the spring behaviour let us assume that the properties and the configuration of the frame is such that the springs will reach the plateau in compression before the unloading phase commence, which corresponds to presented in Figure IV-9 and Figure IV-10.

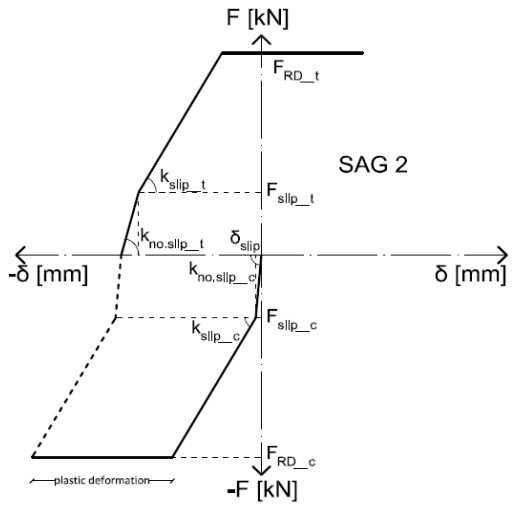

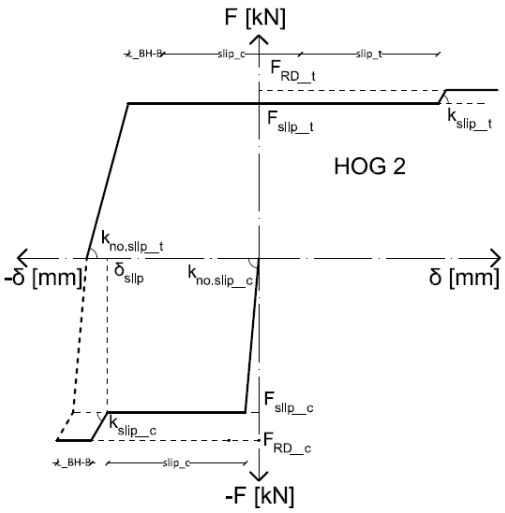

Figure IV-9: F - δ law of the compression spring under sagging bending labelled as SAG 2

Figure IV-10: F - δ law of the compression spring under hogging bending labelled as HOG 2

The first spring to be analysed will be the one named **HOG 2**. As presented in the Figure IV-4 with number **2** this spring belongs to the joint primarily subjected to hogging moment. During Phase 2

this spring is under compression. Before the compression force reaches the slip resistance of the friction damper $\mathbf{F_{slip_c}}$the response of the spring is almost rigid, due to the large stiffness defining the behaviour of that part of the F - δ law. After reaching the $\mathbf{F_{slip_c}}$the slip occurs until the bolts hit the end of the slotted hole. Additional stiffness is provided by the newly activated elements but the value of the stiffness is much lower that the initial one, changing the different behaviour law. Byfurther increasing the force we reach the plateau and bearing of the beam hammer head provides the ductility. Let us assume that after some plastic deformation develops, the membrane forces start to develop in the beams, and therefore in the hinges. This will activate the unloading phase, marked with a dashed line in the Figure IV-10. As the tension forces are progressively developing, the spring will still be in compression but the value of compression force will startto drop. The behaviour law in the unloading phase is governed by the same stiffness values as when the compression force was increasing. If the membrane forces are able togrow further, the spring will finally switch from compression to acting in tension. The spring is now working in tension but the bolts are still in the same position as they were when the slip in compression occurred. Indeed, in the unloading phase the force is still acting in the compression direction, and when it switches to tension the bolts cannot move until the slip resistance is reached. It was concluded that when the spring **HOG 2** starts working in tension, the stiffness governing its behaviour is actually the same one used for defining **SAG 1.** The spring **HOG 2** in tension experiences the same behaviour as **SAG 1**with a small difference in the slip length. When the slip limit is reached in tension, the slip will contain the slip length induced by bearing of the hammer head, the slip of the bolts of the friction damper which occurred while the spring was in compression and the slip length available in the direction of the tension force. The bolts will practically move from one side of the slotted hole to another. Further development of the membrane forces will activate the new components but now in tension until finally the plateau is reached. Theoretically, this is the behaviour that can occur and that is presented in the Figure IV-10. Once again, this scenario is only possible if the configuration, properties are such that the catenary actions develop in this specific way.

The behaviour of the spring **SAG 2** can be described in a similar way. The **SAG 2** corresponds to the spring in compression firstly subjected to sagging bending, located at the upper part of the joint as shown in Figure IV-4. Before the activation of the membrane forces we have almost a rigid behaviour up to the slip of the upper interface. After the slip new components are activated reducing the stiffness which governs the behaviour up to the point where the plateau is reached. Assuming that the membrane forces activate before the ductility limit of the spring is reached, the unloading phase commence. The unloading phase respects the same behaviour law defined by the stiffness in the loading phase, as presented by a dashed line in Figure IV-9. Further potential development of membrane forces would activate the spring in tension. The behaviour of spring **SAG 2**is governed by the same stiffness values as for**HOG** 1. Initial stiffness is valid until the slip in the upper interface occurs, then the modified stiffness governs the behaviour, until finally reaching the plateau.

The values of the stiffness and resistance defining the spring behaviour can be found in Table IV-2.

A comment must be made on the values presented in the table IV-2. As it can be concluded from the presented values the behaviour of the springs **HOG 1**, **HOG 2** and **SAG 1** is defined by the same values as the ones defining the 2-spring model under monotonic loading. The behaviour of the spring **SAG 2**, on the other hand, cannot be defined completely by the using those values.

Table IV-2: Values defining the F-δ laws of the springs

Values defining the F-δ law of the springs				
/	Hogging		Sagging	
	Hog_1_t	Hog_2_c	Sag_1_t	Sag_2_c
F_rd_t [kN]	598.3	490.1	490.1	**829.03**
F_rd_c [kN]	x	-532.4	x	**-818.75**
F_slip_t [kN]	186.6	450.8	450.8	186.6
F_slip_c [kN]	x	-450.8	x	-186.6
k_no.slip_t [mm]	5.934E	6.39E	6.39E	5.934E
k_no.slip_c [mm]	x	45.82E	x	44E
k_slip_t [mm]	1.446E	1.021E	1.021E	1.446E
k_slip_t [mm]	x	1.184E	x	1.832E
δ_slip [mm]	0.15	35.05	35.34	0.2

If we look at the values presented inTable III-1 we can conclude that the weakest component and the component which governs the failure of the spring**SAG 2**should be the column web in shear. But that will not be the case.

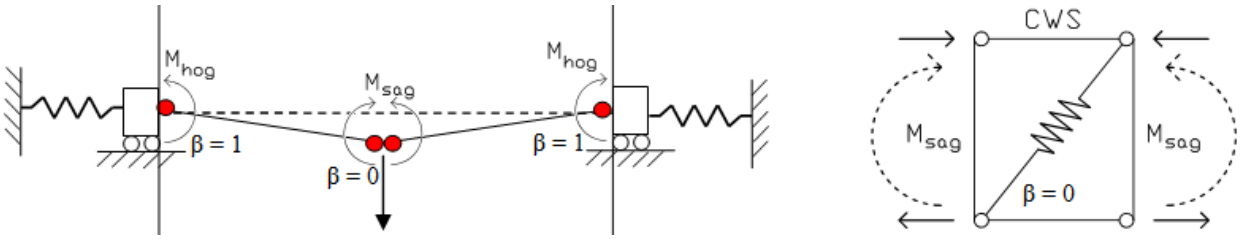

Figure IV-11: Extracted substructure model – column panel in shear under sagging bending

Figure IV-12 shows us the disposition of our model. As mentioned, the extracted substructure is symmetric. Therefore, the moments $\mathbf{M_{sag}}$ acting on the joint subjected to sagging are considered equal. If we observe the behaviour of the column panel, we can see that in this case, the shear forces acting on the panel will annul each other. That is why the transformation parameter **β**, which transforms the shear force acting in the panel to compression and tension force acting at the level of the connection, is in this case equal to zero. According to the recommendations found in the EN 1993-1-8 Table 5.4, for a double-sided joint with balanced bending moments, **β** should be taken as β=0. If we go with this value to the expression for the design resistance of the column panel in shear we obtain the following:

$$F_{RD.CWS} = \frac{0.9 \cdot f_y \cdot A_{vc}}{\beta \cdot \sqrt{3} \cdot \gamma_{M0}} = \text{inf}$$

Therefore, we can conclude that the column panel in shear will not be governing the design resistance of the spring **SAG 2**. The resistance will be governed by the next weakest component. In tension that will be T-stub flange in bending while in compression the governing component is column web in compression.

The design resistance of CWC depends also on the value of **β**. The value **β** is governing the reduction factor **ω**, which accounts for the possible interaction with shear, included in the design resistance equation of the component. Therefore, the $F_{RD.CWC}$will not have the same value as in 2-spring model where was$\beta = 1$. The new value will be obtained by introducing the new **ω,** which for $\beta=0$ is$\omega=1$ according to [7]. Therefore we obtain:

$$F_{RD.CWC.new} = \frac{\omega_{new}}{\omega_{old}} \cdot F_{RD.CWC.old} = \frac{1}{0.83} \cdot F_{RD.CWC.old} = 818.75\text{kN}$$

We have obtained the new value of resistance of the component column web in compression which is governing the failure in compression. The design resistance for the component governing the failure in tension, T-stub web in bending, is the same one calculated when 2-spring model was developed under monotonic loading. The stiffness defining the spring**SAG 2** will remain the same as for monotonic loading. The change of **β**will not influence the stiffness as both CWS and CWC were already considered infinitely stiff.

Having the failure governed by the T-stub in bending in the tension zone provides a ductile failure mode. On the other hand, in the case when the column web in compression is governing the failure, ductility is quite questionable. According to [7] a significant deformation capacity may be expected from this component as long as instability is not governing the failure of the component. In our case the failure will not occur due to instability, but nevertheless it is doubtful whether enough ductility will be provided by this component in order to form a plastic hinge and ensure plastic rotation.Therefore, the result obtained from the analysis shall be analysed with respect to the before mentioned. The discussed matter will be addressed further when the actualresults of the following analysis as obtained and the joint behaviour under the column loss scenario is assessed.

The joint subjected to hogging bending, since the substructure is extracted from themiddle part of the frame, would also have a moment acting on the other side of the joint. As we can't say for sure what is the value of that moment, we will consider the ratio between the one acting on the joint considered in the substructure and the moment on the other side as larger than zero, which would correspond to the value of $\beta=1$ according to [7]. That would mean that the values obtained for the monotonic loading remain correct in case of joint subjected to hogging bending.

The complexity of the prediction of the springs behaviour lies in the fact that the unloading phase can occurs at any point. Depending on the moment when the catenary actions develop and how large is their increment with respect to the vertical displacement (depends on the stiffness of the IAP) the unloading of the compression springscan occur while they are in elastic range before the slip, or after the slip but before plateau is reached. Simply said, at any given time. Therefore, the real behaviour varies for different configurations of the structure and does not have to look as one presented in Figure IV-9 and Figure IV-10.

Since we cannot predict for sure when and whether the unloading phase is going to occur before running the analysis and obtaining some results, it is needed to adequately mathematically and logically define the potential behaviour of the springs in Matlab. From the discussion presented above it can be concluded that defining the general behaviour of the springs, to take into account any possible situation, will be quite challenging.

Therefore, it has been decided to start from a simpler behaviour model and by analysing the obtained results, come to a model which will accurately represent the realistic behaviour of the springs for different values of stiffness belonging to the indirectly affected part of the structure.

The following subchapters will address the routine developed using programing language Matlab and the spring models used to represent the hinge.

IV.4. Substructure routine – Matlab program

We have defined the equations analytically representing the behaviour of the substructure. In order to solve the system we input the value of the vertical displacement **u**and for the chosen input obtain the value of the force **P** which corresponds to the value of the redistributed forcewhich the column is no more able to support. The derived system of equations represents anon-linear system of equations and therefore it is necessary to use iterations and a mathematical solver in order to obtain results.

As mentioned before, University of Liege has developed the analytical procedures for dealing with the problem of a frame subjected to acolumn loss. In some of the available researches regarding this topic as [8], Matlab was used in order to solve the system of equations. Couple of routines made using Matlab which addressed similar problems were available. Therefore, it was decided to form a program used for solving the system of equations by modifying the already existing program.

The program most suiting the considered problem within this thesis was the one connected to the [8]. The Matlab routine developed there has the same number of springs and therefore the same number of equations. In the following, the modified program shall be discussed. The Matlab routine is presented in AppendixB.

The routine consists of a main program named "**substructure_slab1_joint**" and several subprograms.

Main program "**substructure_slab1_joint**" contains the input data related to the frame, position of the springs with respect to the beam axis et cetera. The increment of vertical displacement **u_step** and the maximum value of the vertical displacement **u_limit,** value of **u** when the program stops further calculations, are also presented as input data in the main program. The main program contains also the mathematical solver used for solving the presented system of equations. The function used to solve the equations is called "**fsolve**".The mentioned solver "**fsolve**" calls the equations to be solved from a subprogram named "**myfun_slab1_joint**". In this subprogram the equations are defined.

The equations contain, apart from the equations obtained from geometry, forces equilibrium and compatibility of deformations, the laws defining the behaviour of the springs, 4 of them representing the hinges, and 1 representing the influence of the indirectly affected part. The behaviour of each of the springs are defined as functions in separate subprograms named "**F_spring_hog_1**","**F_spring_hog_2**","**F_spring_sag_1**","**F_spring_sag_2**" for the 4 springs representing the hinge behaviour, and "**fh_linear**" for the spring representing the IAP. Therefore, in order to solve the equations, the solver calls the equations defined in "**myfun_slab1_joint**" which calls the values defining the springs from other subprograms.

The program works like this. Firstly the input data is defined. Then the vector of initial points**x0**is formed. In order to solve the system, the solver uses the **x0**as a starting point for finding the system solution. The values of all the variables forming the equations in "**myfun_slab1_joint**" are at the beginning taken as 0 by forming the first row of the matrix **results** with all zeros. The **u**in the first iteration is defined by summing the previous value of **u**(which is 0)with **u_step** forming the new value of **u** which will be implemented into the equations. The equations are solved for the new value of vertical displacement **u**and the results are stored in a new row of matrix **results**. Results are also stored in a vector **x** which will be used to define the new starting point for solving the system for the next value of **u**. New value of initial points vector **x0**is formedby adding the values stored in **x**, moving the starting point of the away from the previous solution. With the new value of **x0**defined, the equations can be solved for a new value of **u**. The process is repeated until **u_limit**is reached when the program ends the calculations.

As it can be deduced from the presented explanation of the program, several values can influence the accuracy of results. The vector of initial points **x0**, **u_step**, but also function tolerances **TolX** and **TolFun** of the used solver **fsolve**can greatly influence the accuracy of results. In order to have the solver converging until the end of calculation, for each posed problem the right combination of the mentioned parameters has to be used. This will pose a problem latter on when the analysis are conducted as they showed that the program, due to the complexity of the demanded calculations, is quite sensitive to any change of parameters.

IV.5. The primary models of the spring behaviour

As mentioned, the behaviour of the springs depend on variety of parameters and in order to come to asolution which faithfully represents the real behaviour, we will start from a simpler model.

It had been decided that, as a starting point, the springsshould be represented by the simplest models – rigid-plastic behaviour and linear-plastic behaviour. It is obvious that those laws cannot represent the estimated behaviour of all of the springs in reality, but the idea was to run a parametric study in order to see how the program reacts to the change of different parameters such as **x0**, **u_step**, **TolX**, **TolFun**and to see if it is possible to obtain some reasonable results. Also if we analyse in more detail the expected behaviour of the spring presented in Figure IV-7 to Figure IV-10, we can come to a conclusion that it would be possible to represent the behaviour as a combination of several linear-plastic behaviour, and by properly combining them to obtain the full response. The primary results will be analysed a hopefully contribute to making the decision how to proceed with the modelling.

IV.5.1. Testing the program response – rigid plastic and linear plastic behaviour law

Firstly, an attempt of implementing the rigid-plastic behaviour was made. It had been noted that the initial stiffness of the springs is rather high, therefore it was assumed that representing the spring behaviour by using combination of a rigid-plastic behaviours, as presented in Figure IV-2 would not have diminished the credibility of the results.

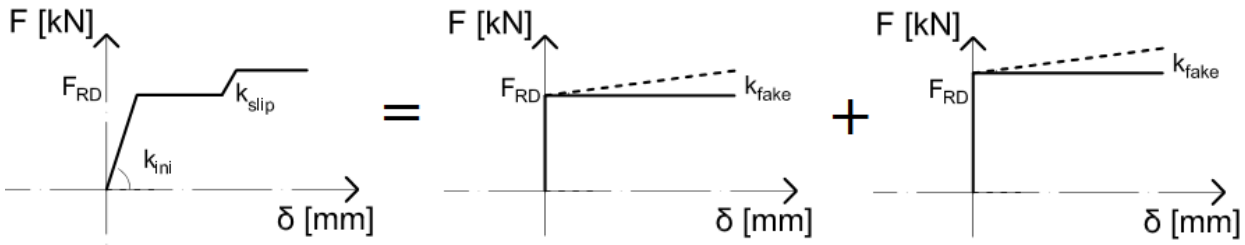

Figure IV-12: General idea how the spring behaviour could be separated into more simple ones using rigid-plastic law

The idea was to split the behaviour of the spring containing the friction damper into 2 behaviour, one representing the behaviour before the slip, the other representing the behaviour after the slip. The same analogy would be used for the remaining springs.

It can be noticed in Figure IV-12 that a concept of "fake stiffness" had been introduced. Namely, the main idea behind the introduction of the so-called "fake stiffness" was to help the program avoid divergence and singularity. If the spring laws were introduced in the program without any stiffness, it would be likely to expect that the solver would not be able to finalize the calculation properly due to the singularity cause by the plateau. Therefore, $\mathbf{K_{fake}}$ was introduced, hoping that reasonable results could be achieved for a value of $\mathbf{K_{fake}}$ which would not significantly affect the expected real behaviour of the springs.

After running the routine made in Matlab several times, modifying the value of $\mathbf{k_{fake}}$ but also the other mention parameters influencing the stability of the solver, it was concluded that the implementation of the present spring model into the routine cannot give reasonable results.

The solver was not able to provide any result unless of the value of $\mathbf{K_{fake}}$was significantly high and even then, there was no consistency. For a small change of $\mathbf{K_{fake}}$the initial value of the force **P**, taken as the value at the beginning of the Phase 3, was significantly varying. Therefore, this idea was abandoned.

The second idea is presented in the Figure IV-13. The principle is the same as in the previous attempt, to split the behaviour of the spring containing the friction damper into 2 behaviour, one representing the behaviour before the slip, the other representing the behaviour after the slip and use the same analogy for other springs.

Presented model is closer to the real behaviour of the expected real behaviour of the springs as it includes the initial and stiffness after the slip. It was expected that the program will have a problem to pass from the linear part to the plastic as the change of the slope in significant. Therefore, the concept of using $\mathbf{K_{fake}}$was retained.

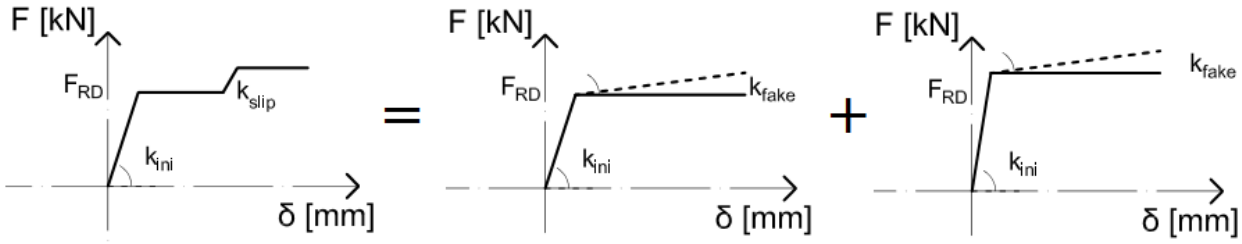

Figure IV-13: General idea how the spring behaviour could be separated into more simple ones using linear-plastic law

The results obtained were encouraging. The solver was able to "catch" the correct solution of the equation system from the beginning and to pass from linear behaviour of the springs to plastic behaviour with a value of $\mathbf{K_{fake}}$which was negligible.

It was concluded at this point that modelling the response of the system by separating it into the behaviour before and after the slip might possible. Before going with the mentioned approach, the decision was made to try to model a more complex behaviour of the spring a see if the program is able to deal with it.

IV.5.2. Simplified-full spring behaviour model

Passing from the first attempt to the here presented model had been a long way. As the analysis done in between will not generally contribute to better understanding of the problem or results, they will not be mentioned. The thing worth mentioning is that the importance of the parameters **x0**, **u_step**, **TolX**, **TolFun**and $\mathbf{K_{fake}}$ was confirmed on the way. It will be latter shown that the valid results are only possible if the right combination of the mentioned parameters is used.

The program was able to deal with the linear-plastic formulation of the spring behaviour and therefore it had been decided to try to model with a behaviour similar to the full behaviour of the springs, but including some simplifications.The idea was to see whether the program solver can deal with the extreme slope changes in the spring laws which correspond to the occurrence of the slip of the friction damper and reaching the design resistance i.e. plateau.

Figure IV-15 presents the potential behaviour of the springs programmed for this model. For the springs fully in tension, SAG 1 and HOG 1, the full behaviour was programmed right away. As the do not enter the unloading phase and therefore have a simpler behaviour, it had been decided to include their full behaviour from the beginning. By doing that, the slip and the activation of new stiffness was considered as well as the slip of the upper interface and the corresponding change of the stiffness.

The simplification of the behaviour was used in case of the springs which are acting primarily in compression, HOG 2 and SAG 2. For the spring HOG 2, the simplification consists of neglecting the behaviour change after the slip, and considering only one approximate stiffness governing the behaviour of the whole unloading phase and the tension phase. The slip resistance was considered as the ultimate spring resistance. As for the SAG 2, full behaviour was considered up to the unloading phase. The behaviour under unloading phase is modelled by approximate value of stiffness while the phase when the spring is in tension is modelled by a stiffness valid before the slip. The plateau is considered to occur when the slip resistance of the upper interface is reached.

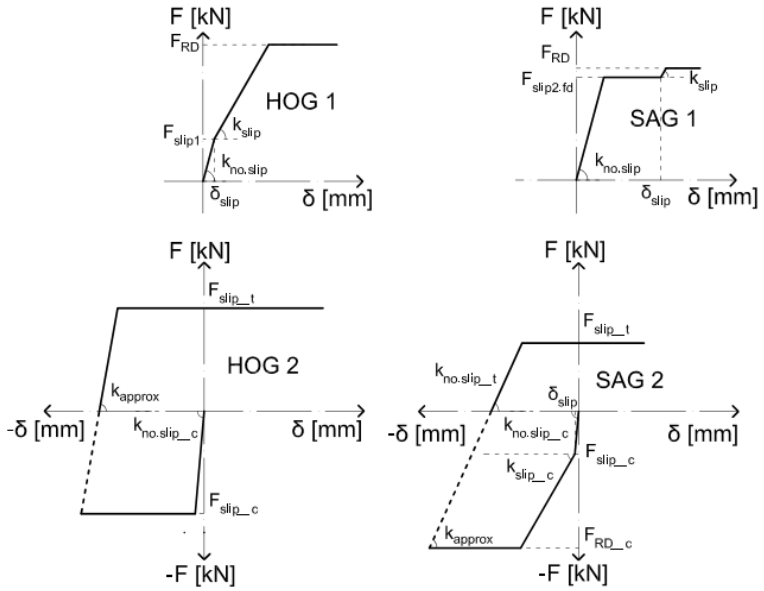

Figure IV-14: Behaviour of the springs considered in the simplified spring model

The values defining the springs are presented in Table IV-3.For better understanding the Figure IV-14 should be compared with Figure IV-7 to Figure IV-10.

Table IV-4: Values defining the simplified spring model

Values defining the F-δ law of the springs				
/	Hogging		Sagging	
	Hog_1_t	Hog_2_c	Sag_1_t	Sag_2_c
F_rd_t [kN]	**598,3**	490,1	**490,1**	**829.03**
F_rd_c [kN]	x	-532,4	x	**-818,75**
F_slip_t [kN]	**186,6**	**450,8**	**450,8**	186,6
F_slip_c [kN]	x	**-450,8**	x	**-186,6**
k_no.slip_t [mm]	**5.934E**	6.39E	**6.39E**	**5.934E**
k_no.slip_c [mm]	x	**45.82E**	x	**44E**
k_slip_t [mm]	**1.446E**	1.021E	**1.021E**	1.446E
k_slip_c [mm]	x	1.184E	x	**1.832E**
k_approx [mm]	x	**26.1E**	x	**22.9E**
δ_slip [mm]	**0,15**	35,05	**35,34**	0,2

Table IV-3: Parameters influencing the result

Kh [kN/m]=	5000
K_fake [kN/m]=	0
u_step [m]=	0,0005
X0 =	0,00001
TolX =	-5
TolFun =	-6

Before running the program the mentioned parameters need to be defined. The parameters which greatly influence the results are presented in Table IV-4. Indeed, due to the complexity of the problem, the solver can experience instability for a small change of any of the parameters. Therefore, to obtain a good result, it is needed to find the suitable combination of the input data and later to analyse the results in detail and check for any inconsistency.

The stiffness of the IAP is taken as 5000 kN/m for the present case. This value is arbitrary and it was considered because the program gives good results which will lead to important conclusions.

The results are presented in the Figure IV-15. In the following obtained results shall be analysed.

In the upper left corner of the Figure IV-15 we can see the P-u curve which represents the response of the analysed substructure. Just as a reminder, **P** corresponds to the force previously supported by the column redistributed to the remaining structure while **u** is the displacement of the upper node of the column lost.

As we can see, the response is linear up to the areamarked in red which corresponds to the beginning of the slip. The red marker highlights the moment when the first springs will reach the slip limit and when the significant rotation of the joint will occur. It should be noted that the mechanism is not formed yet. The plateau in the spring behaviour is caused by the occurrence of the slip of the friction damper.

The part of the curves between red and green markerrepresents the slip of the friction damper until reaching the end stroke limit, highlighted with the green marker. As presented in the F_H - δ_H graph the membrane forces are already developing in this part, even though no plastic hinge developed. This occurs due to the fact that the slip of the damper allows for significant rotation of the joint before the mechanism is formed, in our case around 0.08 rad. The presented feature will be discussed in more detail when the full behaviour is modelled.

marker is reached, which corresponds to the beginning of the development of the membrane forces, we can notice the unloading phase of the spring SAG 2. Since the force in the spring SAG 1 is

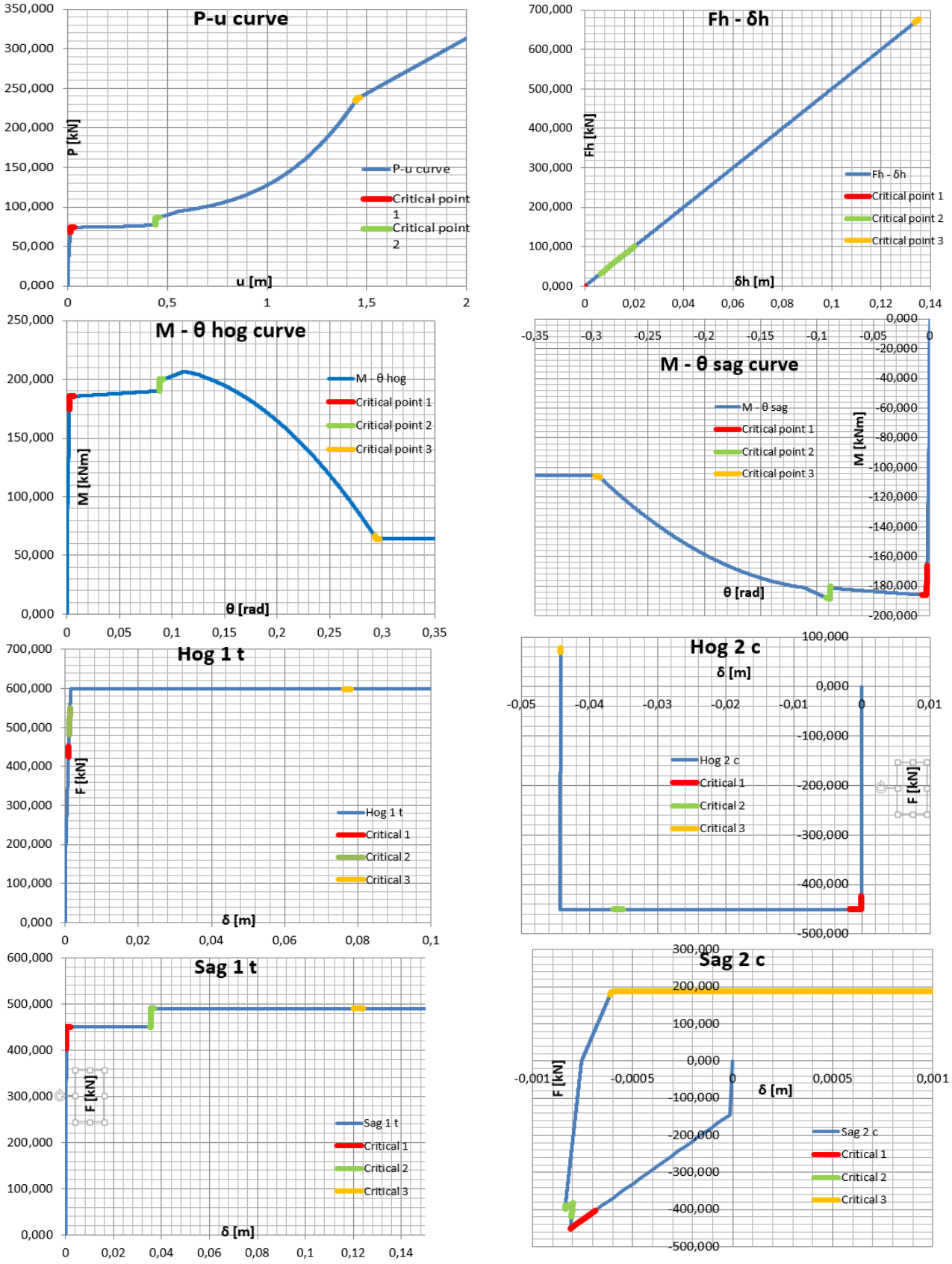

Figure IV-15: Result of the simplified model analysis

constant, if the joint was subjected only to bending moments, the force in the other spring should have also been constant. But, due to the newly added tension actions, the joint is not subject to the pure bending any more but to interaction of M and N, “pushing” the spring SAG 2 towards tension. When the green marker is reached the force in the spring SAG 1 suddenly increases as a consequence of the new activated components after reaching the slip limit, a change of the value of the force in the spring SAG 2 occurs. In order to form an equilibrium, the force in the spring SAG 2 must change direction again and increase in compression. The membrane forces are still there but their increment in this moment is smaller than the increment of the force in the spring SAG 1, leading to such behaviour. The reason why the sudden change in the force direction is visible is the fact that for the unloading phase an approximate value of stiffness was used. Therefore, even though it does not represent completely accurately the expected behaviour of the springs, the simplified model greatly contributed to the understanding of the spring behaviour. At this point it was obvious that a lot of attention should be dedicated to the definition of the spring behaviour in the program, in order to accurately model the possible behaviour.

Interesting behaviour of the springs subjected to sagging can be observed. Namely, until reaching the red marker, the SAG 1 works in tension, while the SAG 2 is in compression. When the red

The green marked represents the moment when the end stroke is reached and when the additional stiffness activates. At this point the mechanism start to form. The structure has no more the first order stiffness and the support is provided by the indirectly affected part.

The membrane forces develop further on as the vertical displacement increases until both of the springs in sagging reach the plateau in tension. The progressive deformation occurs in the hinge at this point (yellow marker). As a consequence of the progressive deformation concentrated in the hinge, membrane force cannot continue to develop. But the **P** force increases further despite the mentioned fact. This comes as a consequence of the second order effects. As the vertical deformation is able to grow even further, the rotation angle raises increasing the value of the projection of the membrane forces. In this way, force **P** can still increase at the expense of the second order effects without any change in the membrane force. The mentioned phenomena is characterized by the presented change of slope in the P - u curve.

All of the above said is valid under the condition of infinite ductility of the elements forming the hinge which is the only limitation for the development of the membrane forces.

Conclusion:

The simplified spring behaviour model provided us with useful information about the phenomena occurring within the general behaviour of the frame equipped with the innovative joint subjected to a column loss is assessed. The sudden change of the direction of the force in the compression spring was noticed, and the lack of accuracy in the used stiffness contributed to it. The change of the behaviour after both of the springs reach the plateau wasnoted, which will prove latter on to be important for the explanation of the obtained results.

The conducted analysis had also highlighted the advantages and drawbacks of the currently used program, allowing for its improvement. To sum it all up in one sentence, the presented simplified model gave a great contribution to the development of what is about to be presented next, and that is the full spring behaviour model.

IV.6. Full spring behaviour model – Parametric study

From the previously conductedanalysis conclusions have been made which lead to the improvement of the programed spring behaviour and to the better understanding of the problem itself. The program had been modified and full expected behaviour of the springs was introduced. Due to the specificity of the possible spring behaviour already explained in the chapter IV.3, programing the full behaviour posed quite a challenge. In order to achieve the full behaviour and cover all the possibilities, part of the spring behaviour had been modelled by comparing the force limits defining the behaviour ($\mathbf{F_{RD.slip}}$, $\mathbf{F_{RD}}$) with the values of the force in the springs obtained in the previous iteration. This makes the program partly sensitive to the change of the iteration step, which shall be latter addressed.

The final model of the spring behaviour is presented in Figure IV-16.The table containing the values defining the presented spring behaviour is included in the figure as a reminder. The modelled behaviour is exactly the same as described in IV.3. As presented by the dashed line some additional stiffness, previously defined as **K_fake**, will be added when necessary to the part of the behaviour which should be fully plastic. In order to avoid divergence and possible singularity, including fake stiffness will prove to be necessary in some cases.

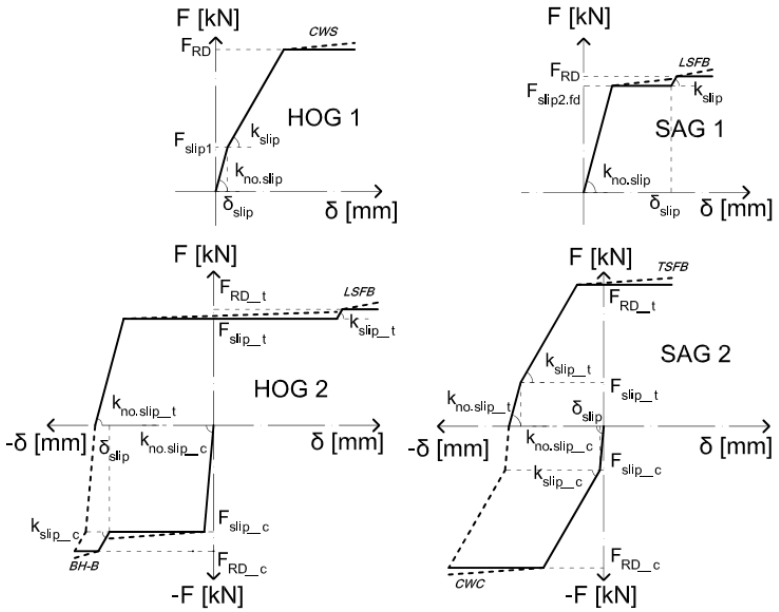

Values defining the F-δ law of the springs				
/	Hogging		Sagging	
	Hog_1_t	Hog_2_c	Sag_1_t	Sag_2_c
F_rd_t	598,3	490,1	490,1	829.03
F_rd_c	x	-532,4	x	-818,75
F_slip_t	186,6	450,8	450,8	186,6
F_slip_c	x	-450,8	x	-186,6
k_no.slip_t	5.934E	6.39E	6.39E	5.934E
k_no.slip_c	x	45.82E	x	44E
k_slip_t	1.446E	1.021E	1.021E	1.446E
k_slip_c	x	1.184E	x	1.832E
δ_slip	0,15	35,05	35,34	0,2

Figure IV-16: Modelled spring behaviour

In the following a parametric study shall be conducted. The idea is to assess the behaviour of the analysed system and the behaviour of the springs representing the innovative joint for different values of the stiffness of the IAP. Therefore, the $\mathbf{K_H}$shall bae varied and for some characteristic cases the results will be presented and commented.All the analysis will be conducted considering infinite ductility of the elements. As no data regarding the real ductility is available the results will be discussed assuming that it will be possible to reach the progressive yielding without the collapse.

It had been mentioned that a set of parameters influences the behaviour of the solver. Figure IV-17contains tables giving the used value of $\mathbf{K_H}$ but also the values of the parameters important for the solver. In order to obtain the solution it is needed to use the right combination of all the parameter in the table.

Kh [kN/m]=	0	Kh [kN/m]=	2500	Kh [kN/m]=	5000	Kh [kN/m]=	10000	Kh [kN/m]=	25000
K_fake [kN/m]=	0	K_fake [kN/m]=	0	K_fake [kN/m]=	20	K_fake [kN/m]=	20	K_fake [kN/m]=	20
u_step [m]=	0,0001	u_step [m]=	0,0005	u_step [m]=	0,0005	u_step [m]=	0,0002	u_step [m]=	0,0005
X0 =	0	X0 =	0	X0 =	0	X0 =	0	X0 =	0
TolX =	-5	TolX =	-5	TolX =	-5	TolX =	-4	TolX =	-5
TolFun =	-6	TolFun =	-6	TolFun =	-6	TolFun =	-5	TolFun =	-6

Figure IV-17: Tables containing values used for chosen K_H

The values of K_H for which the results shall be presented were chosen with the aim of presenting the expected frame response for different possible behaviour of the springs, regarding the beginning of the unloading phase, activating additional elements after slip etc.

IV.6.1. Full spring model 1 – $K_H = 0$

The results of the presented model shall be used for the validation of the Matlab routine. The values of the other parameters of influence are presented in Figure IV-17.

Within this model it is considered that the indirectly affected part provides no lateral stiffness after the mechanism is formed. Consequently, as there is no anchorage provided by the IAP, no membrane forces should develop. It should also be expected that the M –θ (moment-rotation) curve of the joint will look like the one obtained for the monotonic loading as only bending moments should develop (interaction with shear is neglected within the work). The results are presented in the Figure IV-18.

In the upper left corner of the Figure IV-18 we can see the P – ucurve, which represents the main results of the analysis. The other presented data contains the F_H - δ_H diagram, representing the development of the membrane forces, the M – θ curves of both joints and the F – δ diagrams of the springs forming the joint. The markers are used to highlight the changes in the behaviour law of the P – u curve which characterise the response of the analysed structure and to show what is occurring in the joints and springs at that time, leading to this change of behaviour.

The substructure modelling the behaviour of the frame subjected to loss of a column exhibits a linear response up to the occurrence of slip, which is marked in red.

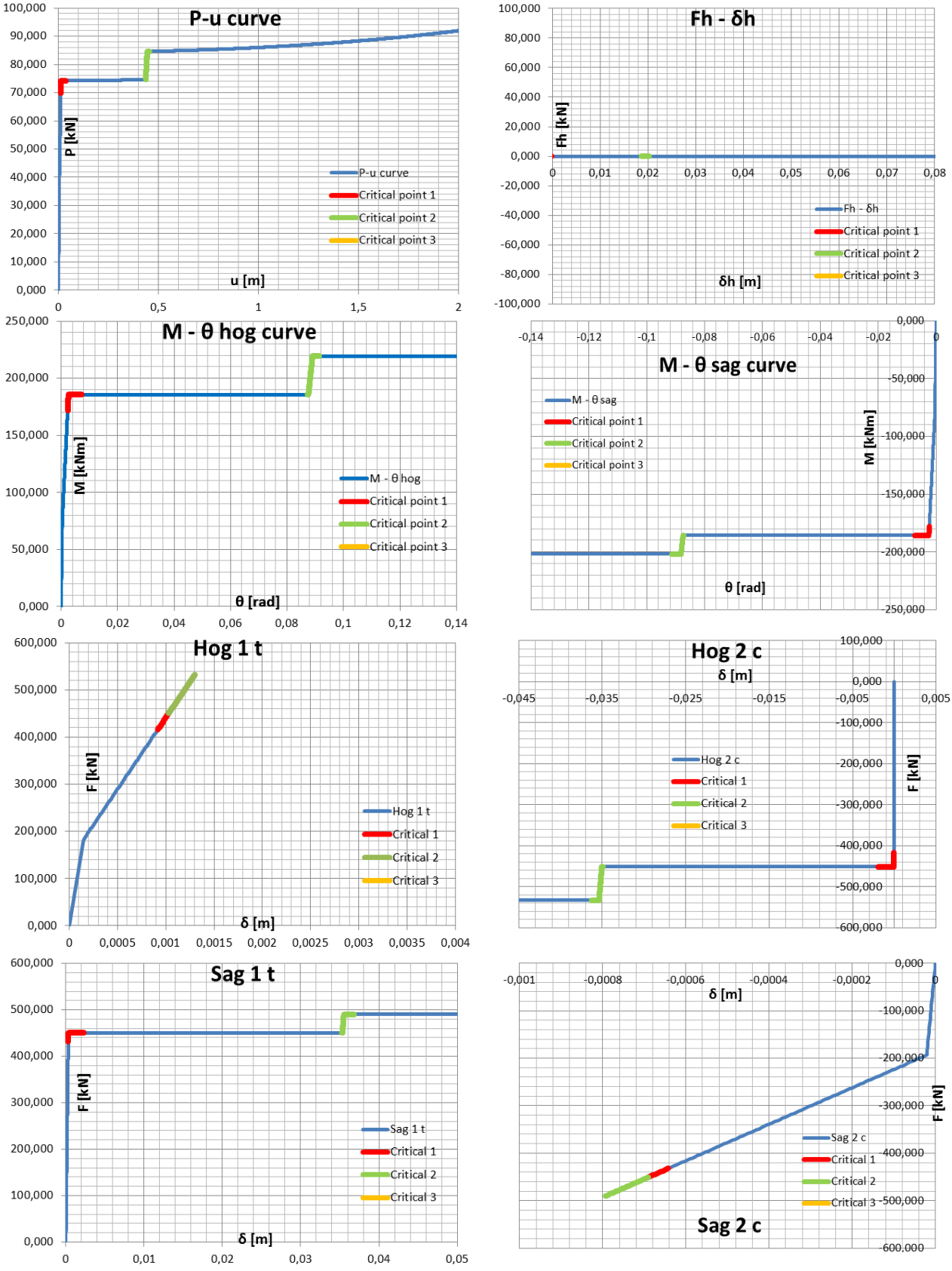

Figure IV-18: Result of the analysis for $K_H = 0$

The distance between red and green marker is characterized by the slip. If we analyse the behaviour of the springs forming the joint presented below, we can notice that when the slip occurs in the one spring containing the friction damper and until it lasts, there is no increment of the force in the other spring. This is perfectly logical since we have 2 springs representing our joint, which is in this case loaded only with bending moment. In order to keep the equilibrium, while one spring has a constant force, the other one needs to have a constant force also.

When the end stroke limit of the slip is reached i.e. when the bolts hit the end of the slotted hole, newly activated components provide additional resistance, highlighted in green. It can be noticed that the force in the springs containing the friction damper starts to increase, and the other spring follows in order to equilibrate.

After the additional resistance is used, the design resistance of the joint is reached and the progressive deformation develops leading to the failure.

Even though the Figure IV-18 shows no development of the membrane forces, and that all the presented diagrams are as expected, some increase in the P force occurs with the increase of vertical deformation according to the programed calculation.

This phenomenawill be explained by using the energy balance postulate. Detailed explanation can be found in IV.6.1.1.

In the following the behaviour of the joints obtained from the Matlab routine with be compared with the expected behaviour derived under monotonic bending in order to validate the routine. It is worth mentioning that even though we changed the law of the spring SAG 2 for the implementation in the program routine, the behaviour is governed by the other springs which remained the same, and therefore we can use the results from the 2-spring model in order to validate the Matlab routine.

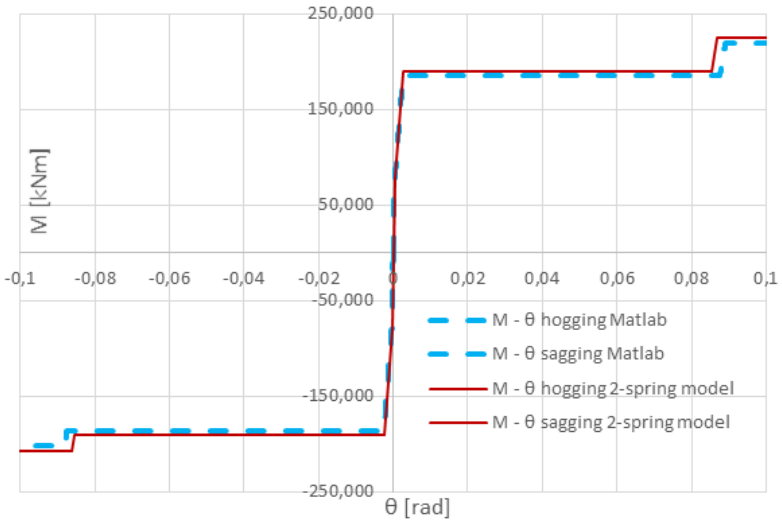

Figure IV-19: Validation of the Matlab routine – Moment-rotation curve

Figure IV-19 shows that there is a good agreement between results. Small difference between the models could be occurring due to the chosen step in the program and other parameters defining the solver. Considering the above said, we can conclude that the Matlab routine provides reasonable results and therefore it can be consider as validated.

IV.6.1.1. Energy balance

In IV.6.1 the model considering no stiffness of IAP was presented. It was shown that even though no membrane forces develop, there is some increment of the P force with the increase od the vertical deformation.

In order to explain the obtained result let us start from the substructure disposition.

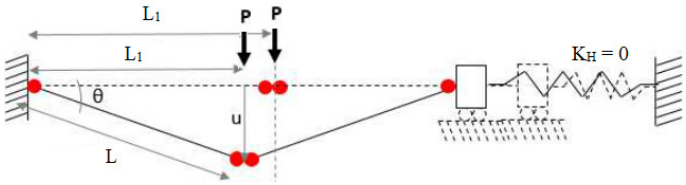

Figure IV-20: Substructure model – initial and deformed shape [Clara]

Figure IV-20 presents the considered substructure in the initial and deformed shape. As we consider the $K_H = 0$ when the mechanism occurs there is nothing to anchorage the membrane forces nor to stop the mechanism from freely moving. Therefore, the presented problem cannot be explained by using the static approach. To explain why the P force increase, we will use the energy balance postulate.

Using the energy balance equation for the deformed shape we obtain:

$$P\,u = 2\,M_{hog.pl}\Theta + 2\,M_{sag.pl}\Theta$$

If we express the vertical deflection as $u = \Theta\,L_1$, obtained from the geometry,and implement it in the previous equation we obtain the following:

$$P\,\Theta\,L_1 = 2\,M_{hog.pl}\Theta + 2\,M_{sag.pl}\Theta\ /:\ \Theta$$

$$P\,L_1 = 2\,M_{hog.pl} + 2\,M_{sag.pl}$$

For each change of vertical deflection u, the value of L_1 will decrease. As the right side of the above presented equation is constant, the only way to keep the energy balance is to have a larger value of force P. Therefore, as the L_1 decreases during the process value of P will consequently increase, explaining the obtained behaviour of the model presented in IV.6.1.

IV.6.2. **Full spring model 2 – K_H = 2500**

In the following the results of the model for which the indirectly affected part has the stiffness of 2500 kN/m will be presented and discussed. Figure IV-17 contains the other relevant parameters used to obtain the presented data, and it can immediately be spotted that a different step of the

vertical displacement was used when compared with the first model. Indeed, the solver was experiencing problems for the other values of the step and the obtained results were not fully explainable.

Looking at the Figure IV-21 representing the result of the analysis, we can notice that the substructure gives an elastic response up to the spot marked in red when the slip occurs.

The behaviour of the part of the P – u curve in-between the red and green marker is characterised by the slip of the friction damper and therefore progressive rotation of the joint up to the stroke limit. None of the components forming the joint have reached their design resistance up to the green marker, hence the substructure is still not in the plastic range and the mechanism in not formed.

Nevertheless, on the graph presented in the upper left corner of the Figure IV-21 we can observe that some membrane forces have developed. This would mean that for the current configuration of the joint the catenary actions can develop before having any plastic deformation. The slip provides the needed deformation for the membrane forces to develop and depending on the stiffness of the IAP, some membrane force will appear.

This kind of behaviour is beneficial in term of robustness, as the innovative joint made the development of the membrane forces possible before the mechanism is formed. In the present case the developed catenary action is not so significant, but with a larger stiffness of IAP, it could prove to be a useful advantage of a frame equipped with the innovative type of connection. The mentioned behaviour will be further studied in the following analysis.

If we look at the behaviour of the joints, for example under hogging, we can notice that after the slip, there is some change in the value of bending moment. For a case when we have only bending this would not be possible because, as previously explained, the forces in the springs have to be in equilibrium so when the one does not change the force in the other spring cannot change either. Therefore, it is obvious that the joint is not subjected to bending moment only anymore, but also to tension force. This can be nicely noticed by looking at the behaviour of the springs forming the joint under hogging. For the spring HOG 2 the part of the curve between red and green marker represents the slip. At the same time we can see in that there is some increment in the tension force in the HOG 1. The part of the curve limited by the red and green marker in the graph HOG 1 represents the change of the force in the spring in order to equilibrate the newly developed membrane force.

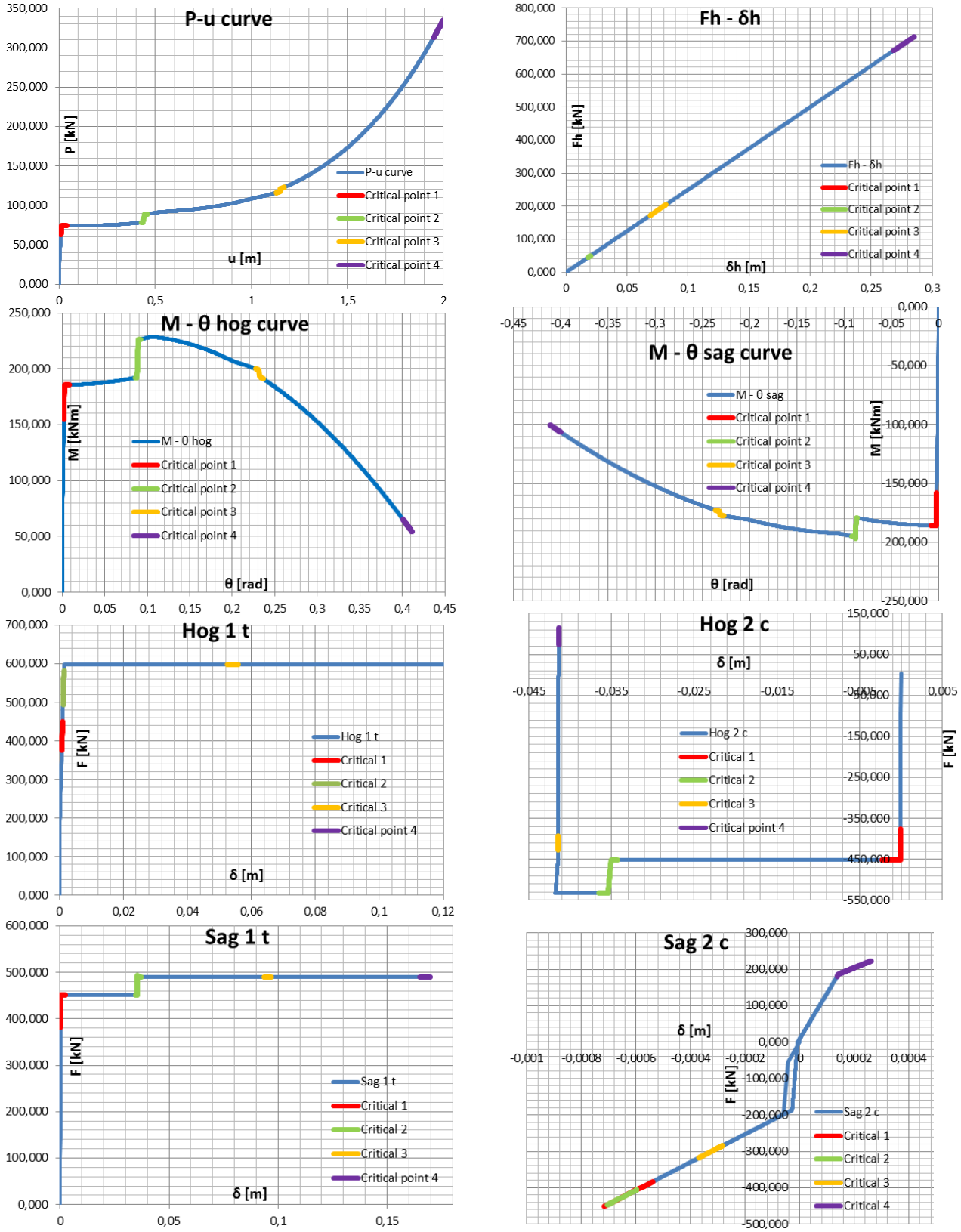

Figure IV-21: Result of the analysis for K_H= 2500

Interesting behaviour can be observed if we look at the springs forming the joint in sagging. Namely, the slip occurs in the tension spring. When the slip occurs membrane forces start to develop. As the membrane forces develop the spring in compression starts to unload in order to equilibrate the new force acting in the joint. When the spring SAG 1 reaches the stroke limit, and additional stiffness activates, the sudden increase of the force in SAG 1 will cause the SAG 2 to change from the unloading phase to the loading in compression (presented with green marker). Due to the fact that the stiffness governing the loading and unloading phase is the same, it is difficult to clearly see what is going on at that point. Luckily, the discussed behaviour was firstly noted in the simplified model where the behaviour is quite clear. After reaching the plateau of the SAG 1,spring SAG 2 will again enter the unloading phase.

For the chosen value of K_H, both of the springs containing friction dampers reach the slip end and activate the new components while the spring SAG 2 does not reach the plateau. The program was able to "catch" all the changes of the spring behaviour laws, from initial stiffness, to the slip, new stiffness, plastic deformation, change of stiffness in the unloading phase etc. A small remark shall be made about the behaviour of the spring SAG 2. Namely, even though it is assumed in the model that the behaviour law is the same for the loading and unloading phase, we can see that when the spring is moving from compression to tension, the behaviour law is not completely the same. From the force value of 186.6 kN, when the slip of the upper interface occurs, the program "misses" a bit the behaviour law of the spring. This occurs due to the fact that such complex behaviour was modelled in the unloading phase by comparing the value of the force in the previous step to the force limit (186.6kN) defining the change in the behaviour. As the stiffness is very high in this part, the behaviour of the spring in influenced in great matter by the chosen step of the vertical displacement. Therefore, due to the mentioned facts, the behaviour law of the spring SAG 2 in not completely the same for loading and unloading phase.

When the green marker is reached, the mechanism starts to form. After passing the green marker the membrane forces continuously increase with deflection, and the springs follow the expected behaviour. As the tension forces increase, the springs which were primarily in compression are in the unloading phase, while the springs in tension have reached the plateau. Assuming that the ductility of the springs is high enough, the analysis had been conducted up to the 2m of vertical displacement.

It should be noted that the reason for the chosen limit is the occurrence of some problem in the solver. The results obtain for the deflection larger then 2m were unexplainable and the solver gave a note that the solution is diverging.

For the presented vertical displacement limit we have not reached the progressive deformation concentrated in the hinge characterised by the change of the slope in P - u. None of the joints have reached the plateau due to the combination of M and N. The values of the force and following behaviour of the spring at the deflection of 2m is marked in purple.

The length of the curve marked in yellow represents a divergence of the solver probably caused by the change of the stiffness in HOG 2. The value of the stiffness is extremely high, almost rigid, and it is assumed that in the combination with the other behaviour laws of the springs induces some divergence.

IV.6.3. **Full spring model 3 – Kh = 5000**

The results of the discussed model are presented in Figure IV-22. By looking at the table containing other parameters of relevance (Figure IV-17) it can be seen that in order to obtain a valid result, it was needed to include the fake stiffness. The minimum value of fake stiffness giving convergence the solver solution was 20kN/m. The idea behind introducing the fake stiffness is to help the solver pass the critical points and finish the analysis. The used value is very small comparing to any of the other values of stiffness and therefore it is assumed that it does not influence the reliability of results. This can also be justified by the fact that the$\mathbf{K_{fake}}$will almost not be visible in the presented results.

The response of the substructure is linear up to the slip. We can notice that the program converges for every used value of $\mathbf{K_H}$ to the same value of force **P** at slip, giving a reason more to trust in the obtained result.

During the slip, membrane forces will start developing and when we reach the green marker, new components will activate inducing an increase in resistance, until both of the springs in tension reach their design resistance (green marker) and the mechanism is formed.

After one of the springs forming the joint reaches plateau, the fact that the other one has not reached the design limit will contribute to the further development of the membrane forces. The behaviour of the springs is generally the same as the one described in IV.6.2. The difference consist of the fact that, in the considered case, the spring HOG 2 will not reach the plateau in tension. The unloading phase will occur just before reaching the plateau but after the new stiffness, provided by the additionally activated components, is activated.

Significant membrane forces develop between the green and yellow marker assuming that the components forming the joints are ductile enough. The yellow marked highlights the area representing the change in the behaviour when the spring HOG 2 reaches the slip in tension. From this point membrane forces are not able to develop anymore. Indeed, as both of the springs have no stiffness at this point, the deformation is developing in the hinge, preventing the development of the membrane forces. This is confirmedby the graphF_H–δ_H,which represents the development of the membrane force.

Butthe force **P** continues to grow, even though the membrane force $F_H$has no increment after the yellow marker. The further increase of the P force can be explained as the influence of the second order effects, as already mentioned in the simplified spring model. As the deformation is concentrated in the hinge the rotation, and accordingly the vertical displacement, will increase further but without inducing any increase in dilatation of the spring representing the IAP. Therefore

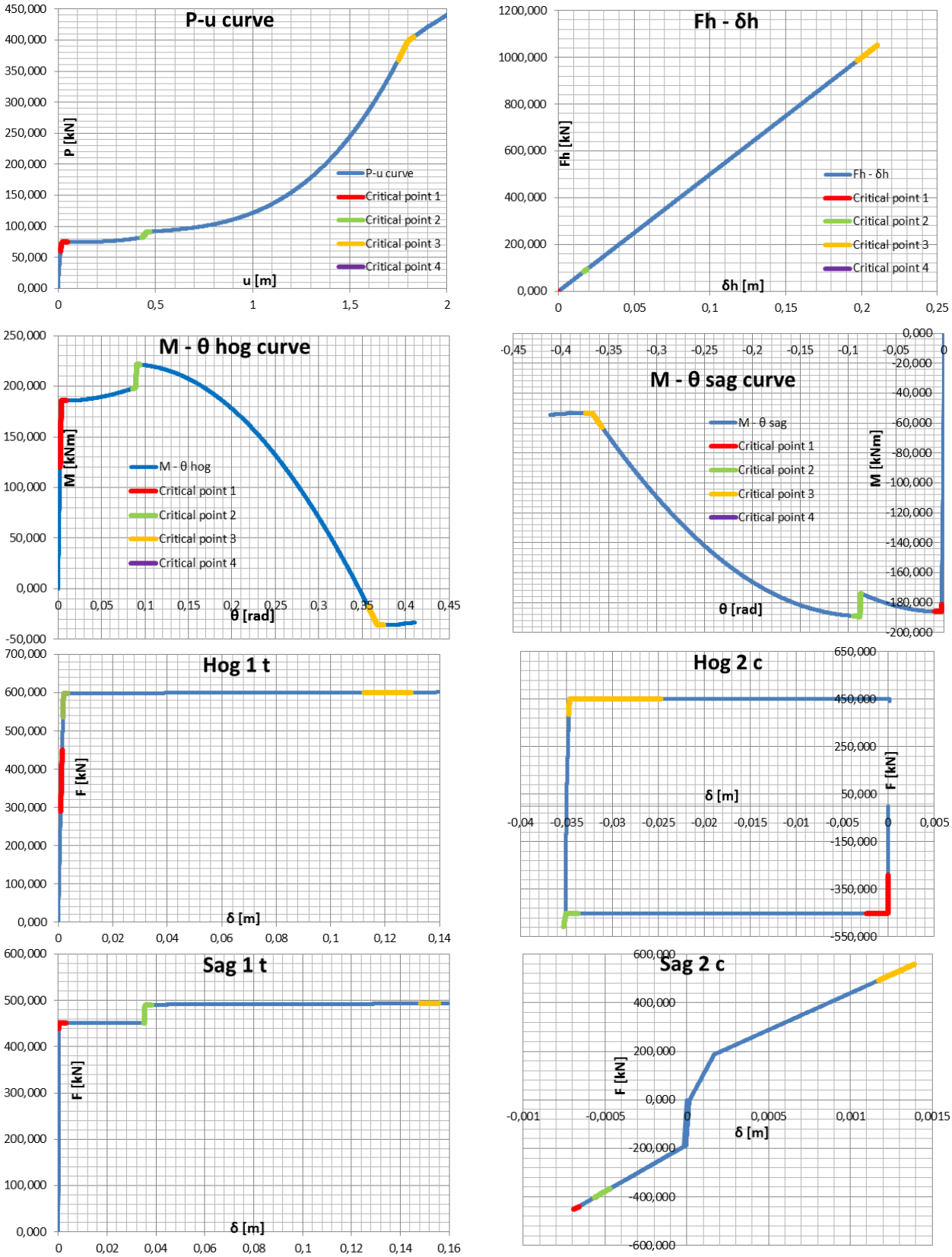

Figure IV-22: Result of the analysis for K_H = 5000

the membrane forces acting remain the same as they were just before the hinge started deforming, but their vertical projection increases due to the different rotation angle. The described situation is illustrated in the Figure IV-23.

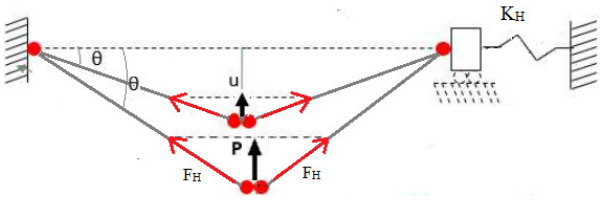

Figure IV-23: Second order effects

Therefore, for the same value of the membrane force in the beam we will have a progressive increase of the force P. The behaviour caused by the second order effect is characterised by the change of the slope in the P-u curve.

The analysis was stopped when the vertical displacement reached 2m. None of the hinges at that point have reached the design limit (previously described situation occurred due to the slip in one spring and reaching the plateau in another) and therefore, the potential full behaviour of the model was not presented.

The model was not able to catch the behaviour of the HOG 2 after vertical displacement reaches 2m. At the end of the calculation you can see that the force in the spring started dropping instead of increasing when the new components activate. This was the reason to terminate the program at 2m of vertical displacement.

IV.6.4. Full spring model 3 – K_H = 10000 kN/m

Model with the horizontal spring stiffness of 10 000 kN/m is the first model where the full potential behaviour of the substructure was reached. For some reason, the change of the K_H from 5000 kN/m to 10 000 kN/m was convenient for the solver, and the program converged to the correct solution during the whole calculation.

The general behaviour of the presented model is the same as for the other models. The main difference between the present model and the one with K_H = 5000 kN/m is the fact that due to the higher stiffness the membrane forces will be larger for the same vertical displacement.The increased stiffness of IAP will cause some changes in the behaviour of the springs.

As presented in the Figure IV-24, the unloading phase of the HOG 2 starts before the stroke limit is reached. The larger increment of $F_H$causes the spring HOG 1 to reach the plateau in tension earlier and consequently the unloading phase of HOG 2 will start earlier than in previous models.

The length between the forming of the mechanism (green) and spot where the other spring of the joint which was primarily loaded in hogging bending reach the slip in tension (yellow) is characterised by the successive rise of the tension forces and the vertical deflection.

The yellow marker highlights the spot when the progressive deformation develops in the hogging joint. As already explained in the previous model, at this point the tension spring of the joint subjected to hogging and tension force has reached the design resistance and the other spring entered the slip zone. As a result we have a deformation concentrated at the level of the hinge leading to the increase of the **P** force due to the second order effects whilethere is no increase in the membrane force.

Assuming that the springs are ductile enough the following could occur. The spring HOG 2 when the slip limit is reached, but now in tension, activates additional resistance. The area representing this behaviour is marked in purple.

In-between the yellow and purple marked the progressive deformation occurs in the hinge under hogging bending and tension, but no membrane forces develop. This is confirmed by the conducted calculation as there is no blue area between the yellow and purple one in the $F_H - \delta_H$ graph. As the spring HOG 2 reaches the end stroke limit (purple), and additional resistance activates, the deformation is no longer just in the joint but in the horizontal spring representing IAP, inducing the further development of the membrane force.

When the additional resistance is consumed i.e. when the design resistance of the HOG 2 is reached, the deformation is again start developing fully in the joint, allowing the increase of the force P due to the second order effects but without any increase of the membrane forces. The limit of the P force which can be redistributed is limited only by the available ductility.

It should once more be emphasised that the obtained results represent a theoretically possible behaviour and that the maximum value of **P** which can be reached in reality depends on the possibility of plastic deformation of the elements forming the joint where the plastic hinge is formed. The joint had been designed so that the area marked in green can be reached for sure, but the further development of the membrane forces is unpredictable without a reliable estimation of the maximum available ductility.

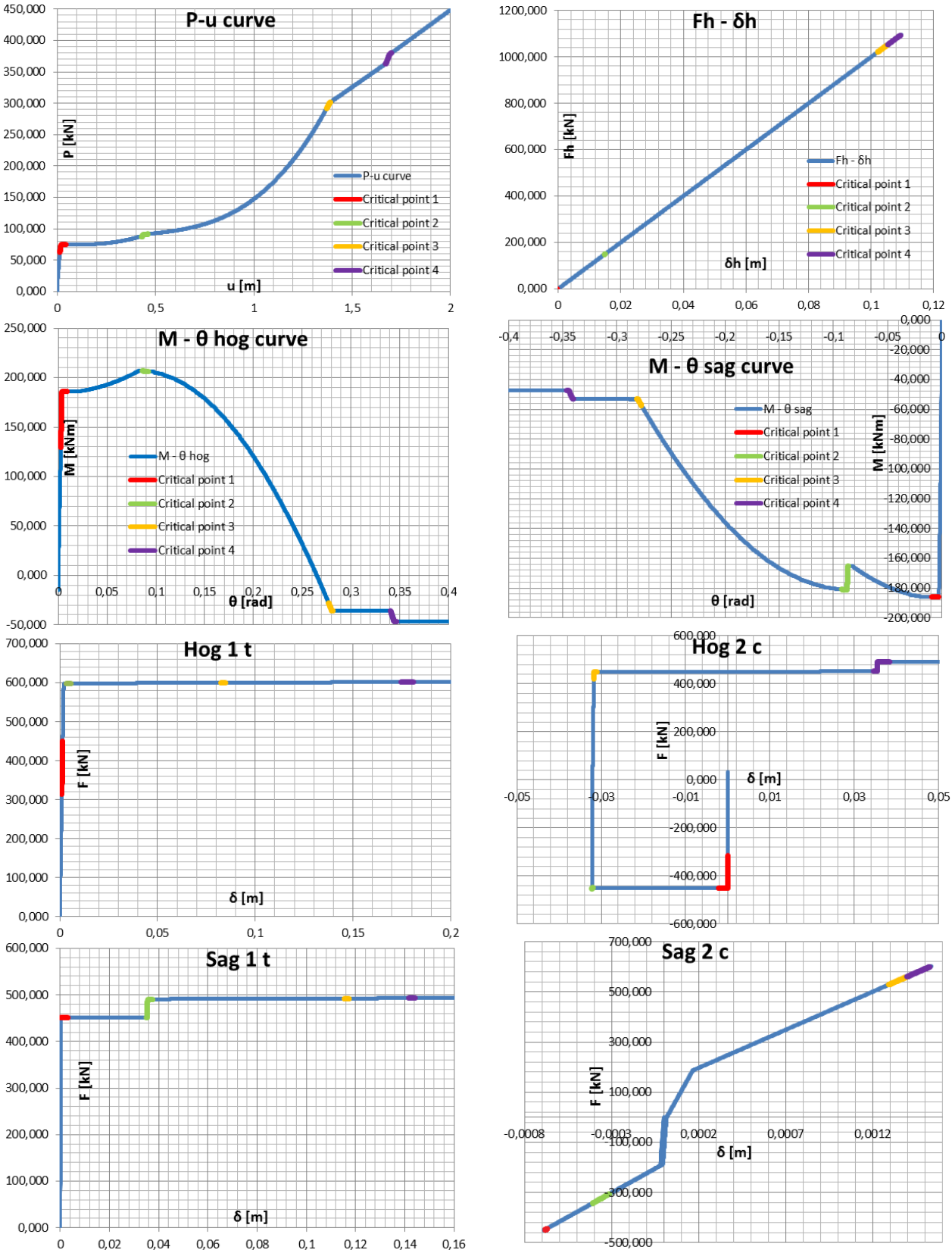

Figure IV-24: Result of the analysis for K_H = 10000

The interaction of bending moments and normal force acting on the joints can be presented as inFigure IV-25.

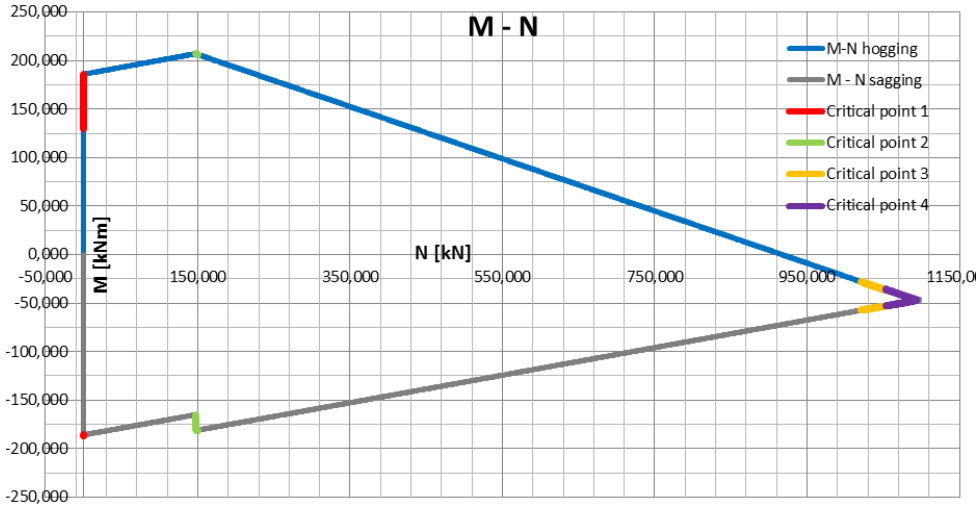

Figure IV-25: Interaction diagram - development of internal forces in the joints during the analysis

A nice illustration of the forces developing and acting in the joints during the simulation of a column loss situation can be presented in term of interaction diagram of bending moments and normal forces, as in Figure IV-25.

We can notice that until the slip is reached (red marker) no tension forces develop. During the slip of the friction damper the tension forces start to develop, loading the joints in combined tension and bending. When the tension reaches a values around 150 kN, the plastic mechanism forms. This is when the mentioned Phase 3 (figure) begins for the analysed configuration of the frame. Catenary actions continue to develop with the increase of vertical deflection until, if the ductility of the joints allows it, we reach the progressive deformation of the plastic hinge. At this point the joint are practically loaded only in tension.

With this model we conclude the parametric analysis in term of detail discussion of the behaviour under specific $\mathbf{K_H}$.

IV.6.5. **Result of the parametrical studyand discussion**

Previously, some characteristic cases of the parametric study were presented and analysed in detail. The study will be extended by including the results of the analysis conducted for different values of K_H in order to explain the general behaviour. It should be noted that some of the analysis had to be stopped before experiencing the full possible behaviour due to the problems occurring in the used

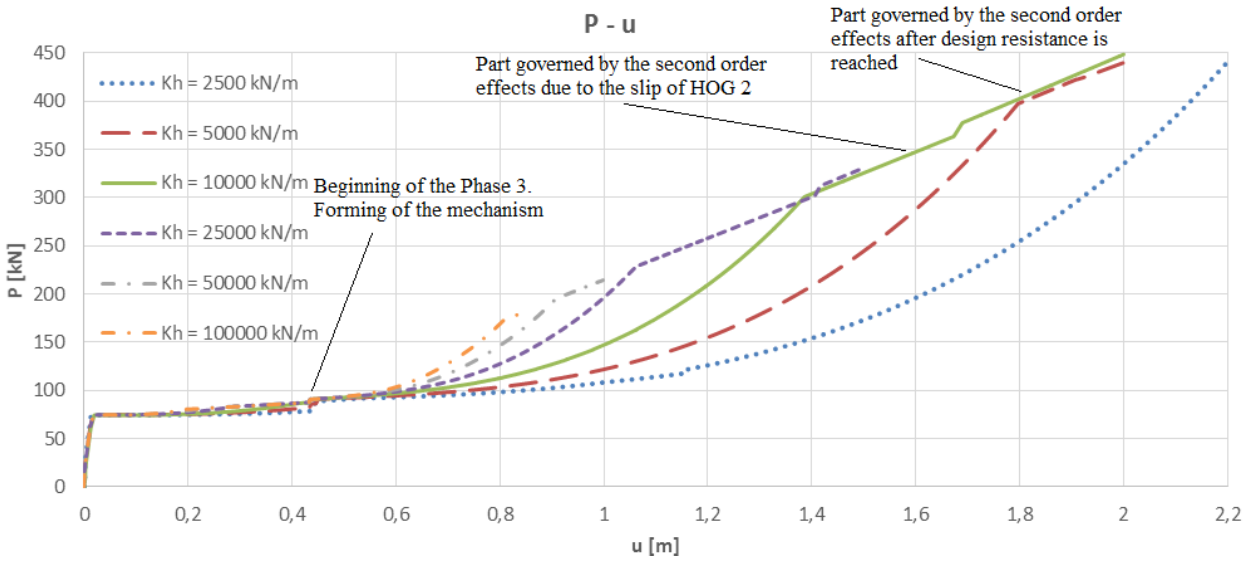

Figure IV-26: Variation of K_H– Results of the parametric analysis – Applied load vs. Vertical deflection

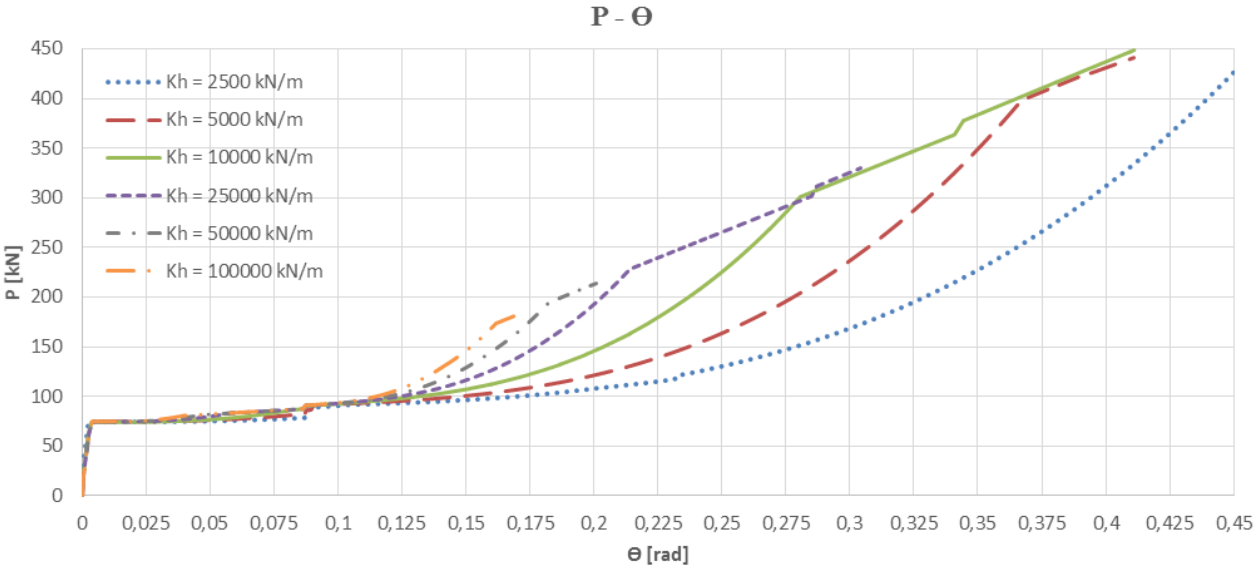

solver.

Figure IV-27: Variation of K_H– Results of the parametric analysis – Applied load vs. rotation of the joint

Figure IV-26 contains graph showing the dependence of the developed**P** force to the vertical displacement of the upper node of the lost column for different values of the stiffness of the indirectly affected part.

The curves representing the substructure behaviour for $\mathbf{K_H}$equalto 2500 kN/m, 5000 kN/m, 10 000 kN/m have already been discussed in detail. The following paragraphs will be dedicated to the analysis and discussion of the result for higher values of $\mathbf{K_H}$ and the obtained result in general.

As visible in the Figure IV-26 regardless of the $\mathbf{K_H}$used, the program converges tothe same value of force **P** before the slip occurs, which is expected since the behaviour of the frame in this part is characterized by the beams and joints subjected to the bending only (the shear force has not considered within the work).

The response after the slip occurs until reaching the stroke end shows that the membrane force start to develop before the mechanism is formed. As anticipated, depending on the stiffness of the IAP the value of the developed tension forces varies from lower, in case of low value of $\mathbf{K_H}$, to higher, in case of having significantly large $\mathbf{K_H}$.

Despite the different behaviour until reaching the slip end caused by the variance of $\mathbf{K_H}$, the response for any $\mathbf{K_H}$ converges to practically the same**P** force at the beginning of the Phase 3, when the mechanism is formed within the substructure. The path to get there is different, but the beginning of the Phase 3 is defined by the same **P** force for any $\mathbf{K_H}$.

Therefore, when we talk about the provided benefit of the innovative frame configuration in terms of robustness, it can be concluded that perhaps there is no real benefit of the development of the membrane forces before forming the mechanism if we only need to redistribute the amount of P force up to the value of P for which the mechanism is formed (if we stay in the Phase 2). That value (labelled as beginning of Phase 3 in Figure IV-28) will be reached ether way just by activation of additional components after the stroke end limit is reached.

Based on the conducted parametric analysis, it seems that the benefit of this joint in term of structural robustness could be that when the mechanism is formed i.e. when the Phase 3 starts, some membrane force have already been activated and therefore for smaller value of plastic rotation the same force can be redistributed when compared to the regular frame assuming the same behaviour of the IAP. This should still be confirmed by further investigation since the used program was not validated by experimental data or data obtained from the numerical simulation.

It should be emphasized that the used substructure model had not been validated for simulation the behaviour during the Phase 2. The influence of beam flexibility and the evenly distributed load to the Phase 2 have been neglected. Therefore, the presented result before the mechanism is formed are approximate, and should be used just for general understanding of the behaviour and the occurring phenomena.

The response of the substructure after the mechanism is formed is greatly defined by the $\mathbf{K_H}$. Even though detailed analysis had not been presented for the cases when the $\mathbf{K_H}$ is larger than 10 000 kN/m, the behaviour can be foreseen based on the previous analysis.

The conducted analysis have showed that the potential deformation concentrated only in the hinge(causing the explained behaviour defined as the second order effect) will always form in the joint subjected to hogging bending(at least for every K_H> 2500 kN/m). Indeed, both springs in hogging will reach the plateau before the springs defining the joint under sagging do. Therefore, when the increment of the membrane force increases due to the larger K_H, the unloading phase for the spring HOG 2 will occur sooner than for K_H = 10 000 kN/m. This will also cause the spring HOG 2 to reach earlier the slip in tension. At that point the deformation is concentrated in the plastic hinge formed in the joint which was under hogging at the beginning of the analysis causing the explained change of behaviour, when the P force increases due to second order effects (Figure IV-29 part second order effect due to slip). Taking into account the before mentioned, it is clear that each time we have a larger increment of membrane forces, the slip in tension of the HOG 2 and later the progressive deformation in the hinge forming in the joint will take place sooner. The latter explains the obtained behaviour in the Figure IV-31 for K_H > 10 000 kN/m. If we compare the result obtained for K_H = 10 000 kN/m and K_H = 25 000 kN/m, we can conclude that the general behaviour is the same, only the part of the curve defined by the increment of P under second order effects develops earlier in case of K_H = 25 000 kN/m which is expected as the HOG 2 will reach the slip in tension sooner for a larger $\mathbf{K_H}$.

After the HOG 1 reaches the plateau and HOG 2 reaches the slip in tension the behaviour is practically the same for all $\mathbf{K_H}$. **P** increases due to the second order effects at this point,and the length of the curve defined by the second order effect depends just of the length of the slip. As the slip has the same length regardless of $\mathbf{K_H}$, we come to a conclusion that after the slip is reached, the behaviour is the same for any $\mathbf{K_H}$.

When the stroke end is reached, some additional stiffness will provide the development of additional catenary action and soon after that, the design limit of HOG 2 is reached, when P can again only increase due to second order effects.

With all of that being said, we can conclude that the result obtained for K_H > 10 000 kN/m are in agreement with the expected behaviour. For each of them the increment of the catenary action is larger, and consequently, the behaviour defined by the second order effects occurs earlier in terms of the reached force **P** and vertical displacement.

The result of the analysis for K_H = 50 000 kN/m and K_H = 100 000 kN/m are presented up to the point when for the first time the second order effects govern the P – u. This had been done party intentionally, to improve the clarity of the figure, partly due to the limitations of the program. But as previously explained, the behaviour after that point can be anticipated.

The presented response of the substructure considered the infinite ductility of the elements forming the frame. In reality, the real response will be limited by the ductility of the elements. As no data is provided regarding the ductility of the elements forming the joint, one can only assume where the collapse will occur. According to the design of the joint, we should always be able to reach the point where the Phase 3 starts. The response of the structure after that point and the amount of the redistributed force is only limited with the ductility of the deforming elements.

For the presented configuration, after the conducted analysis and discussions, it can be concluded that the ductility is mainly demanded from the components column panel in shear and L – stub flange in bending for the springs HOG 1 and SAG 1, respectively. Both of the collapse modes are ductile, which strengthens the belief that significant membrane forces could develop.

As for the springs representing the part of the joints primarily in compression for the spring HOG 2, as shown in the analysis for K_H= 2500 kN/m, the ductility can be demanded from the component bearing of the hammer head flange while the spring is in compression and if the $K_H$is small enough to allow the spring to reach this failure mode. For higher values of the $K_H$the design limit in compression will not be reached, but the ductility of the component governing the design in tension, L – stub flange in bending, could govern the failure of the spring and therefore the joint, assuming that the springs HOG 1 and SAG 1 are ductile enough to allow for the development of the membrane forces up to the point where the design resistance of HOG 2 in tension is reached. Again both of the components from which ductility is demanded are known to experience a ductile failure, which is encouraging.

The spring SAG 2, for the presented configuration, will never govern the failure. As presented in the analysis, the design resistance will never be reached for this spring, not in compression nor in tension. This is a good feature since the failure in compression for this spring would depend from the ductility of the column web in compression. Generally, it is not a good idea to rely on the ductility of components in compression, as they tend to have less ductile behaviour that the ones in bearing, bending or column panel in shear. The failure mode in tension would be governed by the T – stub web in bending, which would again be a ductile failure mode.

As the ductility is not known and it is the only condition to have the force redistribution, it is possible to determine the requested ductility of the joint in order to redistribute a desired value of the force, if the characteristic of the IAP are known. Figure IV-27 represents a graph showing the dependence of the redistributedforce P to the developed rotation of the joint. From the presented graph it is possible to determine the requested rotation of the joint in order to redistribute a certain force.

For example, if the column which is lost supported 150 kN before the loss, and if the indirectly affected part of the frame has stiffness of K_H = 10 000 kN/m (assuming the response of the IAP is linear), from the Figure IV-27 it is possible to read that the requested rotation is around 0.2 rad

i.e.around 11.5 degrees in order to consider the frame robust. From this we can also conclude that the requested plastic rotation would be around 0.12 rad.

The structure is considered robust if it is capable to redistribute the load supported by the lost column without the collapse.

IV.7. Conclusion

From the analysis presented above it can be concluded that for the chosen substructure which had been validated for the simulation of the frame response when subjected to a column loss during Phase 3 (according to [3]), when the hinge forms in the joint it is possible to model the behaviour of the hinge by using the developed 2-spring model approach.

This could possibly, depending of the complexity of the spring behaviour, make the analytical robustness assessment in terms of a column loss situation much more accessible. By modifying the behaviour law of the springs, the same structure of the main program and the used equations could be maintained making the path to the preliminary assessment of structural robustness relatively easy and fast.

The modified Matlab routine has shown that it has its limitations but also that it is able to simulate a very complex behaviour of the substructure model. For the right combination of the parameters of importance (**x0**, **u_step**, **TolX**, **TolFun**, $\mathbf{K_{fake}}$) satisfying result were obtained. The developed routine could be improved further and possibly the high dependence of the mention parameters can be reduced.

The conducted parametric study revealed the detailed behaviour of the substructure simulation the frame. Depending of the stiffness of the indirectly affected part K_H, various behaviour of the springs forming the joints could occur. Therefore, after each analysis, the results should be checked for inconsistencies.

As expected, with the increase of $\mathbf{K_H}$, the developed membrane forces also increase for the same vertical displacement. The analysis demonstrated that the membrane forces will start developing before the mechanism is formed. This could prove to be beneficial because when the mechanism is formed, due to the fact that some membrane forces have developed already, for the same plastic deformation a larger value of force **P** can be redistributed. In other word, since some value of the tension forces is already present in the beam, a smaller plastic rotation is needed to reach the same value of membrane force when compared to a regular frame configuration where the hinges are also formed in the joints. Once again, this should be validated by experiments or numerical models.

It had also been shown that the ductility, for the present configuration and for any value of $\mathbf{K_H}$, is requested from the components forming the joints which generally experience the ductile failure such as column panel in shear, bearing of the hammer head flange, L-stub flange in bending. The

made conclusion strengthens the belief that significant membrane forces could develop within the discussed frame equipped with the innovative joint.

The mentioned features could give the upper hand to the presented joint typology, especially in earthquake prone areas and areas where exceptional events could be expected.

Note: Figures IV-2, IV-3, IV-4, IV-6 and Table IV-1 are taken from [2], [3] and [8], modified to suite the discussed problem within this thesis and then presented.

V GENERAL CONCLUSION AND FUTURE DEVELOPMENT

Component method proved to be a useful tool for reflecting the monotonic behaviour of the innovative connection. Regardless of the fact that the friction damper is not covered as a component within the method, using the component approach the behaviour of the damper was successfully model by representing as a several components in series.

More or less good agreement had been obtained between the experimental behaviour of the joint and the behaviour assessed with the rotational spring model was obtain. Noticeable difference between the behaviour in sagging could be due to the fact that the experimental data represents the response of the joint under cycling loading, or the used way of modelling the behaviour of the friction damper was not accurate enough. The behaviour of the friction damper should be further studied and possibly included in the next update of component method. The possibility of some new components emerging in the innovative connection should also be investigated.

The modelled behaviour of the joint revealed a benefit of the innovative connection in terms of ductility, at it can easily, without any plastic deformation, exceed limit of 35 mrad requested by EC8-1 for ductility class high (DCH).

Newly developed 2-spring joint model used for the monotonic behaviour assessment demonstrated a satisfying agreement when compared with the traditional rotational spring model.The model also proved to be very convenient for reflecting the behaviour of the joint in case of a column loss as it can easily be implemented in the programed routine used for robustness assessment.

As presented, the behaviour law of the components forming the springs of the mentioned 2-spring model was assumed to reach the plateau when the design resistance is reached. For the future development and investigation, the post-limit behaviour of the components and therefore the joint should be included. As the ultimate resistance play a significant role when robustness is assessed, in should be included in the future studies.

The available routine programed in Matlab was successfully modified even though it has some limitations. The program was able to simulate the expected behaviour of the spring and to give logical results. In the future, a research of the program could be done and functions which depend

less of the used step and other parameters of importance could be used. Possibly, if justified, other programing language could be used.

The developed program for the simplified substructure model in combination with the 2-spring behaviour model proved to be a useful and practical tool for assessing the response of a frame further to a column loss. Within the work the most advanced substructure model was used but still in neglects the coupling between the storeys of directly affected part.Therefore an improvement can be made by including the full analytical model, as explain in Chapter II.

The conducted parametrical studyrevealed the general behaviour of the frame equipped with the innovative joint.It was shown that the membrane forces are able to form before the mechanism occurs. Therefore the possible benefit of the innovative connection in terms of robustness could be that with a smaller plastic rotation of the joint we can redistribute the same force when compared to traditional frame.

The amount of redistributed force is limited only by ductility of the deforming elements. It was shown during the analysis that for the considered configuration of the joint the ductility is requested from the components which are generally considered ductile, strengthening the belief that the new type of the connection can experience good behaviour under exceptional situations.

In the future, it would be of great importance to examine the real ductility which can be expected from the joint. By doing that, from the presented graphs, one could read the maximum force which could be redistributed for the given characteristics of indirectly affected part.

References

[1] Lemos A.S.S. (2015). “Numerical Simulation of Connections Designed For Seismic Actions”. Master thesis.University of Coimbra.

[2] Demonceau J.F. (2008). “Steel and composite building frames: sway response under conventional loading and development of membrane effects in the beams further to an exceptional action”. PhD thesis University of Liege.

[3] Huvelle C.;Van-Long Hoang;Jaspart J.P.; Demonceau J.F. “Complrete analytical procedure to assess the response of a frame submitted to a column loss”. University of Liege.

[4] H. N.N. Luu. (2008) Structural response of steel and composite building frames further to an impact leading to the loss of a column. PhD thesis. University of Liege.

[5] Chen W.F., Yoshiaki Goto, Richard Liew J.Y. Stability Design of Semi-Rigid Frames. JOHN WILEY & SONS, INC, 1996, p. 162-163.

[6] CEN (2005), EN 1993-1-8 - Eurocode 3: Design of Steel Structures - Part 1-8: Design of joints, European Committee for standardization, Brussels.

[7] J.-P. Jaspart, K. Weynand "Design of joints in steel and composite structures", ISBN 978-3-433-02985-5, 2016

[8] Huvelle C.; Jaspart J.P.; Demonceau J.F. (2013) “Summary of the analytical method applied to the tests performed in the University of Ghent”. Internal report. University of Liege.

[9] ECCS (1997). “Frame design including join behaviour”. Volume 1.

[10] Mazzolani F.M. (Editor). “Moment Resistant Connections of Steel Frames in Seizmic Areas, Design and Reliability”, 2000.

[11] CEN (2004), EN 1998-1 – Eurocode 8: General rules, seismic actions and rules for buildings – Part 1: General rules and rules for buildings, European Committee for standardization

[12] Iannone, F.; Latour, M.; Piloso, V.; Rizzano, G. (2011). “Experimental Analysis of Bolted Steel Beam-to-Column Connections: Component Identification”. Journal of Earthquake engineering, Vol. 15, pp. 214-244

[13] Latour, M.; Piluso, V.;Rizzano, G. (2015). "Free from damage beam-to-column joints: Testing and design of DST connections with friction pads". Engineering Structures, Vo. 85, pp. 219–233.

[14] Kuhlmann U., Rölle L., Jaspart J.-P., Demonceau J.-F., Vassart O., Weynand K. et al. Robust structure by joint ductility. Final report of the RFCS project n°RFS-CR-04046, 2008.

Appendix A

Calculation of the characteristic of new elements according to EC 3-1-8 for hogging moment:

1. Bolts in shear M20...8.8 used

$f_{yb} := 640\frac{N}{mm^2}$ bolt yeild strength $f_y := 275\frac{N}{mm^2}$

$f_{ub} := 800\frac{N}{mm^2}$ bolt ultimate strength $f_u := 430\frac{N}{mm^2}$

$E := 210GPa$

$\gamma_{m2} := 1$

$d_0 := 21mm$ hole diameter

$d := 20mm$ bolt diameter

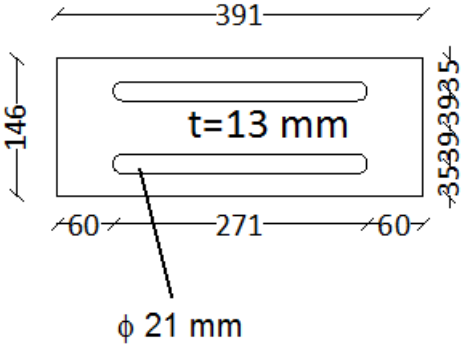

$\alpha_v := 0.6$ $\frac{d^2}{4}\cdot 3.14 = 314\cdot mm^2$

$A_s := 245mm^2$ shredded part area

$m := 2$ number of shear planes

$A_b := \frac{d^2}{4}\cdot\pi = 3.142\times 10^{-4}\,m^2$ shear plane area

It is assumed that the threaded part is not located in the shear plane

$F_{v.rd} := \frac{m\cdot\alpha_v\cdot f_{ub}\cdot A_b}{\gamma_{m2}} = 301.593\cdot kN$ Table 3.4

$n_b := 2$ number of bolt rows working in shear (we have a slotted hole therefore only 2 bolts will be in touch with the plates, both for stiffness and design resistance)

$d_{m16} := 16mm$

$k_{11} := \frac{16\cdot n_b\cdot d^2\cdot f_{ub}}{E\cdot d_{m16}} = 3.048\cdot mm$ Table 6.11

$k_{bs} := k_{11} = 3.048\cdot mm$

2. L cleats in bearing

$F_{b.rd} = \frac{k_1\cdot\alpha_b\cdot f_u\cdot d\cdot t}{\gamma_{m2}}$ $\alpha_b = \min\left(\alpha_d, \frac{f_{ub}}{f_u}, 1\right)$

2.1 Bearing of the upper L cleat (one cleat considered)

$t_{L.cleat} := 15mm$

$e_1 := 60mm$ $\quad p_1 := 60mm$

$e_2 := 31mm$ $\quad p_2 := 999mm$ there is no p.2

$n_{tot} := 1$ total number of bolts working

In the direction of load transfer:

$$\alpha_{d.end.bolt} := \frac{e_1}{3 \cdot d_0} = 0.952 \qquad \alpha_{d.inner.bolt} := \frac{p_1}{3 \cdot d_0} - \frac{1}{4} = 0.702$$

In the direction perpendicular to load transfer:

$$k_{1.edge.bolt} := \min\left(2.8 \cdot \frac{e_2}{d_0} - 1.7, 1.4 \cdot \frac{p_2}{d_0} - 1.7, 2.5\right) = 2.433 \qquad k_{1.inner.bolt} := \min\left(1.4 \cdot \frac{p_2}{d_0} - 1.7, 2.5\right) = 2.5$$

In our case, in the direction of the load transfer we have only end bolts working
When considering the direction perpendicular to the direction of load transfer, the bolts are considered as edge

End edge bolts

$n_{g1} := 0$ number of bolts in the group

$$\alpha_b := \min\left(\alpha_{d.end.bolt}, \frac{f_{ub}}{f_u}, 1\right) = 0.952$$

$$F_{b.rd.1} := \frac{k_{1.edge.bolt} \cdot \alpha_b \cdot f_u \cdot d \cdot t_{L.cleat}}{\gamma_{m2}} = 298.952 \cdot kN$$

Inner edge bolts

$n_{g2} := 1$ number of bolts in the group

$$\alpha_b := \min\left(\alpha_{d.inner.bolt}, \frac{f_{ub}}{f_u}, 1\right) = 0.702$$

$$F_{b.rd.2} := \frac{k_{1.edge.bolt} \cdot \alpha_b \cdot f_u \cdot d \cdot t_{L.cleat}}{\gamma_{m2}} = 220.477 \cdot kN$$

$$F_{b.rd.L2} := \begin{cases} \left(n_{g1} \cdot F_{b.rd.1} + n_{g2} \cdot F_{b.rd.2}\right) & \text{if } F_{v.rd} \geq \max\left(F_{b.rd.1}, F_{b.rd.2}\right) \\ \left(n_{tot} \cdot \min\left(F_{b.rd.1}, F_{b.rd.2}\right)\right) & \text{otherwise} \end{cases}$$

$$F_{b.rd.L2} = 220.477 \cdot kN$$

Stiffness

$$k_{12} = \frac{24 \cdot n_b \cdot k_b \cdot k_t \cdot d \cdot f_u}{E}$$

e_b	is the distance from the bolt-row to the free edge of the plate in the direction of load transfer;
f_u	is the ultimate tensile strength of the steel on which the bolt bears;
p_b	is the spacing of the bolt-rows in the direction of load transfer;
t_i	is the thickness of that component.

$e_b := 60mm$ for hogging moment

e.b in this case equal to the distance to other bolt in direction of load transfer?

$p_b := 60mm$ $n_b := 1$

$t_{L.cleat} = 15 \cdot mm$

$$k_b = \min(k_{b1}, k_{b2}) \quad k_{b1} = \min\left(0.25 \cdot \frac{e_b}{d} + 0.5, 1.25\right) \quad k_{b2} = \min\left(0.25 \cdot \frac{p_b}{d} + 0.375, 1.25\right) \quad k_t = \min\left(1.5 \cdot \frac{t_i}{d_{m16}}, 2.5\right)$$

$$k_{b1} := \min\left(0.25 \cdot \frac{e_b}{d} + 0.5, 1.25\right) = 1.25$$

$$k_{b2} := \min\left(0.25 \cdot \frac{p_b}{d} + 0.375, 1.25\right) = 1.125$$

$$k_t := \min\left(1.5 \cdot \frac{t_{L.cleat}}{d_{m16}}, 2.5\right) = 1.406$$

$$k_b := \min(k_{b1}, k_{b2}) = 1.125$$

$$k_{12} := \frac{24 \cdot n_b \cdot k_b \cdot k_t \cdot d \cdot f_u}{E} = 1.555 \cdot mm$$

for one upper L cleat

$k_{lcw\text{-}b.2} := k_{12} = 1.555 \cdot mm$

2.2 Bearing of the lower L cleat

$t_{L.cleat} := 15mm$

$e_1 := 60mm$ $p_1 := 60mm$

$e_2 := 49mm$ $p_2 := 78mm$

$n_{tot} := 2$ total number of bolts working

In the direction of load transfer:

$$\alpha_{d.end.bolt} := \frac{e_1}{3 \cdot d_0} = 0.952 \qquad \alpha_{d.inner.bolt} := \frac{p_1}{3 \cdot d_0} - \frac{1}{4} = 0.702$$

In the direction perpendicular to load transfer:

$$k_{1.edge.bolt} := \min\left(2.8 \cdot \frac{e_2}{d_0} - 1.7, 1.4 \cdot \frac{p_2}{d_0} - 1.7, 2.5\right) = 2.5$$

$k_{1.inner.bolt} := \min\left(1.4 \cdot \frac{p_2}{d_0} - 1.7, 2.5\right) = 2.5$

In our case, in the direction of the load transfer we have 2 bolts acting as inner bolts (load transf towards in)
When considering the direction perpendicular to the direction of load transfer, all bolts are considered as edge

End edge bolts

$n_{g1} := 0$ number of bolts in the group

$\alpha_b := \min\left(\alpha_{d.end.bolt}, \frac{f_{ub}}{f_u}, 1\right) = 0.952$

$$F_{b.rd.1} := \frac{k_{1.edge.bolt} \cdot \alpha_b \cdot f_u \cdot d \cdot t_{L.cleat}}{\gamma_{m2}} = 307.143 \cdot kN$$

Inner edge bolts

$n_{g2} := 2$ number of bolts in the group

$\alpha_b := \min\left(\alpha_{d.inner.bolt}, \frac{f_{ub}}{f_u}, 1\right) = 0.702$

$$F_{b.rd.2} := \frac{k_{1.edge.bolt} \cdot \alpha_b \cdot f_u \cdot d \cdot t_{L.cleat}}{\gamma_{m2}} = 226.518 \cdot kN$$

$$F_{b.rd.L1} := \begin{cases} \left(n_{g1} \cdot F_{b.rd.1} + n_{g2} \cdot F_{b.rd.2}\right) & \text{if } F_{v.rd} \geq \max\left(F_{b.rd.1}, F_{b.rd.2}\right) \\ \left(n_{tot} \cdot \min\left(F_{b.rd.1}, F_{b.rd.2}\right)\right) & \text{otherwise} \end{cases}$$

$F_{b.rd.L1} = 453.036 \cdot kN$

Stiffness

$$k_{12} = \frac{24 \cdot n_b \cdot k_b \cdot k_t \cdot d \cdot f_u}{E}$$

$e_b := 110mm$ for hogging moment

$p_b := 60mm$ $n_b := 2$

$t_{L.cleat} = 15 \cdot mm$

e_b	is the distance from the bolt-row to the free edge of the plate in the direction of load transfer;
f_u	is the ultimate tensile strength of the steel on which the bolt bears;
p_b	is the spacing of the bolt-rows in the direction of load transfer;
t_i	is the thickness of that component.

$k_b = \min\left(k_{b1}, k_{b2}\right)$ $k_{b1} = \min\left(0.25 \cdot \frac{e_b}{d} + 0.5, 1.25\right)$ $k_{b2} = \min\left(0.25 \cdot \frac{p_b}{d} + 0.375, 1.25\right)$ $k_t = \min\left(1.5 \cdot \frac{t_i}{d_{m16}}, 2.5\right)$

$k_{b1} := \min\left(0.25 \cdot \frac{e_b}{d} + 0.5, 1.25\right) = 1.25$

$k_{b2} := \min\left(0.25 \cdot \frac{p_b}{d} + 0.375, 1.25\right) = 1.125$

$k_t := \min\left(1.5 \cdot \frac{t_{L.cleat}}{d_{m16}}, 2.5\right) = 1.406$

$k_b := \min(k_{b1}, k_{b2}) = 1.125$

$k_{12} := \frac{24 \cdot n_b \cdot k_b \cdot k_t \cdot d \cdot f_u}{E} = 3.11 \cdot mm$

$k_{lcw\text{-}b.1} := k_{12} = 3.11 \cdot mm$

3. Haunch in bearing

No information is available for now for the dimension of haunch so it will be assumed that the haunch has dimension sim to the beam IPE 270 and holes disposition as in L cleats, since they form the friction damper together

$t_{bh} := 13mm$ assumed

$e_1 := 60mm$ $p_1 := 999mm$ does not exist it this case

$e_2 := 35mm$ $p_2 := 74mm$

$n_{tot} := 2$ total number of bolts

In the direction of load transfer:

$\alpha_{d.end.bolt} := \frac{e_1}{3 \cdot d_0} = 0.952$ $\alpha_{d.inner.bolt} := \frac{p_1}{3 \cdot d_0} - \frac{1}{4} = 15.607$

In the direction perpendicular to load transfer:

$k_{1.edge.bolt} := \min\left(2.8 \cdot \frac{e_2}{d_0} - 1.7, 1.4 \cdot \frac{p_2}{d_0} - 1.7, 2.5\right) = 2.5$

$k_{1.inner.bolt} := \min\left(1.4 \cdot \frac{p_2}{d_0} - 1.7, 2.5\right) = 2.5$

In our case, in the direction of the load transfer we have 1 groups of bolts: 2 end bolts
When considering the direction perpendicular to the direction of load transfer, all bolts are considered as edge

End edge bolts

$n_{g1} := 2$ number of bolts in the group

$\alpha_b := \min\left(\alpha_{d.end.bolt}, \frac{f_{ub}}{f_u}, 1\right) = 0.952$

$F_{b.rd.1} := \frac{k_{1.edge.bolt} \cdot \alpha_b \cdot f_u \cdot d \cdot t_{bh}}{\gamma_{m2}} = 266.19 \cdot kN$

Inner edge bolts

$n_{g2} := 0$ number of bolts in the group

$\alpha_b := \min\left(\alpha_{d.inner.bolt}, \frac{f_{ub}}{f_u}, 1\right) = 1$

$$F_{b.rd.2} := \frac{k_{1.edge.bolt} \cdot \alpha_b \cdot f_u \cdot d \cdot t_{bh}}{\gamma_{m2}} = 279.5 \cdot kN$$

$$F_{b.rd.bh} := \begin{cases} \left(n_{g1} \cdot F_{b.rd.1} + n_{g2} \cdot F_{b.rd.2}\right) & \text{if } F_{v.rd} \geq \max\left(F_{b.rd.1}, F_{b.rd.2}\right) \\ \left(n_{tot} \cdot \min\left(F_{b.rd.1}, F_{b.rd.2}\right)\right) & \text{otherwise} \end{cases}$$

$$F_{b.rd.bh} = 532.381 \cdot kN$$

Stiffness

$$k_{12} = \frac{24 \cdot n_b \cdot k_b \cdot k_t \cdot d \cdot f_u}{E}$$

e_b	is the distance from the bolt-row to the free edge of the plate in the direction of load transfer;
f_u	is the ultimate tensile strength of the steel on which the bolt bears;
p_b	is the spacing of the bolt-rows in the direction of load transfer;
t_i	is the thickness of that component.

$e_{b.v} := 60mm$ for hogging moment

$p_{b.v} := 999mm$ does not exist

$n_{b.v} := 2$

$t_{bh} = 13 \cdot mm$

$$k_b = \min\left(k_{b1}, k_{b2}\right) \quad k_{b1} = \min\left(0.25 \cdot \frac{e_b}{d} + 0.5, 1.25\right) \quad k_{b2} = \min\left(0.25 \cdot \frac{p_b}{d} + 0.375, 1.25\right) \quad k_t = \min\left(1.5 \cdot \frac{t_i}{d_{m16}}, 2.5\right)$$

$$k_{b1.v} := \min\left(0.25 \cdot \frac{e_b}{d} + 0.5, 1.25\right) = 1.25$$

$$k_{b2.v} := \min\left(0.25 \cdot \frac{p_b}{d} + 0.375, 1.25\right) = 1.25$$

$$k_{t.v} := \min\left(1.5 \cdot \frac{t_{bh}}{d_{m16}}, 2.5\right) = 1.219$$

$$k_{b.v} := \min\left(k_{b1}, k_{b2}\right) = 1.25$$

$$k_{12.v} := \frac{24 \cdot n_b \cdot k_b \cdot k_t \cdot d \cdot f_u}{E} = 2.995 \cdot mm$$

$$k_{bh} := k_{12} = 2.995 \cdot mm$$

Calculation of the characteristic of new elements according to EC 3-1-8 for sagging moment:

1. Bolts in shear M20...8.8 used

$f_{yb} := 640\frac{N}{mm^2}$ bolt yeild strength $f_y := 275\frac{N}{mm^2}$

$f_{ub} := 800\frac{N}{mm^2}$ bolt ultimate strength $f_u := 430\frac{N}{mm^2}$

$E := 210GPa$

$\gamma_{m2} := 1$

$d_0 := 21mm$ hole diameter

$d := 20mm$ bolt diameter

$\alpha_v := 0.6$ $\frac{d^2}{4}\cdot 3.14 = 314\cdot mm^2$

$A_s := 245mm^2$ shredded part area

$m := 2$ number of shear planes

$A_b := \frac{d^2}{4}\cdot\pi = 3.142\times 10^{-4}\,m^2$ shear plane area

$F_{v.rd} := \frac{m\cdot\alpha_v\cdot f_{ub}\cdot A_b}{\gamma_{m2}} = 301.593\cdot kN$ Table 3.4

$n_b := 2$ number of bolt rows working in shear (we have a slotted hole therefore only 2 bolts will be in touch with the plates, both for stiffness and design resistance)

$d_{m16} := 16mm$

$k_{11} := \frac{16\cdot n_b\cdot d^2\cdot f_{ub}}{E\cdot d_{m16}} = 3.048\cdot mm$ Table 6.11

$k_{bs} := k_{11} = 3.048\cdot mm$

2. L cleats in bearing

$F_{b.rd} = \frac{k_1\cdot\alpha_b\cdot f_u\cdot d\cdot t}{\gamma_{m2}}$ $\alpha_b = \min\left(\alpha_d, \frac{f_{ub}}{f_u}, 1\right)$

2.1 Bearing of the upper L cleat (one cleat considered)

$t_{L.cleat} := 15mm$

$e_1 := 60mm$ $p_1 := 60mm$

$e_2 := 31mm$ $p_2 := 999mm$ there is no p.2

$n_{tot} := 1$ total number of bolts working

In the direction of load transfer:

$$\alpha_{d.end.bolt} := \frac{e_1}{3 \cdot d_0} = 0.952 \qquad \alpha_{d.inner.bolt} := \frac{p_1}{3 \cdot d_0} - \frac{1}{4} = 0.702$$

In the direction perpendicular to load transfer:

$$k_{1.edge.bolt} := \min\left(2.8 \cdot \frac{e_2}{d_0} - 1.7, 1.4 \cdot \frac{p_2}{d_0} - 1.7, 2.5\right) = 2.433 \qquad k_{1.inner.bolt} := \min\left(1.4 \cdot \frac{p_2}{d_0} - 1.7, 2.5\right) = 2.5$$

In our case, in the direction of the load transfer we have only end bolts working
When considering the direction perpendicular to the direction of load transfer, the bolts are considered as edge

End edge bolts

$n_{g1} := 0$ number of bolts in the group

$$\alpha_b := \min\left(\alpha_{d.end.bolt}, \frac{f_{ub}}{f_u}, 1\right) = 0.952$$

$$F_{b.rd.1} := \frac{k_{1.edge.bolt} \cdot \alpha_b \cdot f_u \cdot d \cdot t_{L.cleat}}{\gamma_{m2}} = 298.952 \cdot kN$$

Inner edge bolts

$n_{g2} := 1$ number of bolts in the group

$$\alpha_b := \min\left(\alpha_{d.inner.bolt}, \frac{f_{ub}}{f_u}, 1\right) = 0.702$$

$$F_{b.rd.2} := \frac{k_{1.edge.bolt} \cdot \alpha_b \cdot f_u \cdot d \cdot t_{L.cleat}}{\gamma_{m2}} = 220.477 \cdot kN$$

$$F_{b.rd.L2} := \begin{cases} \left(n_{g1} \cdot F_{b.rd.1} + n_{g2} \cdot F_{b.rd.2}\right) & \text{if } F_{v.rd} \geq \max\left(F_{b.rd.1}, F_{b.rd.2}\right) \\ \left(n_{tot} \cdot \min\left(F_{b.rd.1}, F_{b.rd.2}\right)\right) & \text{otherwise} \end{cases}$$

$F_{b.rd.L2} = 220.477 \cdot kN$

Stiffness

$$k_{12} = \frac{24 \cdot n_b \cdot k_b \cdot k_t \cdot d \cdot f_u}{E}$$

$e_b := 60mm$ for hogging moment

e.b in this case equal to the distance to other bolt in direction of load transfer?

$p_b := 60mm$ $n_b := 1$

$t_{L.cleat} = 15 \cdot mm$

e_b	is the distance from the bolt-row to the free edge of the plate in the direction of load transfer;
f_u	is the ultimate tensile strength of the steel on which the bolt bears;
p_b	is the spacing of the bolt-rows in the direction of load transfer;
t_i	is the thickness of that component.

$k_b = \min(k_{b1}, k_{b2})$ $k_{b1} = \min\left(0.25\cdot\frac{e_b}{d} + 0.5, 1.25\right)$ $k_{b2} = \min\left(0.25\cdot\frac{p_b}{d} + 0.375, 1.25\right)$ $k_t = \min\left(1.5\cdot\frac{t_i}{d_{m16}}, 2.5\right)$

$k_{b1} := \min\left(0.25\cdot\frac{e_b}{d} + 0.5, 1.25\right) = 1.25$

$k_{b2} := \min\left(0.25\cdot\frac{p_b}{d} + 0.375, 1.25\right) = 1.125$

$k_t := \min\left(1.5\cdot\frac{t_{L.cleat}}{d_{m16}}, 2.5\right) = 1.406$

$k_b := \min(k_{b1}, k_{b2}) = 1.125$

$k_{12} := \frac{24\cdot n_b\cdot k_b\cdot k_t\cdot d\cdot f_u}{E} = 1.555\cdot mm$ for one upper L cleat

$k_{lcw\text{-}b.2} := k_{12} = 1.555\cdot mm$

2.2 Bearing of the lower L cleat

$t_{L.cleat} := 15mm$

$e_1 := 60mm$ $p_1 := 60mm$

$e_2 := 49mm$ $p_2 := 78mm$

$n_{tot} := 2$ total number of bolts working

In the direction of load transfer:

$\alpha_{d.end.bolt} := \frac{e_1}{3\cdot d_0} = 0.952$ $\alpha_{d.inner.bolt} := \frac{p_1}{3\cdot d_0} - \frac{1}{4} = 0.702$

In the direction perpendicular to load transfer:

$k_{1.edge.bolt} := \min\left(2.8\cdot\frac{e_2}{d_0} - 1.7, 1.4\cdot\frac{p_2}{d_0} - 1.7, 2.5\right) = 2.5$

$k_{1.inner.bolt} := \min\left(1.4\cdot\frac{p_2}{d_0} - 1.7, 2.5\right) = 2.5$

In our case, in the direction of the load transfer we have 2 bolts acting as inner bolts (load transf towards in)
When considering the direction perpendicular to the direction of load transfer, all bolts are considered as edge

End edge bolts

$n_{g1} := 0$ number of bolts in the group

$\alpha_b := \min\left(\alpha_{d.end.bolt}, \frac{f_{ub}}{f_u}, 1\right) = 0.952$

$$F_{b.rd.1} := \frac{k_{1.edge.bolt} \cdot \alpha_b \cdot f_u \cdot d \cdot t_{L.cleat}}{\gamma_{m2}} = 307.143 \cdot kN$$

Inner edge bolts

$n_{g2} := 2$ number of bolts in the group

$$\alpha_b := \min\left(\alpha_{d.inner.bolt}, \frac{f_{ub}}{f_u}, 1\right) = 0.702$$

$$F_{b.rd.2} := \frac{k_{1.edge.bolt} \cdot \alpha_b \cdot f_u \cdot d \cdot t_{L.cleat}}{\gamma_{m2}} = 226.518 \cdot kN$$

$$F_{b.rd.L1} := \begin{cases} \left(n_{g1} \cdot F_{b.rd.1} + n_{g2} \cdot F_{b.rd.2}\right) & \text{if } F_{v.rd} \geq \max\left(F_{b.rd.1}, F_{b.rd.2}\right) \\ \left(n_{tot} \cdot \min\left(F_{b.rd.1}, F_{b.rd.2}\right)\right) & \text{otherwise} \end{cases}$$

$F_{b.rd.L1} = 453.036 \cdot kN$

Stiffness

$$k_{12} = \frac{24 \cdot n_b \cdot k_b \cdot k_t \cdot d \cdot f_u}{E}$$

$e_b := 110mm$ for hogging moment

$p_b := 60mm$ $n_b := 2$

$t_{L.cleat} = 15 \cdot mm$

e_b	is the distance from the bolt-row to the free edge of the plate in the direction of load transfer;
f_u	is the ultimate tensile strength of the steel on which the bolt bears;
p_b	is the spacing of the bolt-rows in the direction of load transfer;
t_i	is the thickness of that component.

$$k_b = \min\left(k_{b1}, k_{b2}\right) \quad k_{b1} = \min\left(0.25 \cdot \frac{e_b}{d} + 0.5, 1.25\right) \quad k_{b2} = \min\left(0.25 \cdot \frac{p_b}{d} + 0.375, 1.25\right) \quad k_t = \min\left(1.5 \cdot \frac{t_i}{d_{m16}}, 2.5\right)$$

$$k_{b1} := \min\left(0.25 \cdot \frac{e_b}{d} + 0.5, 1.25\right) = 1.25$$

$$k_{b2} := \min\left(0.25 \cdot \frac{p_b}{d} + 0.375, 1.25\right) = 1.125$$

$$k_t := \min\left(1.5 \cdot \frac{t_{L.cleat}}{d_{m16}}, 2.5\right) = 1.406$$

$$k_b := \min\left(k_{b1}, k_{b2}\right) = 1.125$$

$$k_{12} := \frac{24 \cdot n_b \cdot k_b \cdot k_t \cdot d \cdot f_u}{E} = 3.11 \cdot mm$$

$k_{lcw\text{-}b.1} := k_{12} = 3.11 \cdot mm$

3. Haunch in bearing

No information is available for now for the dimension of haunch so it will be assumed that the haunch has dimension sim to the beam IPE 270 and holes disposition as in L cleats, since they form the friction damper together

$t_{bh} := 13mm$ assumed

$e_1 := 60mm$ $p_1 := 999mm$ does not exist it this case

$e_2 := 35mm$ $p_2 := 74mm$

$n_{tot} := 2$ total number of bolts

In the direction of load transfer:

$$\alpha_{d.end.bolt} := \frac{e_1}{3 \cdot d_0} = 0.952 \qquad \alpha_{d.inner.bolt} := \frac{p_1}{3 \cdot d_0} - \frac{1}{4} = 15.607$$

In the direction perpendicular to load transfer:

$$k_{1.edge.bolt} := \min\left(2.8 \cdot \frac{e_2}{d_0} - 1.7, 1.4 \cdot \frac{p_2}{d_0} - 1.7, 2.5\right) = 2.5$$

$$k_{1.inner.bolt} := \min\left(1.4 \cdot \frac{p_2}{d_0} - 1.7, 2.5\right) = 2.5$$

In our case, in the direction of the load transfer we have 1 groups of bolts: 2 end bolts
When considering the direction perpendicular to the direction of load transfer, all bolts are considered as edge

End edge bolts

$n_{g1} := 2$ number of bolts in the group

$$\alpha_b := \min\left(\alpha_{d.end.bolt}, \frac{f_{ub}}{f_u}, 1\right) = 0.952$$

$$F_{b.rd.1} := \frac{k_{1.edge.bolt} \cdot \alpha_b \cdot f_u \cdot d \cdot t_{bh}}{\gamma_{m2}} = 266.19 \cdot kN$$

Inner edge bolts

$n_{g2} := 0$ number of bolts in the group

$$\alpha_b := \min\left(\alpha_{d.inner.bolt}, \frac{f_{ub}}{f_u}, 1\right) = 1$$

$$F_{b.rd.2} := \frac{k_{1.edge.bolt} \cdot \alpha_b \cdot f_u \cdot d \cdot t_{bh}}{\gamma_{m2}} = 279.5 \cdot kN$$

$$F_{b.rd.bh} := \begin{cases} \left(n_{g1} \cdot F_{b.rd.1} + n_{g2} \cdot F_{b.rd.2}\right) & \text{if } F_{v.rd} \geq \max\left(F_{b.rd.1}, F_{b.rd.2}\right) \\ \left(n_{tot} \cdot \min\left(F_{b.rd.1}, F_{b.rd.2}\right)\right) & \text{otherwise} \end{cases}$$

$$F_{b.rd.bh} = 532.381 \cdot kN$$

Stiffness

$$k_{12} = \frac{24 \cdot n_b \cdot k_b \cdot k_t \cdot d \cdot f_u}{E}$$

e_b	is the distance from the bolt-row to the free edge of the plate in the direction of load transfer;
f_u	is the ultimate tensile strength of the steel on which the bolt bears;
p_b	is the spacing of the bolt-rows in the direction of load transfer;
t_i	is the thickness of that component.

$e_{bv} := 60mm$ for hogging moment

$p_{bv} := 999mm$ does not exist

$n_{bv} := 2$

$t_{bh} = 13 \cdot mm$

$$k_b = \min(k_{b1}, k_{b2}) \quad k_{b1} = \min\left(0.25 \cdot \frac{e_b}{d} + 0.5, 1.25\right) \quad k_{b2} = \min\left(0.25 \cdot \frac{p_b}{d} + 0.375, 1.25\right) \quad k_t = \min\left(1.5 \cdot \frac{t_i}{d_{m16}}, 2.5\right)$$

$$k_{b1v} := \min\left(0.25 \cdot \frac{e_b}{d} + 0.5, 1.25\right) = 1.25$$

$$k_{b2v} := \min\left(0.25 \cdot \frac{p_b}{d} + 0.375, 1.25\right) = 1.25$$

$$k_{tv} := \min\left(1.5 \cdot \frac{t_{bh}}{d_{m16}}, 2.5\right) = 1.219$$

$$k_{bv} := \min(k_{b1}, k_{b2}) = 1.25$$

$$k_{12v} := \frac{24 \cdot n_b \cdot k_b \cdot k_t \cdot d \cdot f_u}{E} = 2.995 \cdot mm$$

$$k_{bh} := k_{12} = 2.995 \cdot mm$$

```
clear all
close all

%% Units: kN and m
%% Input data's

global L Es As L0 h_hog h_sag i results u K_fake_1 K_fake_2 yield delta_at_F_0

L0 = 5; %[m] initial lenght of the beam
h_hog = [0.1425 -0.2695]; %[m] distance from the mid-height h = [0.055 -0.07464];
h_sag = [-0.2695 0.1425];
L = 0;%[m] plastic hinge length (in case of a hinge in the joint L=0) L = 3*160/1000
Es = 210000; %[N/mm²] modulus of elasticity of steel
As = 4595;%[mm²] area of the beam IPE 270 cross section, As = 1256.64;
fy = 275; %[MPa] not used
K_fake_1 = 0;%[N/mm]=[kN/m] fake stiffness of the slip
K_fake_2 = 0;%[N/mm]=[kN/m] fake stiffness of the plateu

u_limit = 2.4; %[m] max displacement at the point of col1umn loss
u_step = 0.0005; %[m] iteration step 0.0005 ok


%% Initialisation of the unknowns vector
x0 = 0.0000*ones(1,13); %important for delta limit of springs
%% Resolution

results(1,:) = zeros(1,18);
%results(1,:) = zeros(1,19);

i=2;

while ((results(i-1,1)<u_limit))

    results(i,1)=results(i-1,1)+u_step; %u

    u = results(i,1);

    options = optimset('TolX',1e-5,'TolFun',1e-6,'MaxFunEvals',3000);
    [x,fval,exitflag]=fsolve(@myfun_slab1_joint,x0,options);

     results(i,2:14) = x;

     results(i,15) = results(i,8)*h_hog(1) + results(i,9)*h_hog(2) ;%M+(HOG) default
     results(i,16) = results(i,12)*h_sag(1) + results(i,13)*h_sag(2) ;%M-(SAG)default↙
givin ok springs
     results(i,17) = (results(i,14)*u+results(i,15)-results(i,16))/(L0-results(i,5));%↙
my derivation
     results(i,18) = exitflag;
     results(i,19) = ((results(i,14)/cos(results(i,2)))); %the force in the beam

    x0 = x + (x-results(i-1,2:14)); %do not change

    i=i+1;
end
```

```
%% Graph plot
plot_lim1=find(results(:,1)>1.79,1);
plot_lim2=find(results(:,1)>1.85,1);
plot_lim3=find(results(:,1)>0.47,1);
plot_lim4=find(results(:,1)>0.52,1);
plot_lim5=find(results(:,1)>0.3,1);
plot_lim6=find(results(:,1)>0.35,1);

col1='.g';
col2='.r';
col3='.y';

FIG.fig = 1;
figure(FIG.fig)
hold on
plot(results(:,6),results(:,8),'b','linewidth',2)
plot(results(plot_lim1:plot_lim2,6),results(plot_lim1:plot_lim2,8),col1,'linewidth',↙
1,'MarkerSize',15)
plot(results(plot_lim3:plot_lim4,6),results(plot_lim3:plot_lim4,8),col2,'linewidth',↙
1,'MarkerSize',15)
plot(results(plot_lim5:plot_lim6,6),results(plot_lim5:plot_lim6,8),col3,'linewidth',↙
1,'MarkerSize',15)
xlabel ('delta_1 hog [m]')
ylabel ('F_1 hog [kN]')

FIG.fig = 2;
figure(FIG.fig)
hold on
plot(results(:,7),results(:,9),'b','linewidth',2)
plot(results(plot_lim1:plot_lim2,7),results(plot_lim1:plot_lim2,9),col1,'linewidth',↙
1,'MarkerSize',15)
plot(results(plot_lim3:plot_lim4,7),results(plot_lim3:plot_lim4,9),col2,'linewidth',↙
1,'MarkerSize',15)
plot(results(plot_lim5:plot_lim6,7),results(plot_lim5:plot_lim6,9),col3,'linewidth',↙
1,'MarkerSize',15)
xlabel ('delta_2 hog [m]')
ylabel ('F_2 hog [kN]')

FIG.fig = 3;
figure(FIG.fig)
hold on
plot(results(:,10),results(:,12),'b','linewidth',2)
plot(results(plot_lim1:plot_lim2,10),results(plot_lim1:plot_lim2,12),col1,'linewidth',↙
1,'MarkerSize',15)
plot(results(plot_lim3:plot_lim4,10),results(plot_lim3:plot_lim4,12),col2,'linewidth',↙
1,'MarkerSize',15)
plot(results(plot_lim5:plot_lim6,10),results(plot_lim5:plot_lim6,12),col3,'linewidth',↙
1,'MarkerSize',15)
xlabel ('delta_1 sag [m]')
ylabel ('F_1 sag [kN]')

FIG.fig = 4;
figure(FIG.fig)
hold on
plot(results(:,11),results(:,13),'b','linewidth',2)
```

```
plot(results(plot_lim1:plot_lim2,11),results(plot_lim1:plot_lim2,13),col1,'linewidth',↙
1,'MarkerSize',15)
plot(results(plot_lim3:plot_lim4,11),results(plot_lim3:plot_lim4,13),col2,'linewidth',↙
1,'MarkerSize',15)
plot(results(plot_lim5:plot_lim6,11),results(plot_lim5:plot_lim6,13),col3,'linewidth',↙
1,'MarkerSize',15)
xlabel ('delta_2 sag [m]')
ylabel ('F_2 sag [kN]')

FIG.fig = 5;
figure(FIG.fig)
hold on
plot(results(:,1),results(:,17),'b','linewidth',2)
plot(results(plot_lim1:plot_lim2,1),results(plot_lim1:plot_lim2,17),col1,'linewidth',↙
1,'MarkerSize',20)
plot(results(plot_lim3:plot_lim4,1),results(plot_lim3:plot_lim4,17),col2,'linewidth',↙
1,'MarkerSize',20)
plot(results(plot_lim5:plot_lim6,1),results(plot_lim5:plot_lim6,17),col3,'linewidth',↙
1,'MarkerSize',15)
xlabel ('u [m]')
ylabel ('P [kN]')

FIG.fig = 6;
figure(FIG.fig)
hold on
plot(results(:,5),results(:,14),'b','linewidth',2)
plot(results(plot_lim1:plot_lim2,5),results(plot_lim1:plot_lim2,14),col1,'linewidth',↙
1,'MarkerSize',15)
plot(results(plot_lim3:plot_lim4,5),results(plot_lim3:plot_lim4,14),col2,'linewidth',↙
1,'MarkerSize',15)
plot(results(plot_lim5:plot_lim6,5),results(plot_lim5:plot_lim6,14),col3,'linewidth',↙
1,'MarkerSize',15)
xlabel ('delta_h [m]')
ylabel ('Fh [kN]')

FIG.fig = 7;
figure(FIG.fig)
hold on
plot(results(:,2),results(:,15),'b','linewidth',2)
plot(results(plot_lim1:plot_lim2,2),results(plot_lim1:plot_lim2,15),col1,'linewidth',↙
1,'MarkerSize',15)
plot(results(plot_lim3:plot_lim4,2),results(plot_lim3:plot_lim4,15),col2,'linewidth',↙
1,'MarkerSize',15)
plot(results(plot_lim5:plot_lim6,2),results(plot_lim5:plot_lim6,15),col3,'linewidth',↙
1,'MarkerSize',15)
xlabel ('theta [rad]')
ylabel ('M hog [kNm]')

FIG.fig = 8;
figure(FIG.fig)
hold on
plot((-results(:,2)),results(:,16),'b','linewidth',2)
plot((-results(plot_lim1:plot_lim2,2)),results(plot_lim1:plot_lim2,16),↙
col1,'linewidth',1,'MarkerSize',15)
plot((-results(plot_lim3:plot_lim4,2)),results(plot_lim3:plot_lim4,16),↙
```

```
col2,'linewidth',1,'MarkerSize',15)
plot((-results(plot_lim5:plot_lim6,2)),results(plot_lim5:plot_lim6,16),↙
col3,'linewidth',1,'MarkerSize',15)
xlabel ('theta [rad]')
ylabel ('M sag [kNm]')
```

```
function F = myfun_slab1_joint(x)
%% Input data's
% The same as in the "substrucre.m" file

global L Es As L0 h_hog h_sag i results u K_fake_1 K_fake_2 yield delta_at_F_0

%% Definition of the unknowns
% The vector "x" is the unknowns-vector

theta = x(1);

delta_HOG = x(2);
delta_SAG = x(3);
deltah = x(4);

delta_1_HOG = x(5);
delta_2_HOG = x(6);

F_1_HOG = x(7);
F_2_HOG = x(8);

delta_1_SAG = x(9);
delta_2_SAG = x(10);

F_1_SAG = x(11);
F_2_SAG = x(12);

Fh = x(13);


%% Definition of the equations

F     = [sin(theta)-(u/(L0-2*L+(1000*Fh*(L0-2*L)/(Es*As))))

    cos(theta)-((L0-2*L-deltah - delta_SAG - delta_HOG)/(L0-2*L+(1000*Fh*(L0-2*L)/↙
(Es*As))))% derived and checked

    delta_1_HOG - (delta_HOG+h_hog(1)*theta) % delta_1_HOG should be positive since↙
the spring is in tension
    delta_2_HOG - (delta_HOG+h_hog(2)*theta)

    %giving good spring graphs
    delta_1_SAG - (delta_SAG-h_sag(1)*theta) % delta_1_SAG should be positive since↙
the spring is in tension
    delta_2_SAG - (delta_SAG-h_sag(2)*theta)

    F_1_HOG - F_spring_hog_1(delta_1_HOG,results(i-1,6),results(i-1,8),K_fake_1,↙
K_fake_2)%more complex definition zase 11 F_1_HOG - F_spring_hog_1(delta_1_HOG,results↙
(i-1,6),results(i-1,8))
    F_2_HOG - F_spring_hog_2(delta_2_HOG,results(i-1,7),results(i-1,9),K_fake_1,↙
K_fake_2,i,yield)

    F_1_SAG - F_spring_sag_1(delta_1_SAG,results(i-1,10),results(i-1,12),K_fake_1,↙
K_fake_2)%more complex definition zase 11 F_1_SAG - F_spring_sag_1(delta_1_SAG,results↙
(i-1,10),results(i-1,12))
```

```
    F_2_SAG - F_spring_sag_2(delta_2_SAG,results(i-1,11),results(i-1,13),K_fake_1,↙
K_fake_2,i,yield,delta_at_F_0)

    Fh - (F_1_HOG + F_2_HOG)
    Fh - (F_1_SAG + F_2_SAG)
    Fh - fh_linear(deltah)];

end
```

```
function [FH] = fh_linear(deltah)
%% Input
Kh = 10000; %[N/mm] = [kN/m]
%% Sub-program
%% Formulation 1 - linear
 if deltah<0
      FH = 0;
  else
    FH = Kh*deltah;
  end
```

```
function [F_spring_hog_1] = F_spring_hog_1(delta_1_HOG,delta_prec,F_prec,K_fake_1,↙
K_fake_2) %spring in tension
%% Input
F_tens_ultimate = 598.3; %[kN] ultimate spring strenght
F_slip = 186.6;%[kN] force in the spring at moment of slip F_slip = 186.6;
Es = 210000; %[N/mm²]
K_before_slip = 5.934*Es;%[mm] stiffness of the spring K_before_slip = 5.763*Es;
K_after_slip = 1.446*Es;%[mm] stiffness of the spring
delta_limit = 0.00015; %[m] the value when the law should change
n = 1; % stiffness reduction factor
%% Formulation 1-FULL linear - plastic or fake plastic
%-not working for some reason
% if delta_1_HOG < 0 % same definition as in 9 spring model which works
%     F_spring_hog_1 = 0;
% else
%  if delta_1_HOG < delta_limit
%    F_spring_hog_1 =  max(0,min(F_slip+(K_fake_1/n)*delta_1_HOG,↙
(F_prec+K_before_slip*(delta_1_HOG - delta_prec))));
%  else
%    F_spring_hog_1 =  max(0,min(F_tens_ultimate+(K_fake_2/n)*delta_1_HOG,↙
(F_prec+K_after_slip*(delta_1_HOG - delta_prec))));
%  end
% end

%% Formulation 1.1-FULL linear - plastic or fake plastic
%-not working for some reason
% if delta_1_HOG < 0 % same definition as in 9 spring model which works
%     F_spring_hog_1 = 0;
% elseif delta_1_HOG < delta_limit
%    F_spring_hog_1 =  max(0,min(F_slip+(K_fake_1/n)*delta_1_HOG,↙
(F_prec+K_before_slip*(delta_1_HOG - delta_prec))));
% else
%    F_spring_hog_1 =  max(0,min(F_tens_ultimate+(K_fake_2/n)*delta_1_HOG,↙
(F_prec+K_after_slip*(delta_1_HOG - delta_prec))));
% end

%% Formulation 2 - UGhent
%F_spring_hog_1 = (697.43+(Ks/345)*delta_1_HOG);
%F_spring_hog_1 = F_tens;

%% Formulation 3
%F_spring_hog_1 = min((Ks/345)*delta_1_HOG,F_tens); %case 10 excel

%% Formulation 5 - linear - fake plastic
%-works even for very low value of k_fake!!!
%F_spring_hog_1 =  max(0,min(F_slip+(K_fake_1/n)*delta_1_HOG,(F_prec+K_before_slip*↙
(delta_1_HOG - delta_prec))));
%F_spring_hog_1 =  max(0,min(F_tens_ultimate+(K_fake_2/n)*delta_1_HOG,↙
(F_prec+K_after_slip*(delta_1_HOG - delta_prec))));

%% Formulation 6 - rigid - fake plastic (a bit of slope to avoid singularity)
% -with the if condition can't convergate for any K
% -without if works
```

```
% if delta_1_HOG < 0
%     F_spring_hog_1 = 0;
% else
    %F_spring_hog_1 =  F_tens_ultimate+(K_fake_2/n)*delta_1_HOG;
%     F_spring_hog_1 =  F_slip+(K_fake_1/n)*delta_1_HOG;
% end

%% Formulation 7 - FULL linear - fake plastic - all models the same
%-
if delta_1_HOG < delta_limit % same definition as in 9 spring model which works
    F_spring_hog_1 =  min(F_slip+(K_fake_1/n)*delta_1_HOG,(F_prec+K_before_slip*↙
(delta_1_HOG - delta_prec)));
else
   F_spring_hog_1 =  min(F_tens_ultimate+(K_fake_2/n)*delta_1_HOG,↙
(F_prec+K_after_slip*(delta_1_HOG - delta_prec)));
end

%% Formulation 8 - rigid - linear - fake plastic
%-
 %F_spring_hog_1 =  min(F_tens_ultimate+(K_fake_2/n)*delta_1_HOG,max(F_slip,↙
F_prec+K_after_slip*(delta_1_HOG - delta_prec)));
end
```

```
function [F_spring_hog_2] = F_spring_hog_2(delta_2_HOG,delta_prec,F_prec,K_fake_1,↙
K_fake_2,i,yield) % spring in compression
%% Input
Es = 210000; %[N/mm²]
delta_limit = -0.03505; %[m] the value when the law should change delta_limit =↙
-0.110047
delta_limit_t = 0.03534; %[m] changable value if the plateau in compession is reached
n = 1; % stiffness reduction factor

%Compression behavior
F_c_ult = -532.4; %[kN] ultimate spring strenght
F_slip_c = -450.8;%[kN] force in the spring at moment of slip

K_before_slip_c = 45.82*Es;%[mm] stiffness of the spring K_before_slip = 45.82*Es;
K_after_slip_c = 1.184*Es;%[mm] stiffness of the spring K_after_slip = 1.184*Es;

%Tension behavior

F_t_ult = 490.1; %[kN] ultimate spring strenght
F_slip_t = 450.8;%[kN] force in the spring at moment of slip

K_before_slip_t = 6.39*Es;%[mm] stiffness of the spring K_before_slip = 5.946*Es;
K_after_slip_t = 1.021*Es;%[mm] stiffness of the spring K_after_slip = 1.184*Es;

%% Formulation 1 - approx FULL curve - model 2.1
%- works
% F_c = F_slip_c;
% F_t = F_slip_t;
%
% if delta_2_HOG < delta_prec % if (delta_2_HOG-delta_prec) < 0
%     F_spring_hog_2 = max(F_c+(K_fake_1/n)*delta_2_HOG,F_prec+(K_before_slip_c*↙
(delta_2_HOG - delta_prec)));
% else
%     F_spring_hog_2 = min(F_t+(K_fake_1/n)*delta_2_HOG,F_prec+↙
((K_before_slip_t+K_before_slip_c)/2)*(delta_2_HOG - delta_prec));
% end

% Formulation 2 - approx FULL curve - model 2.2
%- works
% if delta_2_HOG < delta_prec % if (delta_2_HOG-delta_prec) < 0
%     if delta_2_HOG > delta_limit
%         F_spring_hog_2 = max(F_slip_c+(K_fake_1/n)*delta_2_HOG,F_prec+↙
(K_before_slip_c*(delta_2_HOG - delta_prec)));
%     else
%         F_spring_hog_2 = max(F_c_ult+(K_fake_1/n)*delta_2_HOG,F_prec+↙
(K_after_slip_c*(delta_2_HOG - delta_prec)));
%     end
% else
%     if F_prec < 0
%         F_spring_hog_2 = F_prec+K_before_slip_c*(delta_2_HOG - delta_prec);
%     else
%         F_spring_hog_2 = min(F_t_ult+(K_fake_1/n)*delta_2_HOG,↙
F_prec+K_before_slip_t*(delta_2_HOG - delta_prec));
%     end
% end
```

```
%% Formulation 3 - approx FULL curve - model 2.3-works

% if delta_2_HOG < delta_prec % if (delta_2_HOG-delta_prec) < 0
%     if delta_2_HOG > delta_limit
%         F_spring_hog_2 = max(F_slip_c+(K_fake_1/n)*delta_2_HOG,F_prec+↙
(K_before_slip_c*(delta_2_HOG - delta_prec)));
%     else
%         F_spring_hog_2 = max(F_c_ult+(K_fake_1/n)*delta_2_HOG,F_prec+↙
(K_after_slip_c*(delta_2_HOG - delta_prec)));
%     end
% else
%     if F_prec > F_c_ult && F_prec < F_slip_c
%             F_spring_hog_2 =F_prec + K_after_slip_c*(delta_2_HOG - delta_prec);
%     elseif F_prec > F_slip_c && F_prec < 0
%             F_spring_hog_2 =F_prec + K_before_slip_c*(delta_2_HOG - delta_prec);
%     elseif F_prec > 0 && F_prec < F_slip_t
%             F_spring_hog_2 =F_prec + K_before_slip_t*(delta_2_HOG - delta_prec);
%     else %F_prec >= F_slip_t
%             F_spring_hog_2 = F_slip_t;
%     %else
%     end
% end

% %% Formulation 4 - approx FULL curve - model 2.3.2 onlyk_fake added
%
% if delta_2_HOG < delta_prec % if (delta_2_HOG-delta_prec) < 0
%     if delta_2_HOG > delta_limit
%         F_spring_hog_2 = max(F_slip_c+(K_fake_1/n)*delta_2_HOG,F_prec+↙
(K_before_slip_c*(delta_2_HOG - delta_prec)));
%     else
%         F_spring_hog_2 = max(F_c_ult+(K_fake_1/n)*delta_2_HOG,F_prec+↙
(K_after_slip_c*(delta_2_HOG - delta_prec)));
%     end
% else
%     if F_prec > F_c_ult && F_prec < F_slip_c
%             F_spring_hog_2 =F_prec + K_after_slip_c*(delta_2_HOG - delta_prec);
%     elseif F_prec > F_slip_c && F_prec < 0
%             F_spring_hog_2 =F_prec + K_before_slip_c*(delta_2_HOG - delta_prec);
%     elseif F_prec > 0 && F_prec < F_slip_t
%             F_spring_hog_2 =F_prec + K_before_slip_t*(delta_2_HOG - delta_prec);
%     else %F_prec >= F_slip_t
%             F_spring_hog_2 = F_slip_t+(K_fake_1/n)*delta_2_HOG;
%     %else
%     end
% end

%% Formulation 5 - approx FULL curve - model 2.3.2 full even the bearing in tension

if delta_2_HOG < delta_prec % if (delta_2_HOG-delta_prec) < 0
    if delta_2_HOG > delta_limit
        F_spring_hog_2 = max(F_slip_c+(K_fake_1/n)*delta_2_HOG,F_prec+↙
(K_before_slip_c*(delta_2_HOG - delta_prec)));
    else
        F_spring_hog_2 = max(F_c_ult+(K_fake_1/n)*delta_2_HOG,F_prec+(K_after_slip_c*↙
```

```
(delta_2_HOG - delta_prec)));
    end
else
    if F_prec >= F_c_ult && F_prec < F_slip_c
            F_spring_hog_2 =F_prec + K_after_slip_c*(delta_2_HOG - delta_prec);
    elseif F_prec > F_slip_c && F_prec < 0
            F_spring_hog_2 =F_prec + K_before_slip_c*(delta_2_HOG - delta_prec);
    elseif F_prec > 0 && F_prec < F_slip_t
            F_spring_hog_2 =F_prec + K_before_slip_t*(delta_2_HOG - delta_prec);
    elseif F_prec > F_slip_t && delta_2_HOG < delta_limit_t
            F_spring_hog_2 = F_slip_t+(K_fake_1/n)*delta_2_HOG;
    elseif F_prec > F_slip_t && delta_2_HOG > delta_limit_t && delta_2_HOG < 0.0355
           F_spring_hog_2 = F_prec+(K_after_slip_t*(delta_2_HOG - delta_prec));
    else % F_prec > F_slip_t && delta_2_HOG > 0.0359
        F_spring_hog_2 = F_t_ult+(K_fake_1/n)*delta_2_HOG;
    end
end
```

```
function [F_spring_sag_1] = F_spring_sag_1(delta_1_SAG,delta_prec,F_prec,K_fake_1,↙
K_fake_2) %spring in tension
%% Input
F_tens_ultimate = 490.1; %[kN] ultimate spring strenght
F_slip = 450.8;%[kN] force in the spring at moment of slip
Es = 210000; %[N/mm²]
K_before_slip = 6.39*Es;%[mm] stiffness of the spring K_before_slip = 5.946*Es;
K_after_slip = 1.021*Es;%[mm] stiffness of the spring K_after_slip = 1.009*Es;
delta_limit = 0.03534; %[m] the value when the law should change delta_limit = 0.11036
n = 1; % stiffness reduction factor
%% Formulation 1- linear - plastic or fake plastic
% if delta_1_SAG < 0 % same definition as in 9 spring model which works
%     F_spring_sag_1 = 0;
% else
%     if delta_1_SAG < delta_limit
%    F_spring_sag_1 =  max(0,min(F_slip+(K_fake_1/n)*delta_1_SAG,↙
(F_prec+K_before_slip*(delta_1_SAG - delta_prec))));
%     else
%    F_spring_sag_1 =  max(0,min(F_tens_ultimate+(K_fake_2/n)*delta_1_SAG,↙
(F_prec+K_after_slip*(delta_1_SAG - delta_prec))));
%     end
% end

%% Formulation 1.1 FULL - linear - plastic or fake plastic
% if delta_1_SAG < 0 % same definition as in 9 spring model which works
%     F_spring_sag_1 = 0;
% elseif delta_1_SAG < delta_limit
%    F_spring_sag_1 =  max(0,min(F_slip+(K_fake_1/n)*delta_1_SAG,↙
(F_prec+K_before_slip*(delta_1_SAG - delta_prec))));
% else
%    F_spring_sag_1 =  max(0,min(F_tens_ultimate+(K_fake_2/n)*delta_1_SAG,↙
(F_prec+K_after_slip*(delta_1_SAG - delta_prec))));
% end

%% Formulation 2 - UGhent law
%F_spring_sag_1 = (697.43+(Ks/345)*delta_1_SAG);
%F_spring_sag_1 = F_tens;

%% Formulation 3 - linear-plastic law
%F_spring_sag_1 = min((Ks/345)*delta_1_SAG,F_tens); %case 10 excel

%% Formulation 4 - linear - plastic
%F_spring_sag_1 =  min(F_tens_ultimate,(F_prec+K_before_slip*(delta_1_SAG -↙
delta_prec)));

%% Formulation 5 - linear - fake plastic
%F_spring_sag_1 =  min(F_slip+(K_fake_1/n)*delta_1_SAG,(F_prec+K_before_slip*↙
(delta_1_SAG - delta_prec)));
%F_spring_sag_1 =  min(F_tens_ultimate+(K_fake_2/n)*delta_1_SAG,(F_prec+K_after_slip*↙
(delta_1_SAG - delta_prec)));

%% Formulation 6 - rigid - fake plastic (a bit of slope to avoid singularity)
%-Does not work if you activate the IF condition
```

```
% if delta_1_SAG < 0
%    F_spring_sag_1 = 0;
% else
%     F_spring_sag_1 =  F_tens_ultimate+(K_fake_2/n)*delta_1_SAG;
%     F_spring_sag_1 =  F_slip+(K_fake_1/n)*delta_1_SAG;
% end

%% Formulation 7 - rigid-fake plastic (a bit of slope to avoid singularity)
%-works

%F_spring_sag_1 =  F_tens_ultimate+(K_fake_2/n)*delta_1_SAG;
%F_spring_sag_1 =  F_slip+(K_fake_1/n)*delta_1_SAG;

%% Formulation 7 - FULL linear - fake plastic - all models
%-
if delta_1_SAG < delta_limit % same definition as in 9 spring model which works
    F_spring_sag_1 =  min(F_slip+(K_fake_1/n)*delta_1_SAG,(F_prec+K_before_slip*↙
(delta_1_SAG - delta_prec)));
else
   F_spring_sag_1 =  min(F_tens_ultimate+(K_fake_2/n)*delta_1_SAG,↙
(F_prec+K_after_slip*(delta_1_SAG - delta_prec)));
end
end
```

```
function [F_spring_sag_2] = F_spring_sag_2(delta_2_SAG,delta_prec,F_prec,K_fake_1,↙
K_fake_2,i,yield,delta_at_F_0) % spring in compression
%% Input
Es = 210000; %[N/mm²]
delta_limit_1 = -0.00002; %[m] the value when the law should change
n = 1; % stiffness reduction factor

%Compression
F_c_ult = -818.75; %[kN] ultimate spring strenght
F_slip_c = -186.6;%[kN] force in the spring at moment of slip F_slip_c = -186;

K_before_slip_c = 44*Es;%[mm] stiffness of the spring K_before_slip = 44*Es;
K_after_slip_c = 1.832*Es;%[mm] stiffness of the spring

%Tension

F_t_ult = 829.02; %[kN] ultimate spring strenght
F_slip_t = 186.6;%[kN] force in the spring at moment of slip

K_before_slip_t = 5.934*Es;%[mm] stiffness of the spring K_before_slip = 44*Es;
K_after_slip_t = 1.446*Es;%[mm] stiffness of the spring

%% Formulation 0 - approx FULL curve
%- rigid part causes singularity
%if (delta_2_SAG-delta_prec) < 0
% if delta_2_SAG < delta_prec
%     F_spring_sag_2 = max(F_c_ult+(K_fake_1/n)*delta_2_SAG,F_slip_c+(K_after_slip_c*↙
(delta_2_SAG - delta_prec)));
% else
%     F_spring_sag_2 = min(F_t_ult+(K_fake_1/n)*delta_2_SAG,F_prec+K_approx*↙
(delta_2_SAG - delta_prec));
% end

%% Formulation 1 - approx FULL curve without ridig part - model 2.1
%- works
% K_approx = (K_before_slip_c+K_before_slip_t+K_after_slip_c+K_after_slip_t)/3;
%
% if delta_2_SAG < delta_prec %if (delta_2_SAG-delta_prec) < 0
%     if delta_2_SAG > delta_limit_1
%     F_spring_sag_2 = K_before_slip_c*delta_2_SAG;
%     else
%     F_spring_sag_2 = max(F_c_ult+(K_fake_1/n)*delta_2_SAG,F_prec+(K_after_slip_c*↙
(delta_2_SAG - delta_prec)));
%     end
% else
%     F_spring_sag_2 = min(F_t_ult+(K_fake_1/n)*delta_2_SAG,F_prec+K_approx*↙
(delta_2_SAG - delta_prec));
% end

%% Formulation 2 - approx FULL curve without ridig part - model 2.2
%- works
% K_approx_2 = (K_after_slip_c+K_before_slip_c)/2;
%
% %if (delta_2_SAG-delta_prec) < 0
% if delta_2_SAG < delta_prec
```

```
%     if delta_2_SAG > delta_limit_1
%     F_spring_sag_2 = K_before_slip_c*delta_2_SAG;
%     else
%     F_spring_sag_2 = max(F_c_ult+(K_fake_1/n)*delta_2_SAG,F_prec+(K_after_slip_c*↙
(delta_2_SAG - delta_prec)));
%     end
% else
%     if F_prec < 0
%         F_spring_sag_2 = F_prec+(K_approx_2*(delta_2_SAG - delta_prec));
%     else
%         F_spring_sag_2 = min(F_slip_t+(K_fake_1/n)*delta_2_SAG,↙
F_prec+K_before_slip_t*(delta_2_SAG - delta_prec));
%     end
% end

%% Formulation 3 - FULL CURVE - model 2.3
%- I was not able to activate the yield lenght and delta_at_F_0, therefore this↙
complex formulation is useless
%if (delta_2_SAG-delta_prec) < 0
% if delta_2_SAG < delta_prec
%     if delta_2_SAG > delta_limit_1
%         F_spring_sag_2 = K_before_slip_c*delta_2_SAG;
%     else
%         F_spring_sag_2 = max(F_c_ult+(K_fake_1/n)*delta_2_SAG,F_prec+↙
(K_after_slip_c*(delta_2_SAG - delta_prec)));
%         for j=i,
%         if F_spring_sag_2 <= F_c_ult
%         yield(1,j-1) = delta_2_SAG;
%         else
%         yield(1,j-1) = 0;
%         end
%         end
%     end
% else
%     yield_sort = sort(yield(1,:));
%     delta_yield_1 = yield_sort(1,2);
%     delta_yield_2 = yield_sort(1,1);
%     if delta_yield_1 == 0
%         yield_lenght = 0;
%     else
%         yield_lenght = delta_yield_1-delta_yield_2;
%     end
%     %delta_limit_2 = delta_limit_1-yield_lenght;
%
%     if delta_2_SAG < 0 %%%%
%         if F_prec > F_c_ult && F_prec < F_slip_c
%             F_spring_sag_2 =F_prec + K_after_slip_c*(delta_2_SAG - delta_prec);
%         else
%             F_spring_sag_2 =F_prec + K_before_slip_c*(delta_2_SAG - delta_prec);
%            for j=i
%             delta_at_F_0(1,j-1) = delta_2_SAG;
%            end
%         end
%     else
%         delta_limit_3 = yield_lenght+max(delta_at_F_0)+(F_slip_t/K_before_slip_t);
```

```
%         if delta_2_SAG > delta_limit_3
%             F_spring_sag_2 = min(F_slip_t+(K_fake_1/n)*delta_2_SAG,F_prec+↙
(K_before_slip_t*(delta_2_SAG - delta_prec)));
%         else
%             F_spring_sag_2 = min(F_t_ult+(K_fake_1/n)*delta_2_SAG,F_prec+↙
(K_after_slip_t*(delta_2_SAG - delta_prec)));
%         end
%     end
% end

%% Formulation 3 - FULL CURVE - model 2.3.1 - dependant of the step (0.0001↙
reccomended)
%- Simplified full model which will not take into account the full
%theoretical behavior, but the full realistic one
%if (delta_2_SAG-delta_prec) < 0

% F_fake = 0; %[kN] fake condition not to miss the boundary
%
% if delta_2_SAG < delta_prec
%     if delta_2_SAG > delta_limit_1 %F_prec > F_slip_c && F_prec <= 0
%         F_spring_sag_2 = F_prec+(K_before_slip_c*(delta_2_SAG - delta_prec)); %↙
F_spring_sag_2 = K_before_slip_c*delta_2_SAG
%     else
%         if F_prec > (F_slip_c) && F_prec <= 0% cause of the possibility of re-↙
loading when the hog2 spring reaches plateu
%             F_spring_sag_2 = F_prec+(K_before_slip_c*(delta_2_SAG - delta_prec));
%         else
%         F_spring_sag_2 = max(F_c_ult+(K_fake_1/n)*delta_2_SAG,F_prec+↙
(K_after_slip_c*(delta_2_SAG - delta_prec)));
%         end
%     end
% else
%         if F_prec > F_c_ult && F_prec < F_slip_c-F_fake
%             F_spring_sag_2 =F_prec + K_after_slip_c*(delta_2_SAG - delta_prec);
%         elseif F_prec > F_slip_c-F_fake && F_prec < 0
%             F_spring_sag_2 =F_prec + K_before_slip_c*(delta_2_SAG - delta_prec);
%         elseif F_prec > 0 && F_prec < F_slip_t
%             F_spring_sag_2 =F_prec + K_before_slip_t*(delta_2_SAG - delta_prec);
%         else
%             F_spring_sag_2 = min(F_t_ult+(K_fake_1/n)*delta_2_SAG,F_prec+↙
(K_after_slip_t*(delta_2_SAG - delta_prec)));
%         end
% end

%% Formulation 4 - FULL CURVE - model 2.3.2 - dependant of the step (0.0001↙
reccomended) work *
%- Simplified full model which will not take into account the full
%theoretical behavior, but the full realistic one
%if (delta_2_SAG-delta_prec) < 0
% F_fake = 0; %[kN] fake condition not to miss the boundary
%
if delta_2_SAG < delta_prec
    if F_prec > F_slip_c && F_prec <= 0
        F_spring_sag_2 = F_prec+(K_before_slip_c*(delta_2_SAG - delta_prec)); %↙
F_spring_sag_2 = K_before_slip_c*delta_2_SAG
```

```
    elseif F_prec > F_c_ult && F_prec <= F_slip_c
            F_spring_sag_2 = max(F_c_ult+(K_fake_1/n)*delta_2_SAG,F_prec+↙
(K_after_slip_c*(delta_2_SAG - delta_prec)));
    elseif F_prec > 0 && F_prec < F_slip_t
            F_spring_sag_2 =F_prec + K_before_slip_t*(delta_2_SAG - delta_prec);
    elseif F_prec > F_slip_t && F_prec <= F_t_ult
            F_spring_sag_2 = min(F_t_ult+(K_fake_1/n)*delta_2_SAG,F_prec+↙
(K_after_slip_t*(delta_2_SAG - delta_prec)));
    else
    end
else
        if F_prec >= F_c_ult && F_prec < F_slip_c
            F_spring_sag_2 =F_prec + K_after_slip_c*(delta_2_SAG - delta_prec);
        elseif F_prec > F_slip_c && F_prec < 0
            F_spring_sag_2 =F_prec + K_before_slip_c*(delta_2_SAG - delta_prec);
        elseif F_prec > 0 && F_prec < F_slip_t
            F_spring_sag_2 =F_prec + K_before_slip_t*(delta_2_SAG - delta_prec);
        else
            F_spring_sag_2 = min(F_t_ult+(K_fake_1/n)*delta_2_SAG,F_prec+↙
(K_after_slip_t*(delta_2_SAG - delta_prec)));
        end
end
```